NESC GN&C TDT Workshop on 2D Image Motion Optical Transfer Functions, Pointing Performance Analysis, and Requirements

Dr. Mark E. Pittelkau

Independent Consultant
Guidance, Navigation, and Control

Aerospace Control Systems, LLC
35215 Greyfriar Drive
Round Hill, VA 20141-2395
443-286-6902 (c)

mpittelkau@acsinnovations.com
www.acsinnovations.com

About the Instructor

Dr. Mark E. Pittelkau has been an independent consultant since 2005. He was previously with the Applied Physics Laboratory, Orbital Sciences Corporation, CTA Space Systems, and Swales Aerospace (the latter four now Northrop Grumman). His early career at the Naval Surface Warfare Center involved target tracking, gun pointing control, and gun system calibration.

His experience in satellite systems covers all phases of design and operation, including conceptual design, implementation, and testing of attitude control systems, attitude and orbit determination, attitude sensor alignment and calibration, optimal slewing, control-structure interaction analysis, and pointing error analysis. He has participated in post-launch support, including performance analysis, attitude sensor calibration, and anomaly resolution on science spacecraft and high-performance imaging spacecraft.

His current interests include precision pointing, precision attitude determination, and attitude sensor calibration. He is also interested in embedded real-time systems, vision navigation, and autonomous systems. Dr. Pittelkau earned the B.S. and Ph.D. degrees in Electrical Engineering at Tennessee Technological University and the M.S. degree in EE at Virginia Polytechnic Institute and State University. He has published several conference and journal papers on attitude sensor calibration, gyro error modeling, pointing error metrics, and image motion optical transfer functions.

Foreword (1/2)

This course was prepared by the author in support of the NASA GN&C Technical Discipline Team (TDT). The purpose of this two-day course is to inform practicing GN&C engineers, and other system and subsystem engineers, including payload engineers and mission analysts, of methodologies to analyze the pointing performance of spacecraft and to write unambiguous pointing requirements that are relevant to optical payload performance.

It is hoped that the seminar will contribute to a best-practices manual and contribute to accepted and uniform means of requirements definition, validation, and verification.

The course material is designed to address the needs of not only practicing GN&C engineers, but also system and subsystem engineers of other disciplines, payload engineers, mission analysts, and even astronomers who need to understand how they interface to a GN&C subsystem. Much revision is the direct result of active student participation during the presentations and from feedback obtained through course evaluation forms.

Foreword (2/2)

This course material is provided to attendees for their personal use. It is protected by copyright laws and may not be modified, reproduced, scanned, or recorded by any electronic or mechanical means without express written permission by the author. All data and equations are believed to be correct. It is the responsibility of the user of this course material to verify that all data, equations, and results derived therefrom are correct. The author shall not responsible for losses incurred by typographical or other errors or omissions, regardless of whether or when the author has any knowledge of errors or omissions, and the author shall not be obligated to notify the user of this course material of any corrections nor to post corrections. When practical, this author will respond to students' inquiries, remarks, and suggestions after the course.

Dr. Mark E. Pittelkau

What You Will Learn

The focus is on payload imaging performance due to pointing motion. Some historical background on pointing performance analysis is given. The Optical Transfer Function (OTF) and Modulation Transfer Function (MTF) are defined. The imaging performance due to pointing motion is measured by image motion optical transfer functions (IM OTF). IM OTFs are defined for displacement, smear, and jitter motions, which are all rigorously defined. Deterministic and Statistical IM OTFs are briefly derived and graphically illustrated and compared. The IM OTFs are parameterized by pointing error metrics (PEM), which are means and covariances of displacement, smear, and jitter. Emphasis is on procedures and algorithms to evaluate the image motion optical transfer functions and pointing error metrics. Three procedures are covered, which depend on whether the pointing error data is from time-domain simulation, frequency-domain analysis, or stochastic modeling. A method to evaluate the relative contribution of disturbance sources and to identify the most significant contributors is presented. The presentation includes pertinent discussion of flexible structures and control-structure interaction.

No single book can adequately cover this subject, so a book is not required for the course. A list of selected articles, reports, documents, and books is provided for reference and further study. Math is kept to the minimum necessary to convey principles; lengthy derivations are left to the reference material. Graphics are used to illustrate concepts. As with any such learning endeavor, the knowledge gained will be retained and strengthened through actual practice.

Introduction

Introduction – Objectives of the Workshop

- This workshop is a follow-on to the GN&C TDT Jitter Workshop in Oct 2019. [1–5]
  - Topics included Requirements Definition/Flowdown and Programmatic/Contractual issues and barriers
  - The image motion OTF and pointing metrics were presented, but more detail here
- This is an interactive interdisciplinary workshop whose main objectives are to
  1. identify current NASA requirements definition and flowdown process(es) & issues
  2. promote standards & processes for pointing requirements definition and verification
     - mission-level and program level acceptance
     - system-level and subsystem-level processes
     - interdisciplinary/multidisciplinary processes
  3. show how optical system performance is related to pointing performance
  4. provide a formal set of pointing performance definitions and metrics
  5. present methodologies for pointing performance analysis

Objectives (cont'd)

Objectives also include

- Help Systems engineers, Control System engineers, and Optical System engineers understand the physical and mathematical relationships between Pointing Performance and Optical System performance via the Image Motion OTFs.
- Derive Pointing Performance Metrics (PPMs) as parameters in the Image Motion OTFs.
- Discuss Pointing Requirements from payload to structural and control system design and analysis.
- Show how PPMs are used to analyze and manage pointing motion and its contributors.

Introduction – Motivation

- Pointing performance definitions vary widely across programs, industry, agencies
  - Loose connection with optical payload performance (risk of imaging performance)
  - Hidden or excessive margin (risk of additional cost and schedule)
  - Contractual, Programmatic, Organizational issues
- Tighter interdisciplinary/multidisciplinary engineering is needed as future performance requirements become more challenging
  - Need to more tightly couple Optical system design and analysis with Pointing Control system design and analysis, including structural design
  - Facilitate design of more complex systems – multiple optical instruments, wide bandwidth image stabilization, advanced optical systems
  - Inter-discipline communication and coordination
  - Shorter concept-to-flight timelines and cost constraints

Introduction – Approach

- Briefly review traditional definitions of pointing performance.
- Give a brief tutorial on optical system concepts and imageing performance.
- Present methods to evaluate image motion effects on imaging performance.
- Present relevant, consistent, and rigorous definitions and metrics for pointing performance
  - as a basis for requirements definition
  - as a basis for verification
- Present methodologies for pointing performance analysis and verification
  - deterministic and statistical methods of image motion OTF/MTF analysis
  - methods of frequency domain and time-domain analysis of disturbance response
  - a method of relative contributions to pointing metrics from disturbance sources

Introduction – Approach (cont'd)

- Discuss how the IM OTF and corresponding metrics can be incorporated into NASA programs at the program level and in requirements, and implemented into the system engineering process and subsystem levels (GN&C, structures, thermal, optical payload).
- Discuss how the method is applied
  - as a design matures through phases of development, and
  - depending on what information is available about the optical system.
- This presentation and discussions in the workshop may serve as an outline for a section in a Pointing Performance Guidelines or Handbook.

Scope

- The IM OTFs apply to isoplanatic (linear shift invariant, LSI) electro-optical systems with incoherent (noncoherent) radiation geometrically projected onto a detector plane.
  - The OTF for coherent radiation (e.g., laser light) is more complicated and is not addressed in the present framework.
- A Wavefront Transfer Function (WTF) and Statistical WTF have not yet been developed, pending some IR&D. The IM WTF deals with distortion due to motion of optical elements.
- The Pointing Performance Metrics (means and covariances for displacement, smear, jitter) are valid for pointing performance of any optical sensor and other payloads.

Applicability of IM OTF and Pointing Performance Metrics

- Dynamic modeling and analysis of pointing and image motion.
  - Various levels of fidelity/availability of an optical system model considered.
  - Capability to incorporate updated optical system and structural models into the performance analysis.
- The Pointing Performance Metrics have been used on several programs since 2002.
  - or since the initial development at JPL in 1993
- The Pointing Performance Metrics have been revised to include smear motion.
- The Image Motion OTF links Pointing Performance to Image Quality
  - Performance Requirements can now be derived and verified more rigorously.

Two Formal Methodologies

- A statistical description of image motion effects on optical sensor performance
  - Statistical Image Motion OTFs measure expected (mean) IM OTF performance
  - IM OTFs are parameterized by pointing performance metrics (means and covariances).
- A methodology to evaluate pointing performance metrics
  - Frequency-domain analysis is an alternative to time-consuming time-domain simulation and Monte Carlo iterations, thereby reducing time to conduct analyses or permitting more detailed analyses.
  - Relative contribution analysis
    * reveals disturbance sources that are design drivers to pointing performance, and
    * facilitates performance evaluation and updates as models improve.

These complement STOP analysis, which is performed using time-domain simulation.

Benefits of these Formal Methodologies

- Systematic and more Integrated methodology
- Image Motion OTFs are directly relevant to Image Quality
  - Well defined (physical and mathematical model)
  - Clear path from Optical System Performance to Image Motion allocation, then flow down to Pointing Performance Requirements
  - Reduce excess and hidden margin ($\pm$) $\Longrightarrow$ Reduce performance and cost risk
- Displacement, Smear, Jitter Pointing Performance Metrics
  - Equivalent representations in time domain & frequency domain
  - Useful in pointing control system analysis and synthesis
- Windowed Stability metric measures image-to-image displacement (unrelated to IM OTF)

Limitations

- The Statistical Image Motion OTFs augment, but may not replace traditional methods of Image Motion OTF/MTF analysis
  - Methods of numerical evaluation of IM OTF can still be applied.
  - Deterministic IM OTFs are used for specific types of image motion.
- Non-stationary and transient effects may require time-domain simulation
  - Deterministic IM OTFs can be used to evaluate the effect of transient motions.
- IM OTF analysis requires a camera model, which may range from low-fidelity pinhole camera to high-fidelity structural-optical model
  - same limitation in traditional STOP analysis
  - IM OTF requirements can still be derived
  - prior models & updates facilitate IM OTF analysis over the duration of a program
  - camera models may not be available on some programs – may be mitigated

Introduction – Outline

Part 1: Traditional Pointing Error Definitions and Metrics

Part 2: Image Motion Optical Transfer Functions (IM OTF)

Part 3: Requirements Definition, Flow Down, Interfaces, Model Updates

Part 4: Pointing Performance Metrics

Part 5: Reaction Wheel Disturbance Model

Part 6: Summary & Recommendations

Nomenclature & Definitions

Acronyms & Abbreviations

References

Table of Contents

Part 1: Traditional Pointing Error Definitions and Metrics

Part 1: Traditional Pointing Error Definitions and Metrics

- Traditional Pointing Error Definitions
- Limitations and ambiguity of these definitions
- Stability/Jitter Analysis Software Tools
- Some Experiences and Motivation
- Research on Pointing Performance Metrics and Image Motion OTF

Traditional Pointing Error Definitions

- Pointing error is traditionally specified in terms of "jitter", "stability", "quasi-static", and "static" pointing error.
- Jitter and stability are not consistently defined across and within programs [1, 6, 7, 12]. Various definitions exist.
- Line-of-sight (LOS) is not consistently defined.
- Pointing performance requirements must be
  - clear, concise, consistent (not ambiguous, non-conflicting), technically correct, and
  - traceable to [directly related to] (optical) payload performance requirements.
- Though many articles and presentations discuss pointing analysis and test, few discuss pointing and payload requirements and how they are derived.

Some Traditional Stability and Jitter Metrics

- Peak stability (jitter) of the attitude $\Theta(t)$ in a sliding window of width T is

$$\Delta_{\mathsf{p}}(t) = \max_{\tau \in [0,T]} |\Theta(t) - \Theta(t-\tau)|$$

- The peak stability (jitter) metric may be defined

$$\Delta_{\mathsf{p}} = \max_{t \in [-\infty,\infty]} \Delta_{\mathsf{p}}(t)$$

and is sometimes defined as

$$\sigma^2_{\mathsf{ps}} = \mathcal{E}\{(\Delta_{\mathsf{p}}(t))^2\}$$

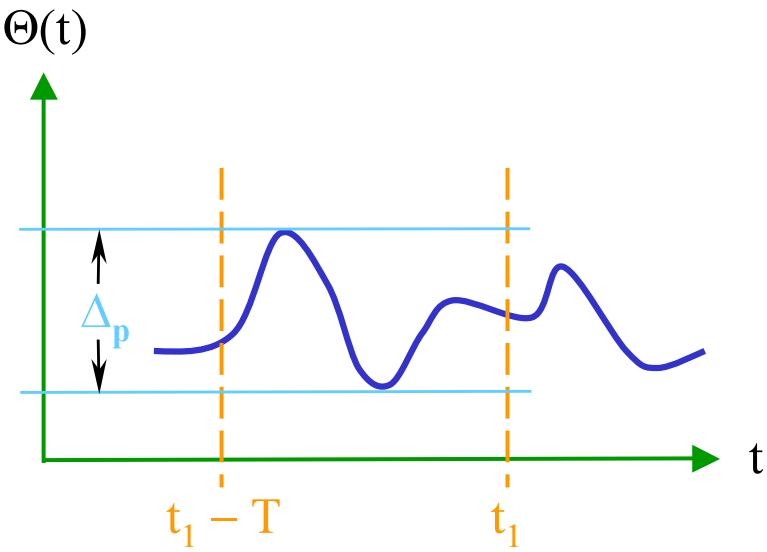

- A method of "pointing stability jitter analysis", in which a probability distribution is computed from a histogram of $\Delta_{\mathsf{p}}(t)$, and pointing accuracy is specified at 99.8% of the distribution, is found in a patent [18] (filed 2003, awarded 2006).

Pointing Error Definitions on GOES-I–M

"Pointing Stability – the peak-to-peak variation of the actual pointing direction over one orbit, per axis."

"Pointing Jitter – the peak-to-peak variations of the actual pointing direction over specific time interval as defined above by each delta Tn, per axis."

The Tn are image scan times.

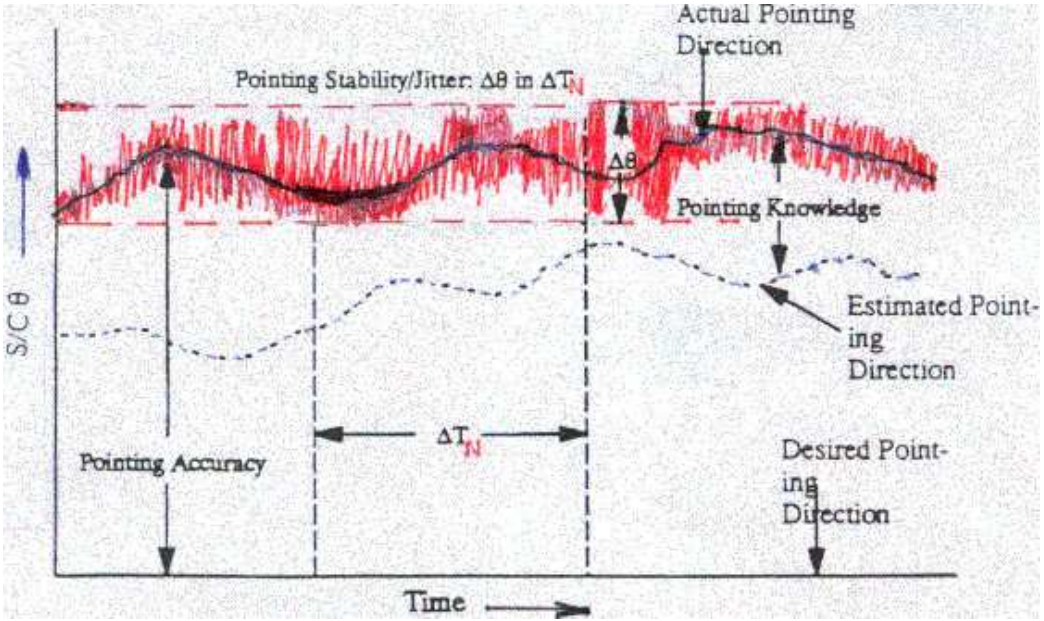

The figure is attributable to John Sudey, Jr. (GSFC), who used it to explain what is meant by pointing accuracy, stability, jitter, and knowledge. He was a proponent of jitter testing. [6–8]

Other Jitter and Stability Definitions

- Jitter is sometimes stated as an angular error over a frequency range. Example: 0.001° over $f = 20$ to 100 Hz ($f \geq 1/T$, where T is the exposure time of the optical sensor).
- Stability is often stated as
  - as a rate, for example, 0.001 deg/sec
  - as a rate over a frequency range, for example, 0.001 deg/sec over 0 to 0.1 Hz
- A maximum rate is often specified to limit smear during an exposure of a detector
- A method was developed at Draper Lab for the EOS-PM mission and is stated in the NOAA I, J, K General Interface Requirements Document (GIRD) [15, 16] (1993, 1994). It measures the peak-to-peak amplitude of a single-harmonic motion over a window of width T. It does not generalize to multiple harmonics.
- Pointing requirements are typically stated as "3σ pointing error" against one or more of the foregoing criteria.

Limitations and Ambiguity of these Definitions

- Known to be very conservative
- Not indicative of optical payload performance
- Difficult to analyze in the time domain
- No mathematical equivalent in the frequency domain
- Not informative – the metrics don't:
  - indicate which are the most offending disturbances
  - reveal what modifications are needed to meet a requirement
- Results can be inconsistent (ex: figures show the same Δ_p, but the effect on optical performance is different)
- Ambiguous definitions: the words "jitter" and "stability" are often used interchangeably.

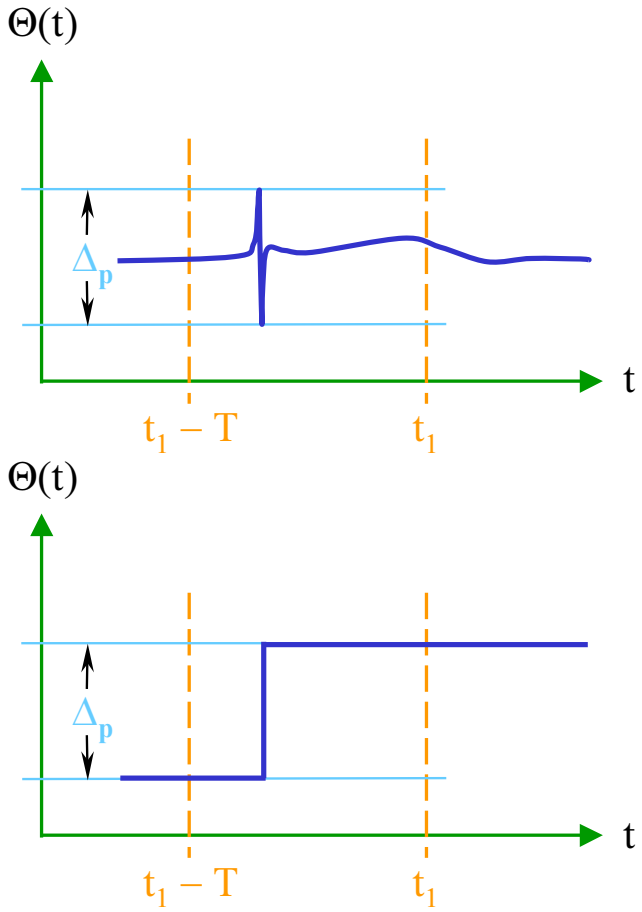

Stability/Jitter Analysis Software Tools

- A Matlab-based program PLATSIM [17] (Ver. 2.0, 1997) is a simulation and analysis tool developed at LaRC that can
  - Compute the time response and frequency response of a system, including flexible-body modes and disturbance inputs.
  - Evaluate the peak stability (jitter) metric. An efficient algorithm computes the peak-to-peak change over a sliding window.
- The Analytic Pointing Performance (APP) tool, implements methods of the ESA Pointing Error Handbook [49] (1993).
- Recent: EllipTool (Blaurock, Elliptical Engineering) has supported several high performance NASA science programs. [5]
- Every organization, and sometimes different programs in an organization, has its own simulation and evaluation software tools and methodologies, either standardized across spacecraft programs, tailored to specific programs, or one-off custom-designed.

Some Experiences and Motivation

- 1991–1993: NOAA I, J, K phase-A study
- 1999: GALEX (Orbital), peak stability metric
- 2000: SORCE (Orbital), 5 imaging instruments: SIM, SOL1, SOL2, TIM, XPS, plus ST, IMU. Proposed weighting functions from Baiocco [28] for PDR.
- 2000: Studied reports on a new Stability Weighting Function by Sirlin, San Martin, Lucke, Baiocco, Bayard (JPL) [26–29].
- 2001–2002: STEREO (APL) [12–14] Pointing requirements driven by the SECCHI coronagraphs (COR1, COR2), EUVI imager (omitted image stabilization system, ISS, that would remove low-frequency motion below 5 Hz); Guide Telescope (GT).
  - Pointing requirements to keep an occulter on the Sun so that stray light is below some level and to maintain resolution
  - ▲ Requirements are based on the peak stability definition, but for radial error.
  - JPL method proposed, but with stability & jitter distinct, windowed stability added.

Research on Pointing Performance Metrics and Image Motion OTF

- "Definitions, Metrics, and Algorithms for Displacement, Jitter, and Stability", 2003 [32, 33] defined jitter, stability, windowed stability, but did not discuss OTFs.
- "Definitions, Metrics, and Algorithms for Displacement, Jitter, and Stability", 2012 [34] connected pointing to image motion OTFs. Smear idea from a diagram in a G&Ski paper [31].
- "Optical transfer functions, weighting functions, and metrics for images with two-dimensional line-of-sight motion", 2016 [35] statistical image motion OTF in 2D with non-zero mean smear. Includes a survey of the literature on Image Motion OTFs.

Part 2: Image Motion Optical Transfer Functions (IM OTF)

Image Motion Optical Transfer Functions (IM OTF)

1. Optical System concepts and technical performance measures
2. Image Motion Optical Transfer Functions
   - Image Motion vs. Line-of-Sight Pointing Motion
   - Camera Model, Geometric Optics
   - Numerically Computed IM OTF
3. Statistical and Deterministic Image Motion OTFs
4. Summary Table of Image Motion OTFs and LSF

1. Optical System Concepts and Technical Performance Measures

- Point Spread Function (PSF)
- Diffraction-limited optics, Resolution
- Spatial frequency response
  - Optical Transfer Function (OTF)
  - Modulation Transfer Function (MTF)
  - Phase Transfer Function (PTF)
- Some optical system technical performance measures (TPMs)
  - Modulation
  - Contrast
  - Resolution
  - MTF Area
  - Strehl Ratio

Point Spread Function (PSF)

The Point Spread Function (PSF) is the image of a point source of light.

- Ideally the PSF is a Dirac delta function so that the image of a sharp point is sharp.
- The PSF can be no smaller than the Fraunhofer diffraction, which is due to the finite aperture of the optics.
- PSF is shaped (enlarged and distorted) by the optical path (atmosphere, optics, detector) and by Image Motion.
- Image motion is potentially a limiting factor in the performance of an optical system.

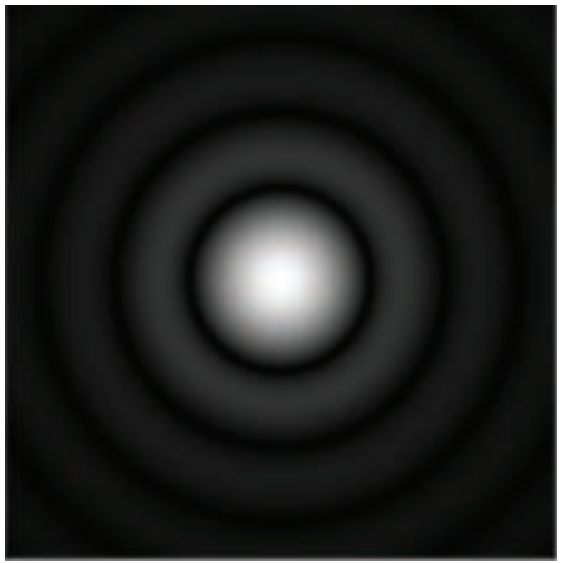

Fraunhofer diffraction
for a circular aperture.

PSF for Diffraction-Limited Optics (Circular Aperture)

- The diffraction PSF $= [2J_1(\pi\rho)/(\pi\rho)]^2$, where ρ is normalized distance. This PSF is well approximated by a Gaussian function $G(\rho; \sigma^2_{\text{psf}})$, normalized so that $G(0; \sigma^2_{\text{psf}}) = 1$.
- The Airy Disc is the bright central region of the PSF.
- The Full-Width Half-Maximum (FWHM) of the PSF is the diameter where $G(x, \sigma^2_{\text{psf}}) = 0.5$, so we have FWHM $= 2.355\sigma_{\text{psf}}$.
- At the diffraction limit, $\sigma_{\text{psf}} = 0.4247$ ($\sigma^2_{\text{psf}} = 0.18$) for a unit diameter FWHM ($2.355\sigma_{\text{psf}} = 1$).
- Gaussian random jitter motion increases the σ^2_{psf}

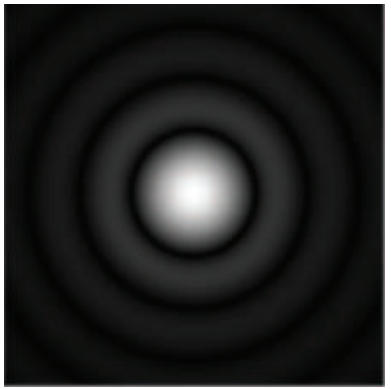

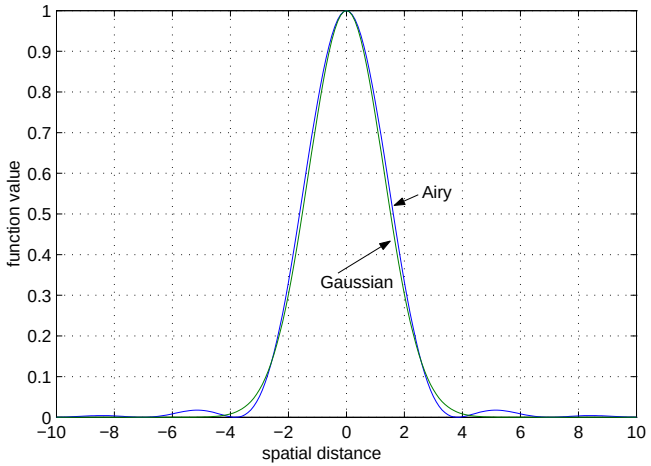

PSF and Gaussian approximation

Effect of Gaussian Random Jitter Motion—Spatial Domain

- In the presence of image motion $p(t)$ with density function $h(p)$, the resulting PSF is

$$G_{\mathsf{e}}(r) = \int_{-\infty}^{\infty} G_{\mathsf{airy}}(x-p)\, h(p)\, \mathrm{d}p$$

- For Gaussian random motion, $h(p) = G_{\mathsf{motion}}(p; \sigma_{\mathsf{J}}^2)$, we get another Gaussian,

$$G_{\mathsf{r}}(x) = G(x, \sigma_{\mathsf{psf}}^2 + \sigma_{\mathsf{J}}^2)$$

- The resulting FWHM is then

$$\mathsf{FWHM} = 2.35(\sigma_{\mathsf{psf}}^2 + \sigma_{\mathsf{J}}^2)^{1/2}$$

- The Gaussian random motion over an exposure interval T is called **jitter**.
- The relevant metric is the **jitter variance** σ_{J}^2.
- Jitter *widens the PSF* and thus *reduces the resolution* of the optical system.

Spatial Frequency

- The spatial frequency $\boldsymbol{\xi}$ (sometimes $\boldsymbol{\nu}$) in the two dimensions x and y on a focal plane is

$$\boldsymbol{\xi} = \begin{bmatrix} \xi_x \\ \xi_y \end{bmatrix} \qquad \text{cycles per unit length}$$

- $\xi = |\boldsymbol{\xi}|$ is the reciprocal of the spatial wavelength λ
- The units of $\boldsymbol{\xi}$ are typically cycles/mm, also called line pairs per mm or lp/mm.
- The angular wavenumber $\boldsymbol{k}$ is defined by

$$\boldsymbol{k} = 2\pi\boldsymbol{\xi} \qquad \text{rad per unit length}$$

- The magnitude of $\boldsymbol{k}$ is $k = |\boldsymbol{k}| = \dfrac{2\pi}{\lambda}$.
- The units of $\boldsymbol{k}$ are typically rad/mm for λ in mm.

OTF, MTF, PTF

Point Spread Function is the spatial impulse response of an optical sensor.

Optical Transfer Function (OTF) of an isoplanatic (linear shift invariant, LSI) electro-optical system, $\mathrm{OTF}_{\mathrm{system}}(\boldsymbol{\xi})$, is the 2D spatial Fourier Transform (FT) of the PSF for incoherent (noncoherent) radiation geometrically projected onto the detector plane. (More simply, the OTF is the spatial-frequency response of an optical sensor.)

Modulation Transfer Function (MTF) is the magnitude of the OTF,

$$\mathrm{MTF}(\boldsymbol{\xi}) = |\,\mathrm{OTF}(\boldsymbol{\xi})\,|$$

Phase Transfer Function (PTF) is the phase shift as a function of frequency,

$$\mathrm{OTF}(\boldsymbol{\xi}) = \mathrm{MTF}(\boldsymbol{\xi})\,\exp(-i\,\mathrm{PTF}(\boldsymbol{\xi}))\,, \qquad \mathrm{PTF}(\boldsymbol{\xi}) \equiv \Theta(\boldsymbol{\xi})$$

FT of an Image is the product of the system OTF and the FT of the object,

$$\mathrm{FT}_{\mathrm{image}}(\boldsymbol{\xi}) = \mathrm{OTF}_{\mathrm{system}}(\boldsymbol{\xi})\;\mathrm{FT}_{\mathrm{object}}(\boldsymbol{\xi})$$

Modulation and Contrast

Modulation Depth is the amplitude of the irradiance variation divided by the average irradiance, $M = (A_{\text{max}} - A_{\text{min}})/(A_{\text{max}} + A_{\text{min}})$. Note A_{max} and A_{min} are positive.

Contrast is defined as the modulation depth M. The contrast is maximum when $M = 1$, where $A_{\text{min}} = 0$. The contrast is zero when $M = 0$, where $A_{\text{max}} = A_{\text{min}}$.

Contrast Transfer Function (CTF) is the sensor's response to a square wave input signal comprising alternating white and black line pairs. The sensor's response to the line pairs has maximum and minimum intensities A_{max} and A_{min}. The CTF is related to the MTF. The MTF is a function of sinusoidal lines, which are more difficult to generate than a square wave input.

Resolution Loss, Phase Reversal, and Low Contrast

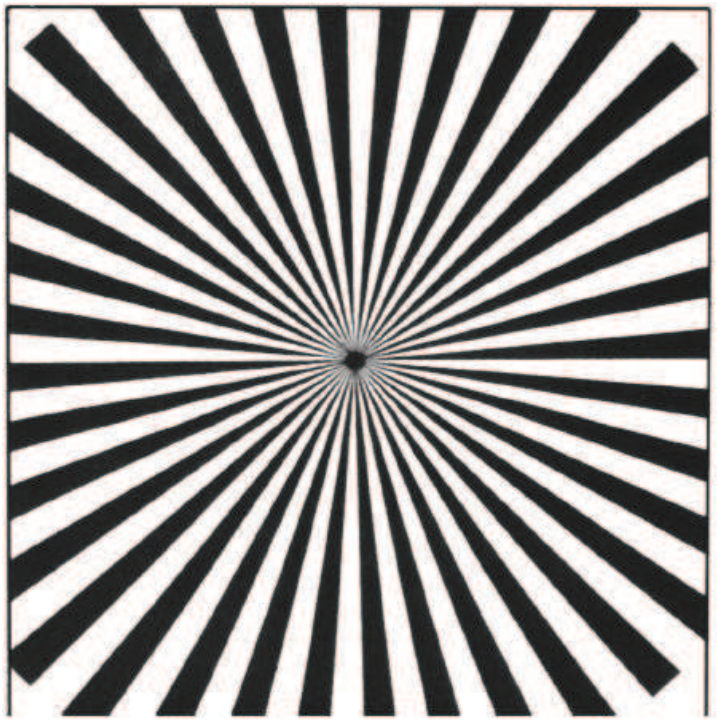

Original sharp image

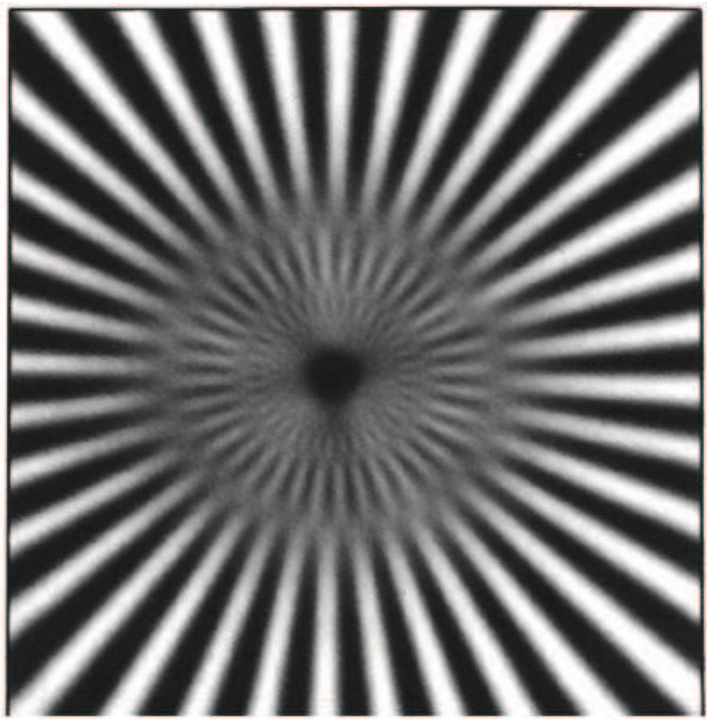

Slightly defocused image

Resolution

- Resolution can be defined as the smallest detail or the smallest black and white line pair that can be distinguished. The line pair is indistinguishable when $A_{\text{max}} = A_{\text{min}}$, where the contrast is zero.
- Sspatial resolution of the optical system limits the modulation depth of the image. Resolution depends also on the MTF.
- Resolution can also be defined to be where FWHM $= 0.5$.
- Resolution is limited also by the detector's sensitivity and noise.
- Resolution is limited also by the spatial sampling of the detector array to approximately 2 pixels. The FWHM should not be greater than about 1 pixel, so $\sigma_{\text{psf}} \lesssim 1$ pixel.
- Resolution can be subjective in human perception.

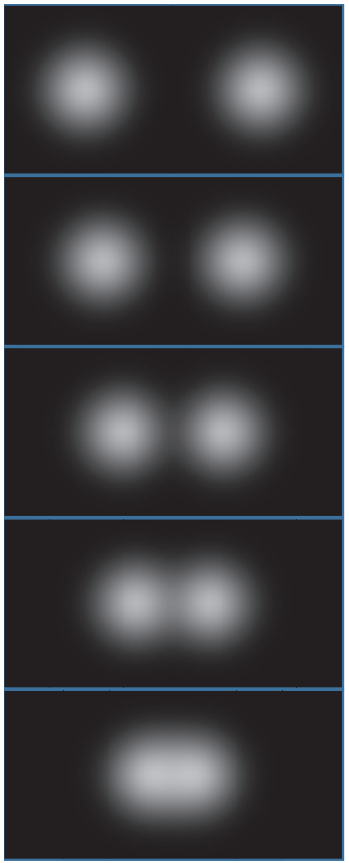

Resolution Depends on the MTF and Detector Noise

The limiting resolution of A and B is the same, but the performance of A is better than B.

The limiting resolution of C is less than that of A and B, but its performance is slightly better than A in mid-frequencies.

NEM is the Noise Equivalent Modulation

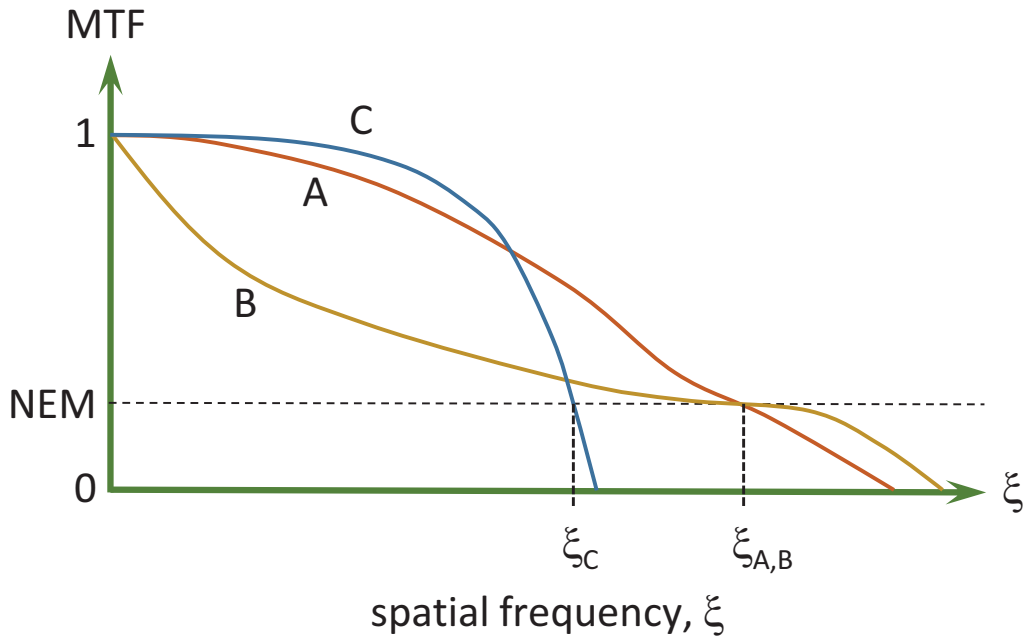

Image-Quality Performance Measured by MTF Area (MTFA)

Image-Quality performance can be measured by the MTF Area (MTFA).

The MTFA is the area between the MTF and the NEM curves over a frequency range of interest, typically from $\xi = 0$ up to ξ_A at the resolution limit.

The best performance is achieved by the system that has the largest MTFA.

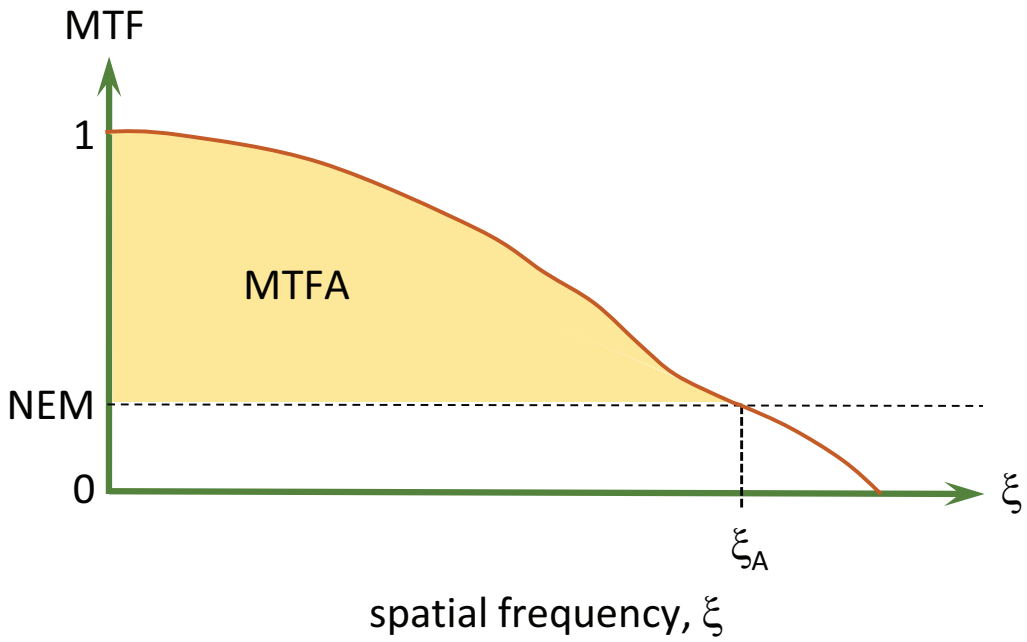

Strehl Ratio

The Strehl ratio S is a useful single-number performance specification. It compares the actual optical performance to the diffraction-limited optical performance.

The Strehl ratio is defined as the ratio of actual intensity to diffraction-limited intensity I,

$$S = \frac{I_{\text{actual}}}{I_{\text{diffraction}}} = \frac{\int_{\boldsymbol{\xi}} \text{MTF}_{\text{system}}(\boldsymbol{\xi})\, \mathrm{d}\boldsymbol{\xi}}{\int_{\boldsymbol{\xi}} \text{MTF}_{\text{diffraction}}(\boldsymbol{\xi})\, \mathrm{d}\boldsymbol{\xi}}$$

There is an equivalent calculation in the spatial domain can be made. (Omitted here.)

$S \geq 0.8$ indicates excellent image quality (relative to the diffraction limit).

Note: The foregoing are not the only optical performance measures, but illustrate the role of the OTF, which is our focus here.

Previous Results for Pointing Error [Performance] Metrics

- PEMs for displacement and jitter originally developed at JPL by Sirlin and San Martin (1990) [26], Lucke, Sirlin, San Martin (1992) [27], Bayard (2000, 2004) [29, 30].
- PEMs developed at APL, published in 2003, define Point-to-Point Stability and Windowed Stability, and includes displacement and jitter [32, 33]. All are 1D.
- The PEMs defined in 2003 are included in the ESA Performance Error Engineering Tool (PEET) [46–52]. The latest was published in 2012.
  "Performance", "pointing", and "error" are used synonomously.
- Image Motion OTFs for 1D displacement, zero-mean smear, and *new* jitter. 2012, [34].
- This presentation includes results from SPIE paper published in 2016 [35].
  - Extends results from 2012 to 2D and non-zero-mean Gaussian random smear.
  - Main result is the 2D statistical smear OTF with *new* shift, smear, jitter PPMs.

Deterministic Image Motion OTF

- Optical Engineering papers* derive the image motion OTF for
  - uniform linear motion (smear)
  - higher order smear – quadratic/parabolic (smile), cubic (frown), exponential
  - pure tone/sinusoidal motion
    - integral number of cycles per exposure
    - non-integral number of cycles per exposure
    - 0 to 2 sinusoidal cycles, including fractional cycles, with an initial phase angle
  - Gaussian random motion (jitter)
  - various other effects such as shutter and time delay integration (TDI)
- Smear and sinusoidal amplitude and phase are traditionally treated as deterministic.
- All image motion is analyzed in the time domain.
- Pointing system design and analysis are not considered directly.

* See [35] for citations.

2. Image Motion OTF (outline)

- Image Motion vs. Line-of-Sight poomting motion
- Camera model, Geometric Optics
- Image motion model, displacement, smear, jitter
- Mathematical model for Image Motion OTF
- Numerical methods to compute the Image Motion OTF from time-domain data

Image Motion vs. Line-Of-Sight (LOS) Pointing Motion

- Image motion on a focal plane is due to the relative motion of the observed object, pointing motion of the optical sensor, and motion of its optical elements of the sensor.
- Image motion due to changes in the aspect of the object is not considered here.
- LOS relative pointing motion and Image motion are synonymous, *but are not the same*!
  - Image motion is interior to the sensor, on the focal plane of a camera or telescope.
  - LOS relative pointing motion is exterior to the sensor (referenced to a boresight frame*).
  - They differ not just geometrically, but possibly due to structural modes along the optical path, as well as motion of articulated optical elements.

$\Longrightarrow$ We are primarily concerned with image motion on the focal plane.

$\Longrightarrow$ The relative LOS motion is caused by the relative rotational and translational motion of the object and sensor.

*I demand that the boresight axis be labeled the z-axis by edict.

Geometric Optical Sensor (Camera, Telescope) Model

- The image motion $\boldsymbol{p}(t)$ on the focal plane can be modeled by

$$\boldsymbol{p}(t) = \begin{bmatrix} x(t) \\ y(t) \end{bmatrix} = \boldsymbol{c}\big(\boldsymbol{X}(t), \boldsymbol{\theta}(t)\big)$$

- The function $\boldsymbol{c}\big(\boldsymbol{X}(t), \boldsymbol{\theta}(t)\big)$ is a camera model parameterized by relative translation $\boldsymbol{X}$ and relative attitude $\boldsymbol{\theta}$ motions. A pinhole camera is the simplest geometric model.
- More generally, the camera model comprises multiple moving elements involving structural modes, multiple mirrors, lenses, prisms, mechanisms, and detectors.

$$\boldsymbol{p}(t) = \begin{bmatrix} x(t) \\ y(t) \end{bmatrix} = \boldsymbol{c}\big(\boldsymbol{d}(t)\big)$$

  $\boldsymbol{d} = \boldsymbol{\Phi_d}\,\boldsymbol{q}$ is a vector of translational and rotational modal displacements,
  $\boldsymbol{\Phi_d}$ is a matrix of mode shapes and mode slopes at points along the optical path,
  $\boldsymbol{q}$ is a vector of structural normal modes (including rigid body modes).
- There can be multiple optical sensors or multiple focal planes in an optical sensor.

Image Motion Model / Relative LOS Pointing Motion Model

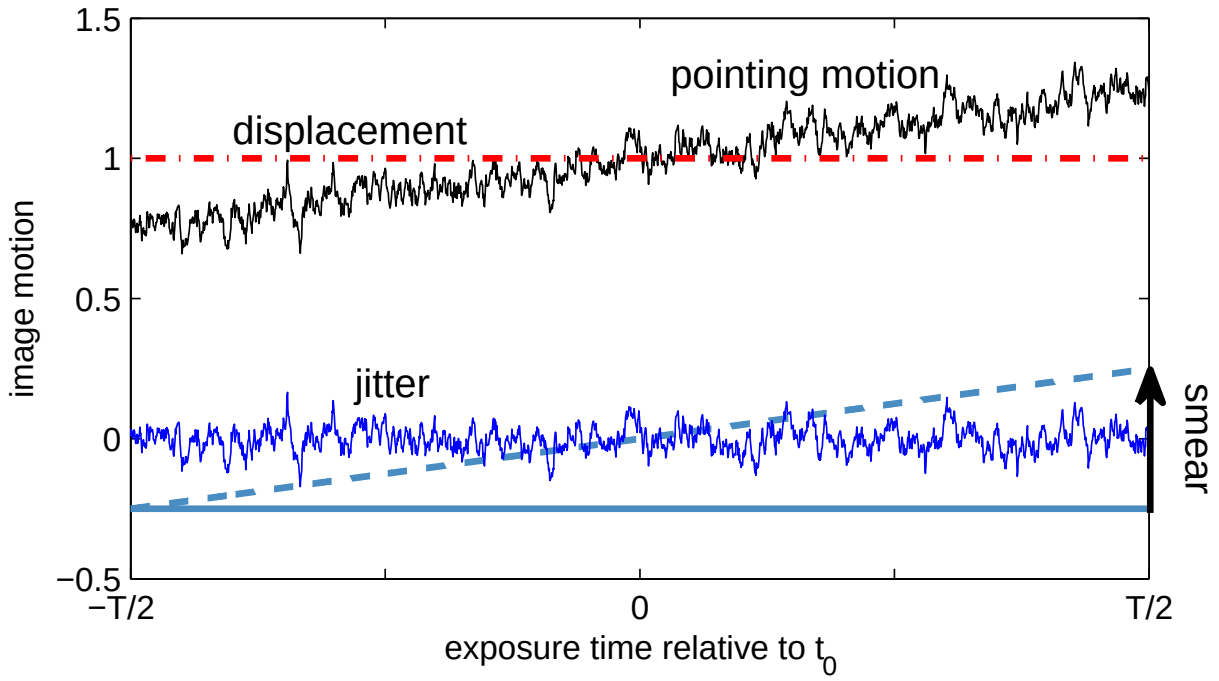

$$\boldsymbol{p}_o = \boldsymbol{p}_o(t_0) = \text{displacement}$$

$$\boldsymbol{v}_o = \boldsymbol{v}_o(t_0) = \text{smear rate}$$

$$\boldsymbol{s}_o = T\boldsymbol{v}_o = \text{smear}$$

$$\boldsymbol{\psi}(t) = \text{jitter motion}$$

$$\boldsymbol{p}(t) = \boldsymbol{p}_o + (t - t_0)\boldsymbol{v}_o + \boldsymbol{\psi}(t) \qquad t \in [t_0 - T/2,\, t_0 + T/2] \equiv \mathcal{I}(t_0)$$

$$\boldsymbol{p}(t_0 + \alpha) = \boldsymbol{p}_o + \alpha\boldsymbol{v}_o + \boldsymbol{\psi}_o(\alpha) \qquad \alpha \in [-T/2,\, T/2]\,, \quad \boldsymbol{\psi}_o(\alpha) = \boldsymbol{\psi}(t_0 + \alpha)$$

Model Assumptions

- $\boldsymbol{p}(t)$ is either
  - Gaussian and wide-sense stationary (WSS)
  - Non-Gaussian and fourth-order stationary (FOS)

  $\Longrightarrow \boldsymbol{p}_o$, $\boldsymbol{v}_o$, and $\boldsymbol{\psi}(t)$ are WSS or FOS Gaussian random variables.
- $\boldsymbol{p}_o$, $\boldsymbol{v}_o$, and $\boldsymbol{\psi}(t)$ are independent.
- $\boldsymbol{\psi}(t)$ is zero mean.
- The displacement and smear rate depend on the centroid time t_0,

  $$\boldsymbol{p}_o = \boldsymbol{p}_o(t_0)$$
  $$\boldsymbol{v}_o = \boldsymbol{v}_o(t_0)$$
- The coherence time τ_c of the jitter is short relative to the exposure time, $\tau_c \ll T$.

Jitter Coherence Time (1/2)

- The coherence time is obtained from a second-order Taylor series approximation of the autocovariance $\boldsymbol{C}(\tau_c)$ of $\boldsymbol{\psi}(t)$,

$$\tau_c = \left[-2\boldsymbol{C}_{\boldsymbol{\psi}}(0)/\boldsymbol{C}''_{\boldsymbol{\psi}}(0)\right]^{1/2}$$

  $\boldsymbol{C}''_{\boldsymbol{\psi}}(\tau)$ is the second derivative of $\boldsymbol{C}_{\boldsymbol{\psi}}(\tau)$ with respect to τ.

- Another definition (not used here) is

$$\tau_c = \frac{1}{\boldsymbol{C}_{\boldsymbol{\psi}}(0)} \int_0^\infty \boldsymbol{C}_{\boldsymbol{\psi}}(\tau)\,\mathrm{d}\tau$$

- The coherence time is computed per-channel when $\boldsymbol{C}_{\boldsymbol{\psi}}$ is a matrix.

Jitter Coherence Time (2/2)

- Compute the autocorrelations from the inverse Fourier Transform of the power spectral density $\boldsymbol{S}_{\boldsymbol{\psi}}(\omega)$ of $\boldsymbol{\psi}(t)$,

$$\boldsymbol{C}_{\boldsymbol{\psi}}(\tau) = \frac{1}{2\pi}\int_{-\infty}^{\infty} \boldsymbol{S}_{\boldsymbol{\psi}}(\omega)\, e^{-j\omega\tau}\, \mathrm{d}\omega$$

$$\boldsymbol{C}''_{\boldsymbol{\psi}}(\tau) = \frac{1}{2\pi}\int_{-\infty}^{\infty} -\omega^2 \boldsymbol{S}_{\boldsymbol{\psi}}(\omega)\, e^{-j\omega\tau}\, \mathrm{d}\omega$$

- Evaluating $\boldsymbol{C}_{\boldsymbol{\psi}}(\tau)$ and $\boldsymbol{C}''_{\boldsymbol{\psi}}(\tau)$ at $\tau = 0$ yields

$$\boldsymbol{C}_{\boldsymbol{\psi}}(0) = \frac{1}{2\pi}\int_{-\infty}^{\infty} \boldsymbol{S}_{\boldsymbol{\psi}}(\omega)\, \mathrm{d}\omega$$

$$\boldsymbol{C}''_{\boldsymbol{\psi}}(0) = \frac{1}{2\pi}\int_{-\infty}^{\infty} -\omega^2 \boldsymbol{S}_{\boldsymbol{\psi}}(\omega)\, \mathrm{d}\omega$$

Model Parameters, aka Pointing Performance Metrics (PPM)

Model Parameters

Accuracy	$\boldsymbol{m} = \mathcal{E}\{\boldsymbol{p}(t)\}$	$\boldsymbol{\Sigma}_{\mathsf{A}} = \mathrm{cov}\{\boldsymbol{p}(t)\}$
Displacement	$\boldsymbol{\mu} = \mathcal{E}\{\boldsymbol{p}_o\}$	$\boldsymbol{\Sigma}_{\mathsf{D}} = \mathrm{cov}\{\boldsymbol{p}_o\}$
Smear Rate	$\boldsymbol{\rho} = \mathcal{E}\{\boldsymbol{v}_o\}$	$\boldsymbol{\Sigma}_{\mathsf{R}} = \mathrm{cov}\{\boldsymbol{v}_o\}$
Smear	$\boldsymbol{s} = T\boldsymbol{\rho}$	$\boldsymbol{\Sigma}_{\mathsf{S}} = T^2\boldsymbol{\Sigma}_{\mathsf{R}}$
Jitter	$\mathbf{0} = \mathcal{E}\{\boldsymbol{\psi}(t)\}$	$\boldsymbol{\Sigma}_{\mathsf{J}} = \mathrm{cov}\{\boldsymbol{\psi}(t_o)\}$

System Optical Transfer Function

- Recall that the Point Spread Function (PSF) is the image of a point source of light and is shaped by various effects in the optical path such as atmospheric effects, the spatial frequency response of the optics and detector, and Image Motion.
- The OTF of an optical system is

$$\mathrm{OTF}_{\mathsf{system}}(\boldsymbol{\xi}) = \mathrm{OTF}_{\mathsf{motion}}(\boldsymbol{\xi})\ \mathrm{OTF}_{\mathsf{detector}}(\boldsymbol{\xi})\ \mathrm{OTF}_{\mathsf{optics}}(\boldsymbol{\xi})\ \mathrm{OTF}_{\mathsf{atmosphere}}(\boldsymbol{\xi})$$

- The FT of the image is the product of the system OTF and the FT of the object,

$$\mathrm{FT}_{\mathsf{image}}(\boldsymbol{\xi}) = \mathrm{OTF}_{\mathsf{system}}(\boldsymbol{\xi})\ \mathrm{FT}_{\mathsf{object}}(\boldsymbol{\xi})$$

- Image Display OTF and Human Visual System (HVS) OTF are omitted here.
- Image restoration algorithms use an estimate of $\mathrm{OTF}_{\mathsf{motion}}(\boldsymbol{\xi})$ and inverse filtering.
- $\boldsymbol{\xi} = \begin{bmatrix} \xi_x \\ \xi_y \end{bmatrix}$ is the 2-D spatial frequency, typically in lp/mm (line pairs per millimeter)

Single-Image Image Motion OTF

- The Image Motion OTF for a single image is

$$K(\boldsymbol{\xi}, t_0) = \frac{1}{T} \int_{t_0 - T/2}^{t_0 + T/2} \exp(i2\pi \boldsymbol{\xi}^T \boldsymbol{p}(t)) \, \mathrm{d}t$$

  where $\boldsymbol{\xi}$ is the 2D vector of spatial frequencies. [35, §3, §3.1]
- The image motion OTF $K(\boldsymbol{\xi}, t_0)$ depends on the image motion $\boldsymbol{p}(t)$ during a single exposure over the interval $\mathcal{I}(t_0)$.
- If an analytical form of $\boldsymbol{p}(t)$ is known, $K(\boldsymbol{\xi}, t_0)$ can in principle be computed analytically
- If $\boldsymbol{p}(t)$ is a stochastic process, the Statistical Image Motion OTF can be evaluated,

$$\begin{aligned} \mathrm{OTF}_{\mathsf{motion}}(\boldsymbol{\xi}) &= \mathcal{E}\{K(\boldsymbol{\xi}, t_0)\} \\ &= \mathcal{E}\left\{ \frac{1}{T} \int_{t_0 - T/2}^{t_0 + T/2} \exp(i2\pi \boldsymbol{\xi}^T \boldsymbol{p}(t)) \, \mathrm{d}t \right\} \end{aligned}$$

Numerically Computed IM OTF

- The motion OTF can be computed numerically from time-domain data (simulated or instrumentation – test or in-flight)
  - Direct estimation of motions: smear, smile, frown, sinusoidal, etc., and their OTFs.
  - Compute the 2D FT of the motion by integration and averaging.
  - Approximate PSF as a 2D histogram of the motion. Compute the 2D FT of the PSF.
  - Method of Moments.
- These numerical methods would have to be used with Monte Carlo simulation to obtain a statistical smear OTF, which is time-consuming and may not be practical.
- A numerically computed IM OTF could be used to cross-check the closed-form statistical IM OTF, derived next.
- Numerical methods to compute an IM OTF are used for verification.
  They do not help in writing pointing requirements based on an IM OTF allocation.

Numerically Computed IM OTF

- It is *incorrect* to compute the IM OTF in x and y separately, and then multiply them.
  - The smear OTF is *not separable* in x and y.
  - The jitter OTF is separable under a (unknown) coordinate transformation.
- The numerical estimate is evaluated over K, N, and a fine 2D grid of frequencies.

▲ It is difficult to compute the Image Motion OTF this way!

  - The numerical IM OTF requires significant computation, unless the number of frequency points and time points are small.
  - The required number of samples and the required sample rate are not clear.
  - Multirate contributions to $\boldsymbol{p}(t_n)$ require resampling.
  - This OTF calculation requires a lot of time-domain data, does not make use of temporal-frequency domain data, and does not reveal how pointing error sources contribute to the Image Motion OTF.

Numerically Computed IM OTF – Integration & Averaging (1/2)

- Compute the IM OTF from the spatial FT of image motion $\boldsymbol{p}(t)$.
  Use rectangular integration of $\exp(i2\pi\boldsymbol{\xi}^T\boldsymbol{p}(t))$ and averaging
  - Requires evaluation over a fine grid of frequencies and time average over many Monte Carlo realizations of the pointing motion. Involves significant computation.
  - The necessary number of samples and sample rate are not clear.
  - Multirate contributions to the image motion $\boldsymbol{p}(t)$ require resampling.
  - Does not make use of frequency domain data and does not reveal how error sources contribute to the Image Motion OTF.

Numerically Computed IM OTF – Integration & Averaging (2/2)

Before evaluating the statistical IM OTF, let's look at a numerical estimate based on time-domain samples of $\boldsymbol{p}(t)$, either measured or from a simulator.

- For $2N+1$ discrete samples $\boldsymbol{p}(t_n)$ in an exposure interval, numerical integration yields

$$H(\boldsymbol{\xi}, t_k) = \frac{1}{2N+1} \sum_{n=-N}^{N} \exp(-j2\pi \boldsymbol{\xi}^T \boldsymbol{p}(t_k + \alpha_n)) \,, \qquad \alpha_n \in \mathcal{I}(t_n)$$

- The expectation can be approximated by a Monte Carlo ensemble average. If $\boldsymbol{p}(t)$ is an ergodic process, use a time average from K intervals centered on centroid times t_k,

$$\begin{aligned} \mathrm{OTF}_{\mathsf{motion}}(\boldsymbol{\xi}) &\simeq \frac{1}{K} \sum_{k=0}^{K} H(\boldsymbol{\xi}, t_k) \\ &= \frac{1}{K(2N+1)} \sum_{k=0}^{K} \sum_{n=-N}^{N} \exp(-j2\pi \boldsymbol{\xi}^T \boldsymbol{p}(t_k + \alpha_n)) \,, \qquad \alpha_n \in \mathcal{I}(t_n) \end{aligned}$$

Numerically Computed IM OTF – Histogram Method

- The PSF (or LSF) can be computed by simulating the image motion (time domain).
  - Observation: The PSF and LSF are probability density functions (PDF)
  - Drop image motion points into the bins of a 2D (1D) histogram to approximate a PSF (LSF).
  - Compute the 2D (1D) Fourier Transform of the approximate PSF (LSF) to obtain an MTF.
- See the literature survey and Refs 10–15 in [35].

Numerically Computed IM OTF – Method of Moments

See Ref 16 in [35]

Expand the OTF in a Taylor series

$$\mathrm{OTF}(\omega) = \sum_{n=0}^{\infty} \frac{1}{n!} \left. \frac{\partial^n \mathrm{OTF}(\omega)}{\partial \omega^n} \right|_{\omega=0} \omega^n$$

$$\frac{\partial^n \mathrm{OTF}(\omega)}{\partial \omega^n} = \frac{\partial^n}{\partial \omega^n} \left. \int_{-\infty}^{\infty} \mathrm{LSF}(x) \exp(-j\omega x)\, \mathrm{d}x \right|_{\omega=0}$$

$$= (-j)^n \int_{-\infty}^{\infty} x^n \,\mathrm{LSF}(x)\, \mathrm{d}x$$

$$= \mathcal{E}\{x^n\} = m_n \qquad n\text{th order moment of } x$$

Numerically Computed IM OTF – Method of Moments (cont'd)

We can compute the nth moment m_n directly from $x(t)$

$$m_n = \mathcal{E}\{x^n\} = \frac{1}{T}\int_{t_a}^{t_a+T} x^n(t)\,\mathrm{d}t \simeq \frac{1}{M}\sum_{i=1}^{K} x_i^n$$

And finally the OTF can be approximated with a finite number of terms

$$\mathrm{OTF}(\omega) \simeq \sum_{n=0}^{N} \frac{m_n}{n!}\,(-j\omega)^n$$

Faster convergence if central moments are used ($m = m_0$ or $m = \frac{1}{2}[\max_i x_i + \min_i x_i]$)

$$M_n = \frac{1}{K}\sum_{i=1}^{K}(x_i - m)^n$$

$$\mathrm{OTF}(\omega) \simeq \exp(-j\omega m)\sum_{n=0}^{N} \frac{M_n}{n!}\,(-j\omega)^n$$

See the reference to calculate the truncation error and for other details.

3. Statistical Image Motion OTF (IM OTF) (outline)

- Motivation to derive a statistical smear OTF
- Derive statistical Image Motion OTFs for
  - shift (displacement, offset)
  - smear
  - jitter
  - sinusoidal/harmonic motion
- Illustrate the IM OTFs
  - parameterization in terms of Pointing Metrics (PM)
  - characterization, frequency response
  - compare to deterministic image motion OTFs
  - derive a statistical smear line spread function (LSF)
- Summary Table of Image Motion OTFs and LSF

Motivation for a Statistical Smear OTF

- Numerical methods to evaluate the PSF/IM-OTF are arduous and less informative.
- Smear specifications have been based on the deterministic smear OTF (sinc function).
  - Deterministic smear OTF applies to individual images with known smear length.
- Specifications for deterministic smear are traditionally based on a known or specified upper bound, or based on a 2σ or 3σ smear length.
  - 2σ is typically specified. 3σ is too conservative. Upper bound may not be known.
  - Can lead to margin on top of margin. (Margin is included in the OTF budget and in a pointing budget)

Motivation for a Statistical Smear OTF (cont'd)

- Statistical smear OTF describes the *average smear* effect of an ensemble of images or on a single image with *a priori* unknown but random smear.
  - A *statistical* description of the Image Motion OTF for random smear is more useful than the deterministic smear OTF.
  - A *statistical* description of the Image Motion OTF for sinusoidal motion is related to both the statistical smear OTF and the jitter OTF.
- Smear should not be lumped in with jitter.
  - Smear and jitter affect image quality differently.
  - Pointing error metrics prior to 2012 modeled jitter with smear included. *Smear and jitter are now separated.*

Statistical Image Motion OTF (IM OTF)

- For $\alpha = t - t_0 \in [-T/2,\, T/2]$ we have

$$\exp(i2\pi\boldsymbol{\xi}^T\boldsymbol{p}(t)) = \exp(i2\pi\boldsymbol{\xi}^T\left[\,\boldsymbol{p}_o + \alpha\boldsymbol{v}_o + \boldsymbol{\psi}_o(\alpha)\,\right])$$

$$= \underbrace{\exp(i2\pi\boldsymbol{\xi}^T\boldsymbol{p}_o)}_{\text{displacement}}\ \underbrace{\exp(i2\pi\boldsymbol{\xi}^T\alpha\boldsymbol{v}_o)}_{\text{smear}}\ \underbrace{\exp(i2\pi\boldsymbol{\xi}^T\boldsymbol{\psi}_o(\alpha))}_{\text{jitter}}$$

- $\boldsymbol{p}_o$, $\boldsymbol{v}_o$, and $\boldsymbol{\psi}(\alpha)$ are independent random variables (more on this later)
- The **Statistical Image Motion OTF** is the time-average of $\mathcal{E}\left\{\,\exp(i2\pi\boldsymbol{\xi}^T\boldsymbol{p}(t))\,\right\}$

$$\mathrm{OTF}_{\mathsf{motion}}(\boldsymbol{\xi}) = \underbrace{\mathrm{OTF}_{\mathsf{D}}(\boldsymbol{\xi})}_{\text{displacement}}\ \underbrace{\mathrm{OTF}_{\mathsf{S}}(\boldsymbol{\xi})}_{\text{smear}}\ \underbrace{\mathrm{OTF}_{\mathsf{J}}(\boldsymbol{\xi})}_{\text{jitter}}$$

- The image motion OTF for Gaussian random motion is the well known jitter OTF.

Statistical Smear OTF

$$\mathrm{OTF}_{\mathsf{S}}(\boldsymbol{\xi}) = \frac{\sqrt{\pi}}{2q}\,\exp(-r^2)\,\Re(\mathrm{erfz}(q+ir))$$

$$q^2 = \frac{1}{2}\pi^2\boldsymbol{\xi}^T\boldsymbol{\Sigma}_{\mathsf{S}}\boldsymbol{\xi}\,, \qquad r^2 = \frac{(\boldsymbol{\xi}^T\boldsymbol{s})^2}{2\boldsymbol{\xi}^T\boldsymbol{\Sigma}_{\mathsf{S}}\boldsymbol{\xi}}$$

$\mathrm{erfz}(\cdot)$ is the complex error function (often denoted erf)

$\Re(\cdot)$ is the real part of its complex argument

- $\mathrm{OTF}_{\mathsf{S}}(\boldsymbol{\xi})$ is **not separable** in the two coordinates.
- The statistical smear OTF is the expected value (ensemble average) of the deterministic smear OTF when the smear is random.
- The deterministic smear OTF applies to individual images with known smear. The statistical smear OTF describes the average effect of random smear on many images.

Statistical Smear OTF – 2D Illustrations

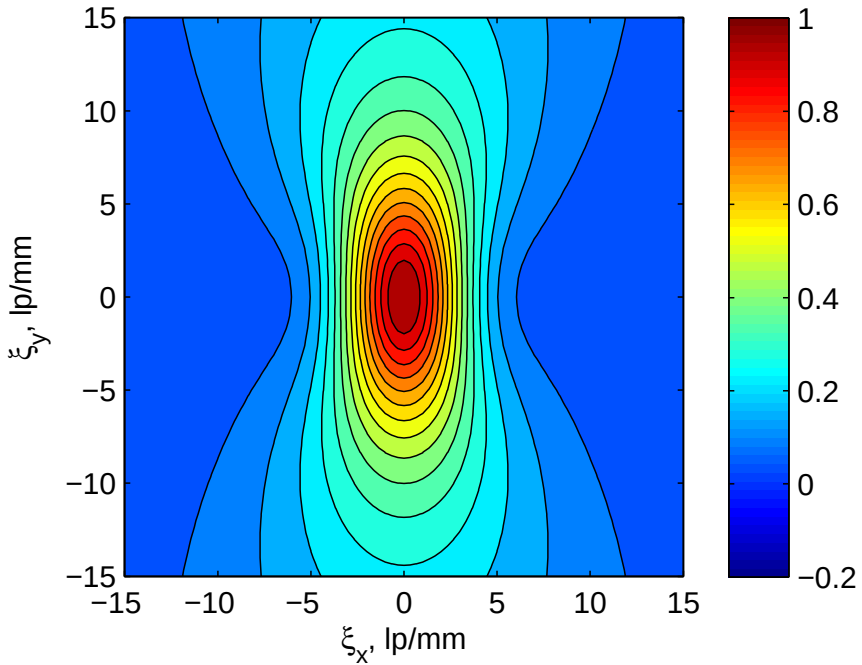

$s_x = 0.2,\ s_y = 0$ mm

$\sigma_x = \sigma_y = 0.1$ mm, $\sigma_{xy} = 0$

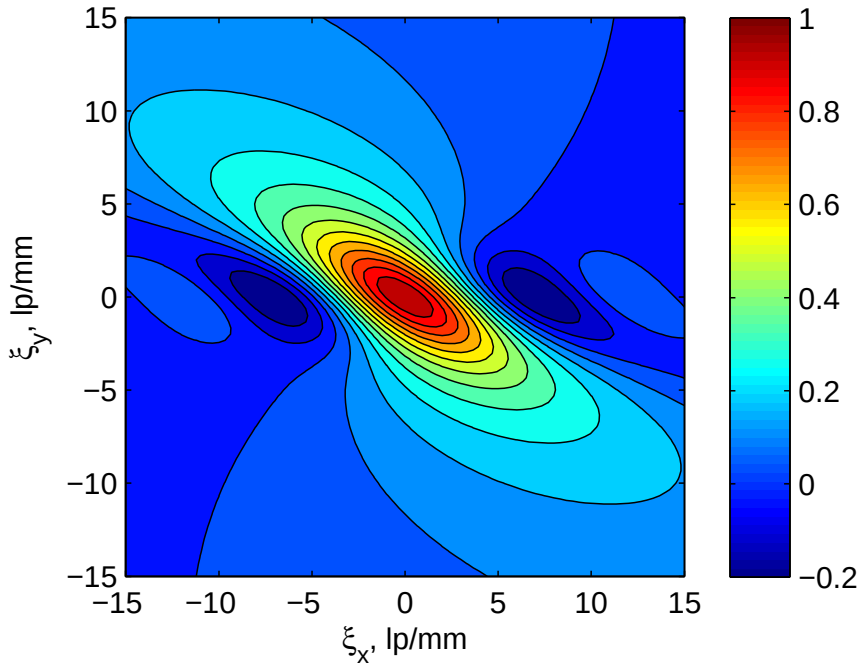

$s_x = s_y = 0.2$ mm

$\sigma_x = 0.02,\ \sigma_y = 0.2$ mm, $\sigma_{xy} = 0$

Contour plots of statistical smear OTF (in two dimensions of spatial frequency)

Statistical Smear OTF – 1D Illustrations

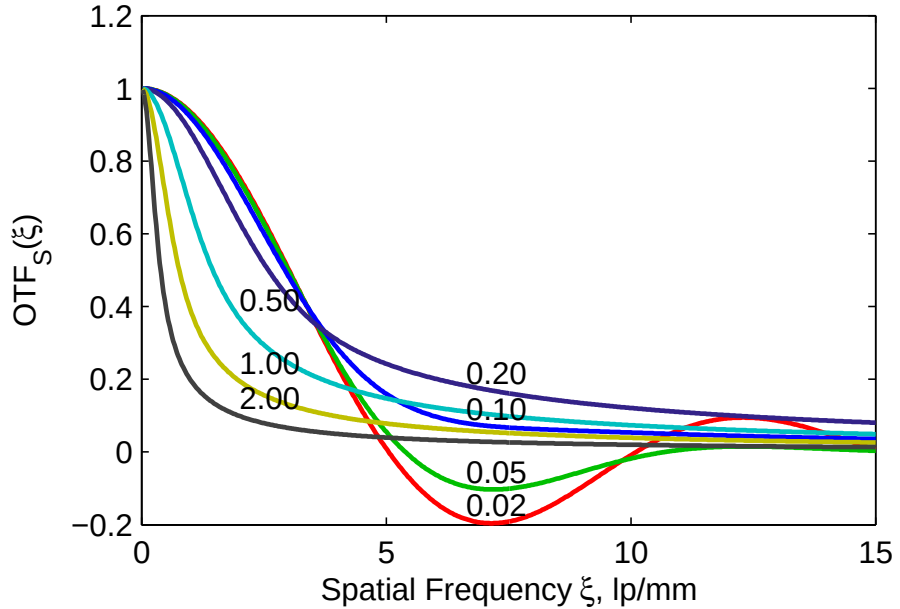

Mean smear $s = 0.2$ mm

Smear dispersion σ_S ranging from 0.02 to 2.0 mm

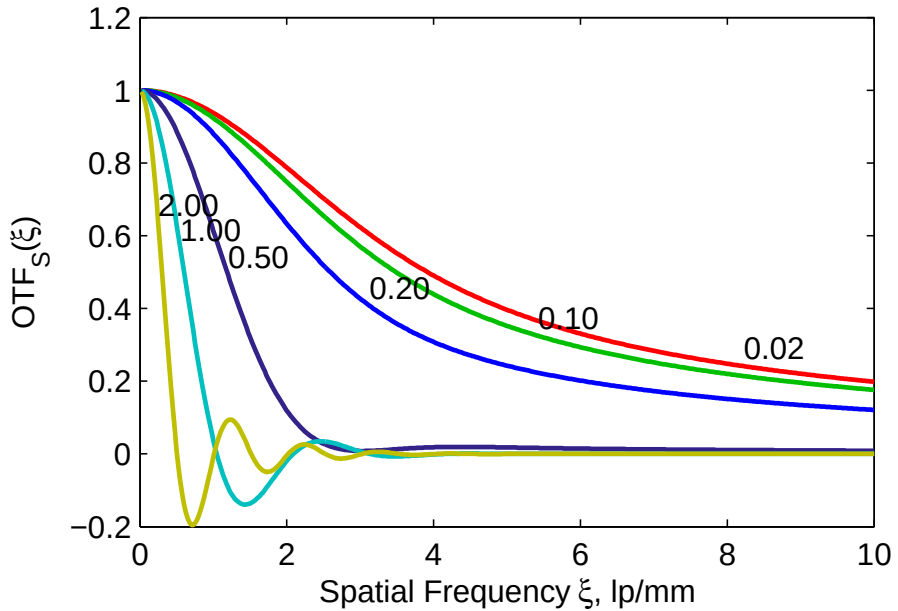

Smear dispersion $\sigma_S = 0.2$ mm

Mean smear s ranging from 0.02 to 2.0 mm

Statistical smear OTF (in one dimension of spatial frequency)

Statistical Smear OTF – Limiting Cases

Statistical Smear OTF, $s = 0$

$$\mathrm{OTF}_{\mathsf{S}}(\boldsymbol{\xi}) = \frac{\sqrt{\pi}}{2q}\,\mathrm{erf}(q)$$

$$q^2 = \frac{1}{2}\pi^2 \boldsymbol{\xi}^T \boldsymbol{\Sigma}_{\mathsf{S}} \boldsymbol{\xi}$$

Deterministic Smear OTF, $\boldsymbol{\Sigma}_{\mathsf{S}} = \mathbf{0}$

$$\mathrm{OTF}_{\mathsf{S}}(\boldsymbol{\xi}) = \exp(-r^2)\,\mathrm{erfz}(ir)$$

$$\mathrm{OTF}_{\mathsf{SD}}(\boldsymbol{\xi}) = \mathrm{sinc}(\pi \boldsymbol{\xi}^T \boldsymbol{s})$$

$$\mathrm{MTF}_{\mathsf{SD}}(\boldsymbol{\xi}) = \left|\,\mathrm{sinc}(\pi \boldsymbol{\xi}^T \boldsymbol{s})\,\right|$$

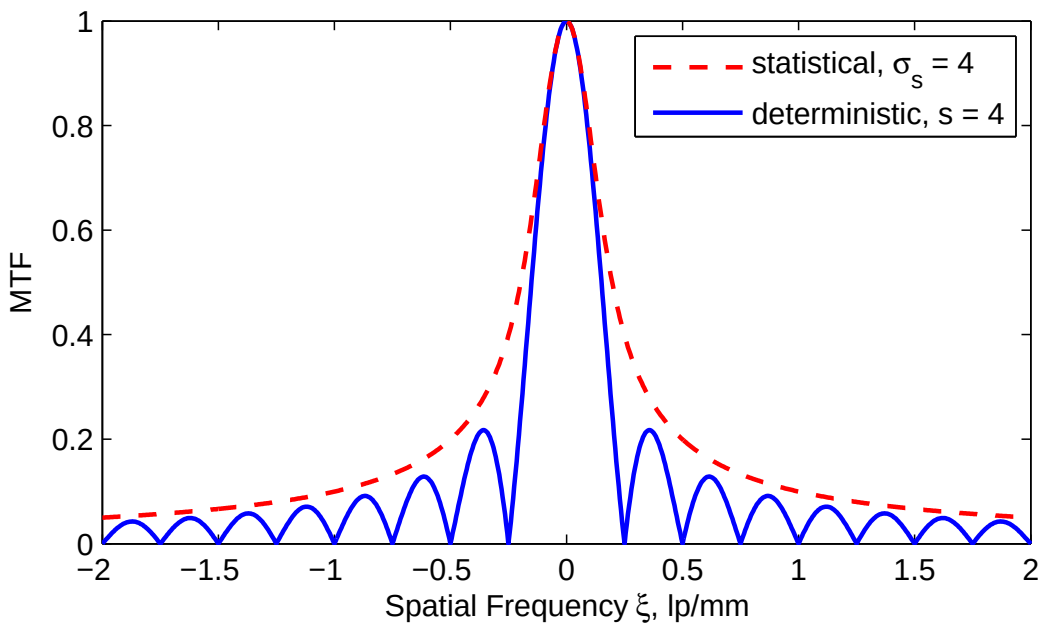

$\mathrm{MTF}_{\mathsf{S}}(\boldsymbol{\xi})$ with $s = 0$, $\sigma_s = 4$ (red dash line)

$\mathrm{MTF}_{\mathsf{SD}}(\boldsymbol{\xi})$ with $s = 4$, $\sigma_s = 0$ (solid blue line)

A worst case deterministic s corresponds to $1\sigma_{\mathsf{s}}$ (not $2\sigma_{\mathsf{s}}$ or $3\sigma_{\mathsf{s}}$) !

Optical engineers have used $s = 2\sigma_{\mathsf{s}}$ in the deterministic smear OTF, $\mathrm{OTF}_{\mathsf{S}}(\boldsymbol{\xi})$

Deterministic and Statistical Smear LSF

The **Deterministic Smear LSF** is a boxcar function, length $s = |\boldsymbol{s}| = |\boldsymbol{v}T|$, height $1/s$

$$\mathrm{LSF}_{\mathsf{SD}}(x) = \begin{cases} 1/s & |x| < s/2 \\ 0.5/s & |x| = s/2 \\ 0 & |x| > s/2 \end{cases}$$

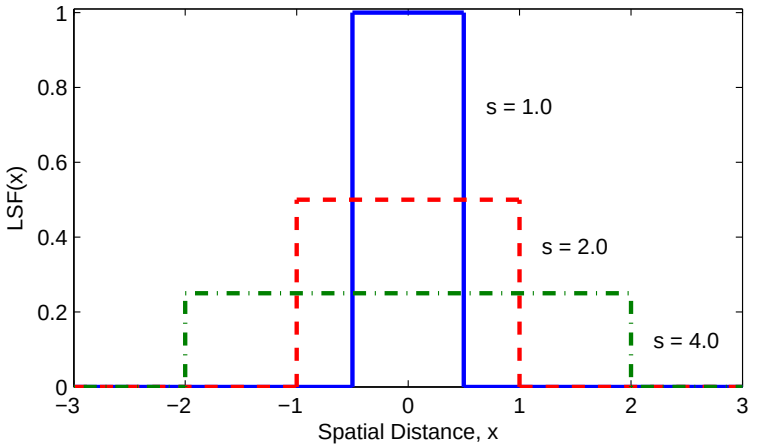

The **Statistical Smear LSF** is an ensemble average of Gaussian random boxcar functions.

$$\mathrm{LSF}_{\mathsf{S}}(x) = \frac{1}{\sigma_{\mathsf{S}}\sqrt{2\pi}}\left[-\mathrm{Ei}(-2(x/\sigma_{\mathsf{S}})^2)\right]$$

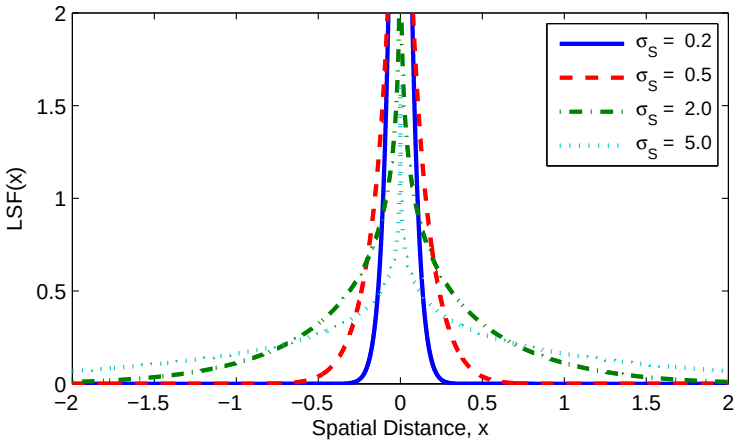

Gaussian Jitter PSF

The **Gaussian Jitter PSF** is due to Gaussian random motion.

The Gaussian PSF is

$$\mathrm{PSF}_{\mathsf{J}}(x) = \frac{1}{2\pi|\boldsymbol{\Sigma}_{\mathsf{J}}|}\exp\left(-\frac{1}{2}\boldsymbol{x}^T\boldsymbol{\Sigma}_{\mathsf{J}}^{-1}\boldsymbol{x}\right)$$

By the Central Limit Theorem, a sum of many independent random motions of various distributions approximates a Gaussian.

For random motion to qualify as jitter, its coherence time must be much shorter than the exposure time.

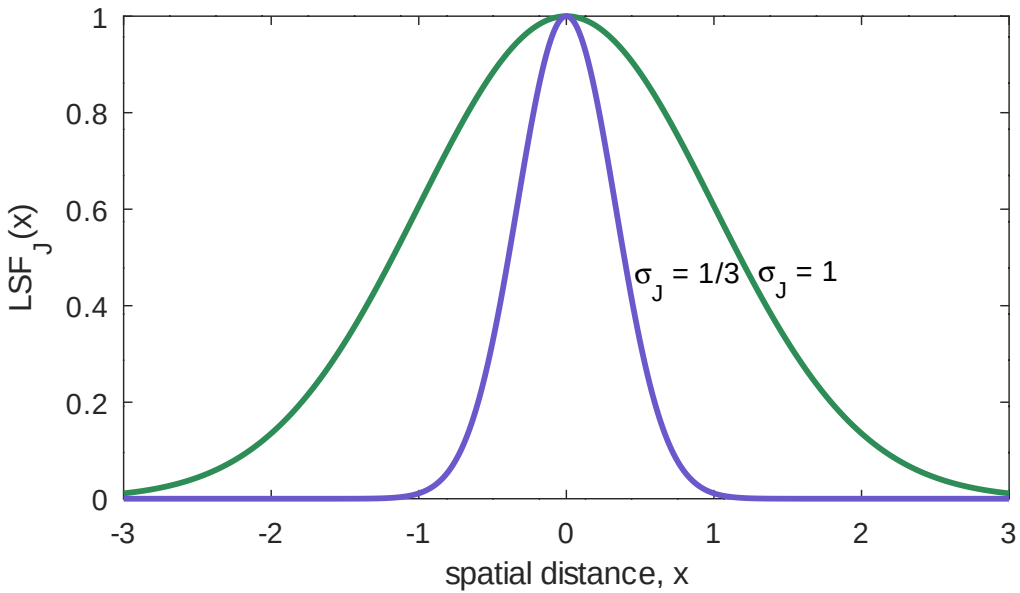

The jitter LSF here is a 1D cross section of the 2D PSF.

LSFs are shown for $\sigma_{\mathsf{J}} = 1$ and $\sigma_{\mathsf{J}} = 1/3$.

Statistical Jitter OTF

The **Statistical Jitter OTF** is the FT of the Gaussian PSF.

The Gaussian Jitter OTF is

$$\mathrm{OTF}_{\mathrm{J}}(\boldsymbol{\xi}) = \exp\left(-2\pi^2 \boldsymbol{\xi}^T \boldsymbol{\Sigma}_{\mathrm{J}} \boldsymbol{\xi}\right)$$

By the Central Limit Theorem, a sum of many independent random motions of various distributions approximates a Gaussian.

For random motion to qualify as jitter, its coherence time must be much shorter than the exposure time.

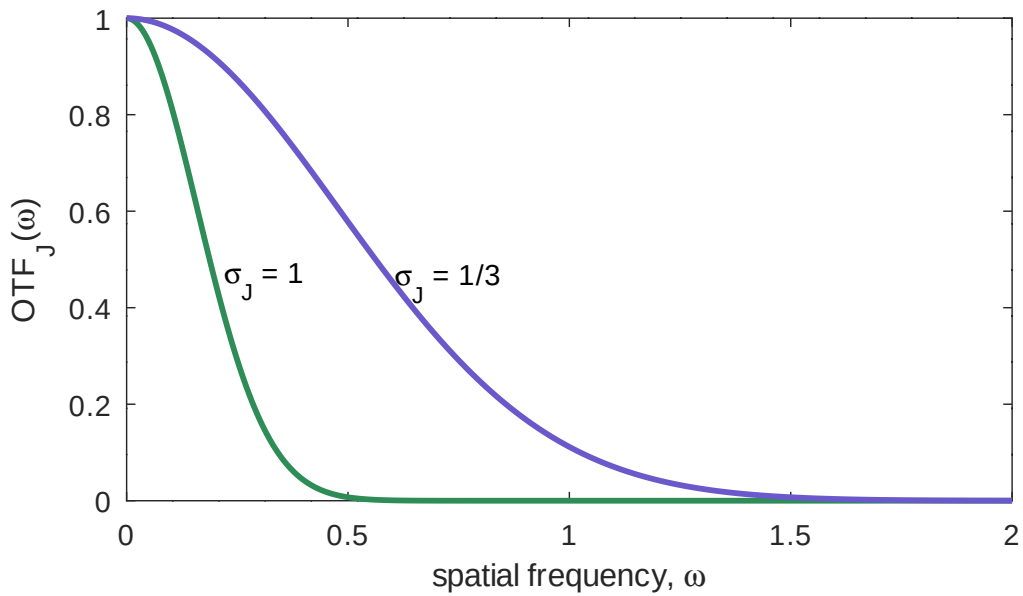

The jitter OTF here is a 1D cross section of the 2D PSF

OTFs are shown for $\sigma_{\mathrm{J}} = 1$ and $\sigma_{\mathrm{J}} = 1/3$.

Statistical Smear and Jitter OTF Comparison

Statistical Smear OTF, $s = 0$

$$\mathrm{OTF}_{\mathsf{S}}(\boldsymbol{\xi}) = \frac{\sqrt{\pi}}{2q}\,\mathrm{erf}(q)$$

$$q^2 = \frac{1}{2}\pi^2 \boldsymbol{\xi}^T \boldsymbol{\Sigma}_{\mathsf{S}} \boldsymbol{\xi}$$

Statistical Jitter OTF

$$\mathrm{OTF}_{\mathsf{J}}(\boldsymbol{\xi}) = \exp\left(-2\pi^2 \boldsymbol{\xi}^T \boldsymbol{\Sigma}_{\mathsf{J}} \boldsymbol{\xi}\right)$$

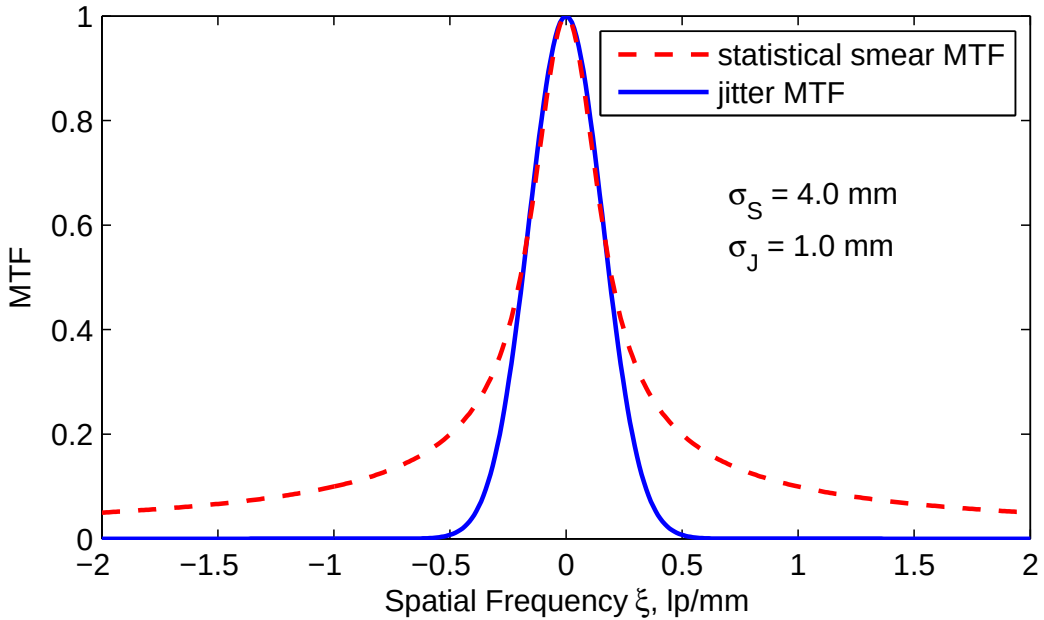

- The jitter OTF is **not separable** in the two coordinates, except for a coordinate trans.
- In this example, smear and jitter pointing error almost equal, $\sigma_{\mathsf{S}}/\sqrt{12} \simeq 1.15 \sim \sigma_{\mathsf{J}}$
- The statistical smear MTF is larger at higher spatial frequencies than the jitter MTF.
- Empirical evidence has shown that imaging systems tolerate smear better than jitter.

Harmonic Motion LSF

1D harmonic motion

$$p(t) = d \sin \omega t$$

The velocity is

$$v(t) = \omega d \cos \omega t$$

Exposure $I(p)$ is inversely proportional to velocity

$$I(p) = \frac{A}{v} = \frac{A}{\omega d \cos \omega t} = \frac{1}{d\pi \sqrt{1 - (p/d)^2}}$$

We choose $A = \omega d$ so that $\int_{-d}^{d} I(p)\,\mathrm{d}p = 1$.

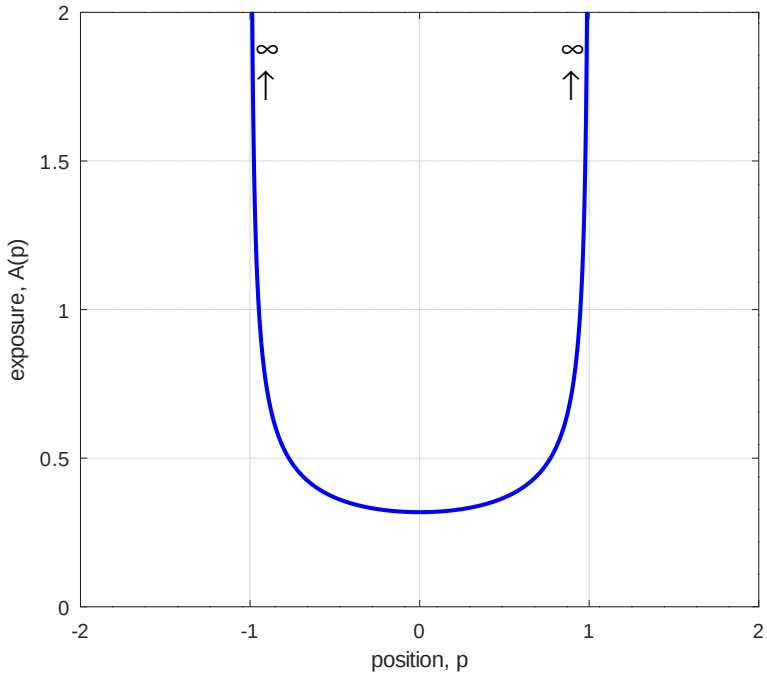

Line Spread Function (LSF) for harmonic motion, $d = 1$

Harmonic Motion OTF (1/2)

- Suppose the image motion is due only to m cycles of a single-frequency vibration of amplitude d $(= a/2)$ along one direction during the exposure period T.

$$p(t) = d\sin(\omega t)\,, \quad T = \frac{2\pi m}{\omega}\,, \quad m = \frac{\omega T}{2\pi}$$

  - If m is an integer, the image motion OTF is a Bessel function [23, 24]

$$\mathrm{OTF}_{\mathsf{H}}(\xi) = J_0(2\pi\xi d) \quad \text{for integral } m$$

  - If m is not an integer, then [24, 25]

$$\mathrm{OTF}_{\mathsf{H}}(\xi) \to J_0(2\pi\xi d) \quad \text{as} \quad m \to \infty$$

- Single-frequency sinusoidal vibration with 0 to 2 cycles (and fractional cycles) and various phase angles is analyzed in [25].

Harmonic Motion OTF (2/2)

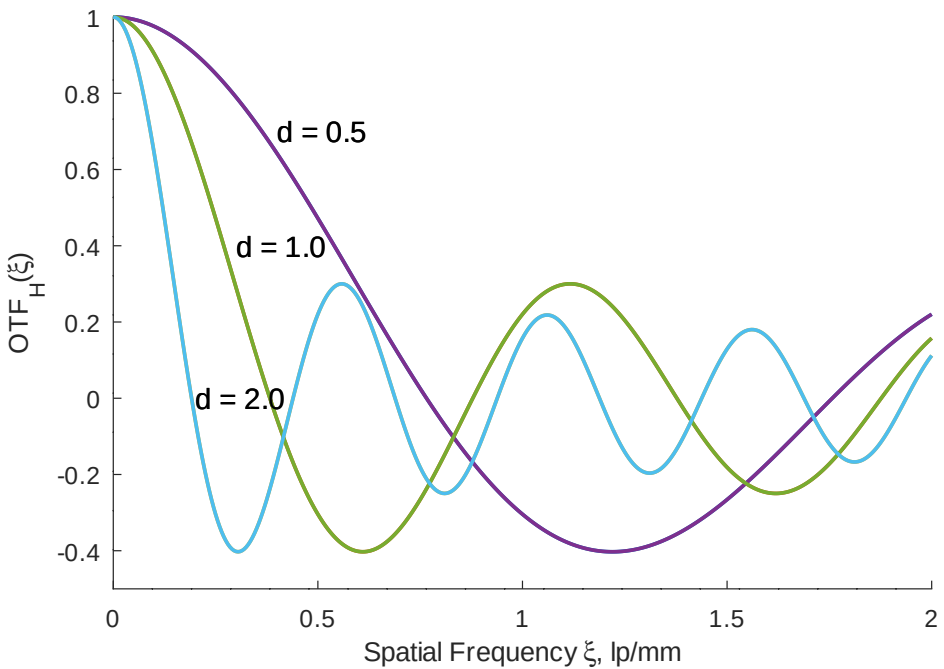

Harmonic OTF for sinusoidal amplitudes
$d = 0.5,\ 1,\ 2$ **lp/mm**

Unpublished numerical results:

- The average $\mathrm{OTF}_{\mathsf{H}}$ for one sinusoid with Gaussian random amplitude d, $\sigma_d = (s/2)/\sqrt{2}$, is nearly $\mathrm{OTF}_{\mathsf{S}}$.
- The $\mathrm{OTF}_{\mathsf{H}}$ for a sum of $n \gtrsim 3$ sinusoids with r.m.s. amplitude $(s/2)/\sqrt{2}$ is $\mathrm{OTF}_{\mathsf{J}}$ with $\sigma_j = s/4$.
- Is the harmonic OTF separable from the statistical smear OTF ?
  (They may be tangled together in an integrand when computing the time average OTF.)

Summary of Image Motion OTFs and LSF

Displacement OTF	deterministic	$\mathrm{OTF}_{\mathsf{D}}(\boldsymbol{\xi}) = \exp(-i2\pi\boldsymbol{\xi}^T\boldsymbol{\mu})$
Smear OTF	statistical	$\mathrm{OTF}_{\mathsf{S}}(\boldsymbol{\xi}) = \dfrac{\sqrt{\pi}}{2q}\,\exp(-r^2)\,\Re(\mathrm{erfz}(q+ir))$ $q^2 = \frac{1}{2}(\pi T)^2\boldsymbol{\xi}^T\boldsymbol{\Sigma}_{\mathsf{R}}\boldsymbol{\xi} = \frac{1}{2}\pi^2\boldsymbol{\xi}^T\boldsymbol{\Sigma}_{\mathsf{S}}\boldsymbol{\xi}$ $r^2 = \dfrac{(\boldsymbol{\xi}^T\boldsymbol{\rho})^2}{2\boldsymbol{\xi}^T\boldsymbol{\Sigma}_{\mathsf{R}}\boldsymbol{\xi}} = \dfrac{(\boldsymbol{\xi}^T\boldsymbol{s})^2}{2\boldsymbol{\xi}^T\boldsymbol{\Sigma}_{\mathsf{S}}\boldsymbol{\xi}}$
Smear OTF	statistical, $\boldsymbol{s}=\mathbf{0}$	$\mathrm{OTF}_{\mathsf{S}}(\boldsymbol{\xi}) = \dfrac{\sqrt{\pi}}{2q}\,\mathrm{erf}(q)$
Smear OTF	deterministic, $\boldsymbol{\Sigma}_{\mathsf{S}}=\mathbf{0}$	$\mathrm{OTF}_{\mathsf{S}}(\boldsymbol{\xi}) = \mathrm{sinc}(\pi\boldsymbol{\xi}^T\boldsymbol{s})$
Smear LSF (1D)	statistical, $\boldsymbol{s}=\mathbf{0}$	$\mathrm{LSF}_{\mathsf{S}}(x) = \dfrac{1}{\sigma_{\mathsf{S}}\sqrt{2\pi}}\left[-\mathrm{Ei}(-2(x/\sigma_{\mathsf{S}})^2)\right]$
Jitter OTF	statistical	$\mathrm{OTF}_{\mathsf{J}}(\boldsymbol{\xi}) = \exp\!\left(-2\pi^2\boldsymbol{\xi}^T\boldsymbol{\Sigma}_{\mathsf{J}}\boldsymbol{\xi}\right)$
Harmonic OTF	deterministic	$\mathrm{OTF}_{\mathsf{H}}(\xi) = J_0(2\pi\xi d)\,, \quad p(t) = d\sin(\omega t)$

4. A New Paradigm for V&V of System Performance

- The Statistical IM OTFs measure average OTF/WTF* performance and are useful for requirements definition and verification.
- The Statistical IM OTFs and Pointing Performance Metrics** (PPMs), along with a methodology and procedures to evaluate the PPMs, enable a multidisciplinary and integrated design and analysis methodology (or paradigm) to couple optical (payload) engineering with mechanical and control systems (bus) engineering.
- It does not purport to automatically or completely replace other established methodologies for performance analysis, including the use of well-known deterministic IM OTF/WTF, but augments our portfolio of methodologies.

* A Statistical Wavefront Transfer Function (WTF) has not yet been developed.

** "Pointing Error Metrics" (PEM) is a misnomer in the context of Image Motion. It seems appropriate to call them Pointing Metrics (PMs). Pointing Performance Metrics (PPMs) can refer to the IM OTFs or the PMs.

Part 3: Requirements Definition, Flow Down, Interfaces, Model Updates

Requirements Definition, Flow Down, Interfaces, Model Updates

- Requirements Validation & Verification
- What is the Pointing Requirements Definition Process?
- Where does a Pointing Requirement apply?
- Payload-Bus Interfaces
- Pointing, More Generally
- How does the New Paradigm fit into the Real World?
- Image Motion MTF Allocation from an MTF budget
- OTF, IM OTF, and Pointing Requirements Definition
- Optical Model Availablity, Fidelity, and Updates

Requirements Validation & Verification [11, §4]

Definitions

- Validation and validate mean to show that something is appropriate to a purpose.
- Verification and verify mean to show that something performs as intended.

Document Rationale for the Requirements

- Reason for the Requirement
- Relationships (to expected operations, conops)
- Assumptions
- Constraints

Valid Technical Performance Requirements

- Written Correctly
- Technically Correct
  (traceable, valid assumptions, essential)
- Satisfy Stakeholders
- Complete
- Feasible (achievable)
- Verifiable
- Consistent (not ambiguous or conflicting)
- Unique (not redundant)
- Necessary (not over-specified)

What is the Pointing Requirements Definition Process?

- Discuss current practice and compare with the New Paradigm.
- Pointing performance requirements are derived from optical performance requirements.
  - How? By whom? [Mission scientists, CONOPS, MRD, Optical or Systems Engr]
  - What assumptions are made?
  - [How] is image motion allocated from an image performance requirement?
  - [How] is a pointing requirement derived from an image motion requirement?
  - Can the pointing requirement *and* image motion allocation be verified?
- It should be understood that a pointing requirement, however stated, *may be verifiable, but may not verify the image motion allocation to the image performance requirement.*
  - Image motion effects depend on characteristics of the pointing motion.
  - The pointing requirements may not indicate true image performance, or may be too conservative, thus incurring risk to performance, cost, and schedule.

Where does a Pointing Requirement apply?

- Pointing requirements are referred to some physical interface between the bus and payload. Definitions vary . . .
  - pointing defined by a LOS fixed to some mechanical reference frame
  - designated body-fixed (bus) coordinate frame defined for attitude determination
  - coordinate frame defined at the bus-payload mechanical interface, with one axis (notionally) aligned to an optical boresight axis
  - optical system boresight axis, defined externally
  - optical system focal plane, geometric camera model, simple or complex
- Coordinate frame definitions can be important to in-flight alignment calibration. Intermediate body-fixed frames are not observable.
- Image motion may be evaluated by optical system engineers, separately from GN&C, but they need particular data to do so.

Payload–Bus Interfaces

- Separate payload and bus structural model:
  - requirements may include forces and torques or displacements and rates
  - LOS pointing established at the payload-bus interface for GN&C pointing analysis
- Combined payload and bus structural model:
  - structural damping and frequencies can be much different in separate structures than in a combined structure
  - bus and optical payload structural models are updated periodically, usually not at the same time or same frequency

Pointing, More Generally

- Think of "Pointing" in a more abstract sense.
  - Pointing is not the orientation of a single element, but of a collection of elements along an optical path from detector to target, including the detector.
  - Pointing motion is not the motion of a single element, but the motion of elements along an optical path from detector to target, including motion of the detector.
  - LOS Pointing can be defined as a ray from the perspective center of the optical detector to a point on a target.
- Image motion is computed from structural motion and a geometric camera model.
  - Equivalent to STOP analysis. STOP analysis uses optical element displacements and ray tracing to obtain PSF motion and WFE (distortion) in the time-domain.
  - The image motion OTF is the spatial frequency-domain equivalent.
  - The image motion OTFs are analytical forms that are useful to define performance requirements and to evaluate performance.

How does the New Paradigm fit into the Real World?

The practical utility of the New Paradigm may be fairly questioned

- Who uses it?
- Will the methodology be accepted across NASA programs? How do we encourage it?
- If we put it into a Pointing Guidelines Handbook, will it be ignored?
- The New Paradigm seems to require a high-fidelity geometric camera model. Is it practical to base pointing requirements on it?
- How does the New Paradigm work with established inter-disciplinary and multi-disciplinary processes?
- Is the New Paradigm supported by established processes?

We have to examine the current requirements definition and verification processes to find out how requirements are derived from optical payload performance requirements.

Image Motion OTF Complements Traditional STOP Analysis

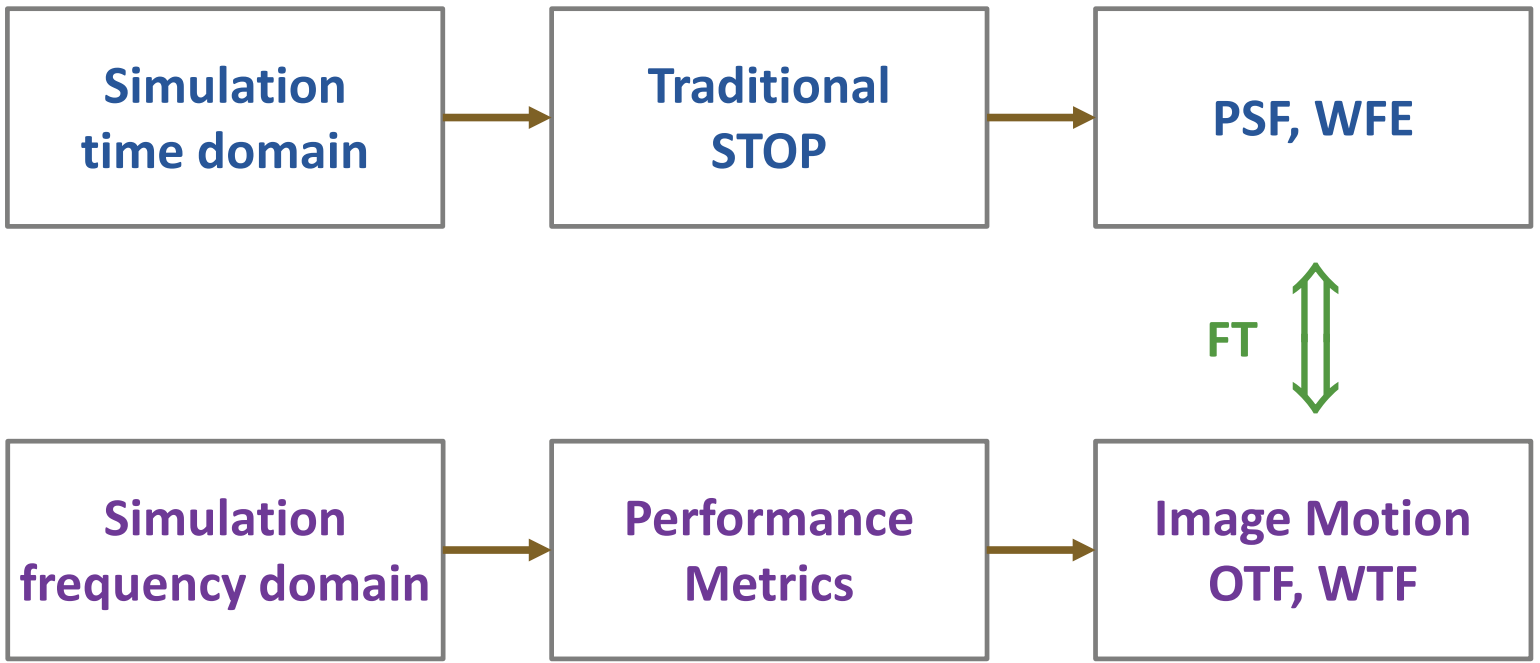

- Frequency domain analysis has an advantage of speed, and often accuracy, over time-domain analysis

Image Motion OTF Allocation from an MTF budget

- Optical engineers derive pointing requirements from an Image Motion allocation from a system OTF.
- Image Motion MTF results from various motions: displacement, smear, smile, frown, harmonic, jitter.
- These motion effects may be removed, to some extent, from an image in post-processing, provided sufficient detail exists in the image.
- A fast steering mirror (FSM) can remove some image motion, but introduces other optical problems.

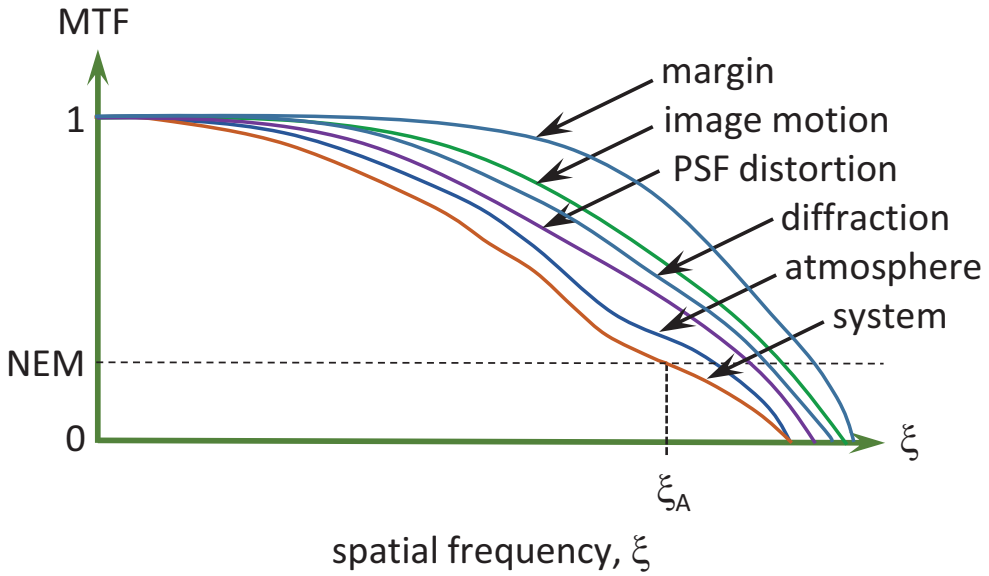

- MTFs are multiplied, not added!
- The optical system MTF is the product of contributing MTF effects.
- The system MTF includes plenty of margin.

IM OTF and Pointing Requirements Definition

- Image Motion OTFs provide a direct connection between imaging performance and pointing performance
  - derive pointing requirements from an IM OTF requirement (inverse problem)
  - evaluate the IM OTF from pointing performance (forward problem)
- Requirement allocation from an imaging system OTF to Pointing Metrics (PMs)
  1. The IM OTF is an allocation from the imaging system OTF (negotiable?)
  2. The IM OTF is allocated to OTF_D, OTF_S, OTF_J (non-obvious tradeoff)
  3. Derive requirements on the Pointing Metrics (PM) $\boldsymbol{\mu}$, $\boldsymbol{\rho}$ or $\boldsymbol{s}$, $\boldsymbol{\Sigma}_\mathsf{D}$, $\boldsymbol{\Sigma}_\mathsf{S}$, $\boldsymbol{\Sigma}_\mathsf{J}$ from requirements on OTF_D, OTF_S, OTF_J. (may be difficult for OTF_S)

▷ Inverse Problem (Pointing requirements from IM OTF) is traditional, but not necessary.
▷ The Forward Problem is easier (compute the IM OTFs from an image motion analysis).
▷ The allocations in 1 and 2 are not likely to be negotiable, particularly after they are set.

OTF and IM OTF Requirements Definition (cont'd)

- *OTFs are multiplied, not added!*
  - OTF margins are not linear-additive and they vary with spatial frequency.
    - $-\log(\text{OTF margin})$ can be added, but varies with spatial frequency.
  - The Inverse Problem is difficult for these two reasons (nonlinear, frequency varying).
    - Also there may be no closed form for the inverse of $\mathrm{OTF}_{\mathrm{S}}(\boldsymbol{\xi})$.
  - The Forward Problem is much easier.
- MTF Area (MTFA) and spatial bandwidth (the spatial frequency where the OTF crosses the NEM) may lead to a useful inverse solution.
- Some work is needed to specify the inverse, in consultation with optical engineers.
  - For now, solve the Forward Problem to see if a design meets an IM OTF requirement.

Can the PPM Requirements be Validated and Verified?

For PPM requirements to be valid, they must align with reality:

- Are the requirements linking the optical subsystem and the pointing control subsystem supported by organizational and contractual interfaces?
- Can the required Pointing Performance Metrics be validated? What are the technical, contractual, and organizational limitations?
- Is a geometric optical model available? Do we have, or will we have, an Image Motion and Wavefront Error sensitivity model? When will the models be available?
- How often will the models updated, and how accurate are they expected to be?
- Will the optics and bus structural models be coupled or uncoupled?

Optical Model Availability

- The geometric optical model is just a function (a matrix) that maps displacements and motions of structural elements to image motion.
- Motion in the optical path and image motion can be evaluated by GN&C, provided that a geometric optical model and structural model are available.
- There is usually an initial baseline or reference design for a camera
  - Optical sensor performance requirements are defined by mission scientists and stated in an MRD, *usually well in advance of a bus design.*
  - The baseline or reference design for an optical sensors is often an existing design.
  - Rarely is there no information about an optical payload.
- Optical system error budgets and allocations are made at the outset of a design.
  - Allocations may be adjusted as the optical system design proceeds.
  - The image motion allocation is fixed once the MRD is written and RFP is issued.

Optical Model Fidelity

- A geometric optical model could range from a simple pinhole model to a full geometric optical model with structural displacements modeled, depending on
  - the level pf performance required
  - program cost and schedule
  - class of spacecraft
  - design timeline and phases of design
  - ability to update structural models
  - contractual and organizational constraints
- Model fidelity and uncertainty are always of concern, *regardless of whether pointing performance requirements are traditional or based on image motion OTFs.*
- The performance evaluation tool chain should permit rapid re-evaluation as payload and bus structural model updates become available.

No Optical Model Available

- In some situations an optical model is not available or can't be used because either
  - The optical system has not yet been designed, behind schedule, not released, or
  - The pointing requirements are at the optical payload-bus mounting interface,
  - Contractual or proprietary reasons, or programmatic or institutional reasons.
  - The instrument designer can't give it to the control system designer for security reasons (if the optical system and its pointing performance are SCI).
- In any of these situations, there are ways to proceed. (discussed later)

Part 4: Pointing Performance Analysis

Pointing Performance Analysis

- Controller, Dynamics, Disturbance, and Noise modeling and analysis
- Pointing Performance Metrics
- Methods to compute the Pointing Performance Metrics (Covariance Matrices $\mathbf{\Sigma}_X$)
  - Frequency response
  - Lyapunov equation
  - Time response (2 methods)
- Optical sensor (Camera, Telescope) models, sensitivity models
- Relative and cumulative contribution from disturbance sources
  - worst offenders
  - sensitivities
- What to do If Pointing Requirements are not Met

1. Pointing Motion Model and Pointing Performance

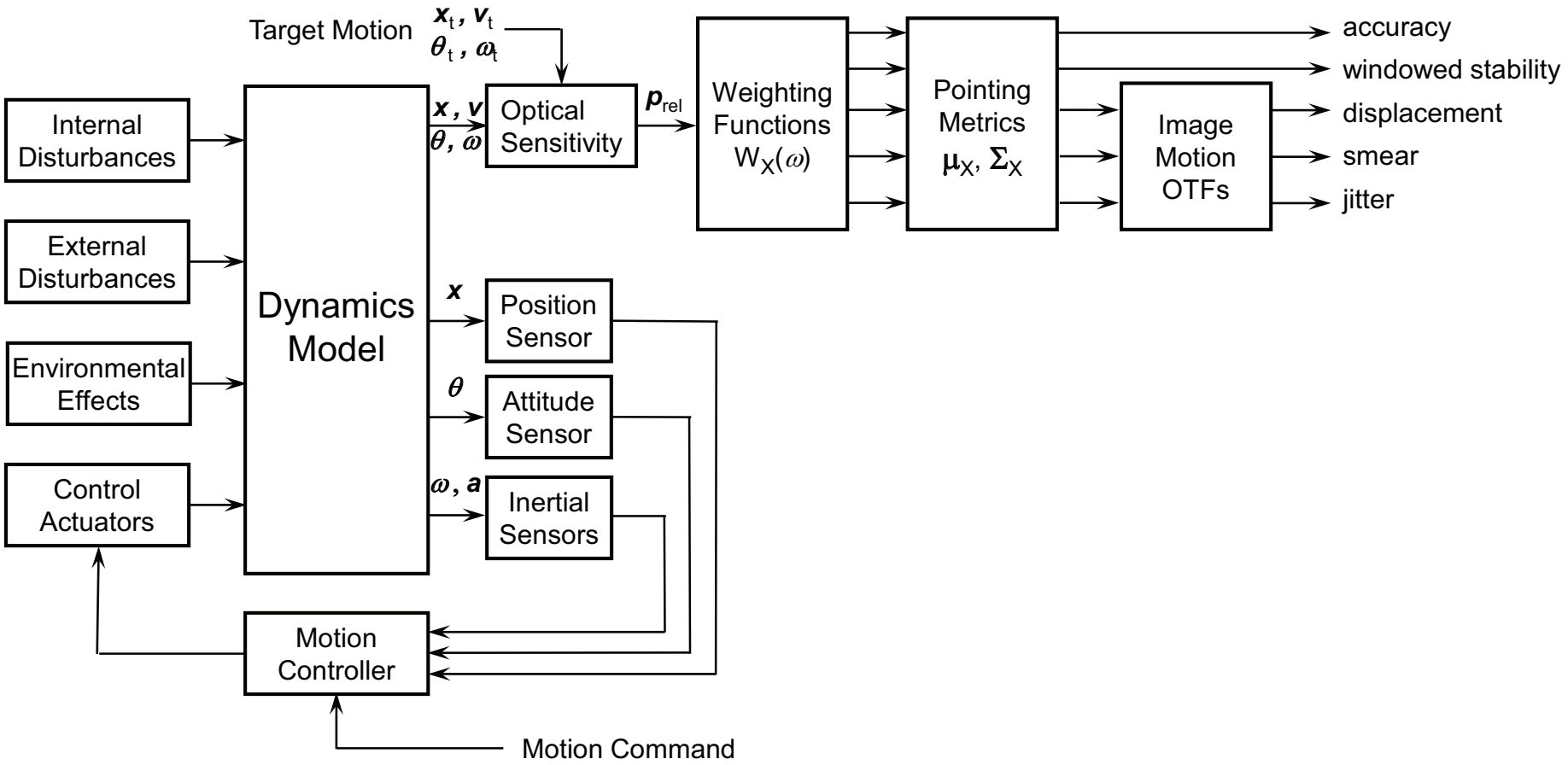

Dynamics Model and Controller Interconnection

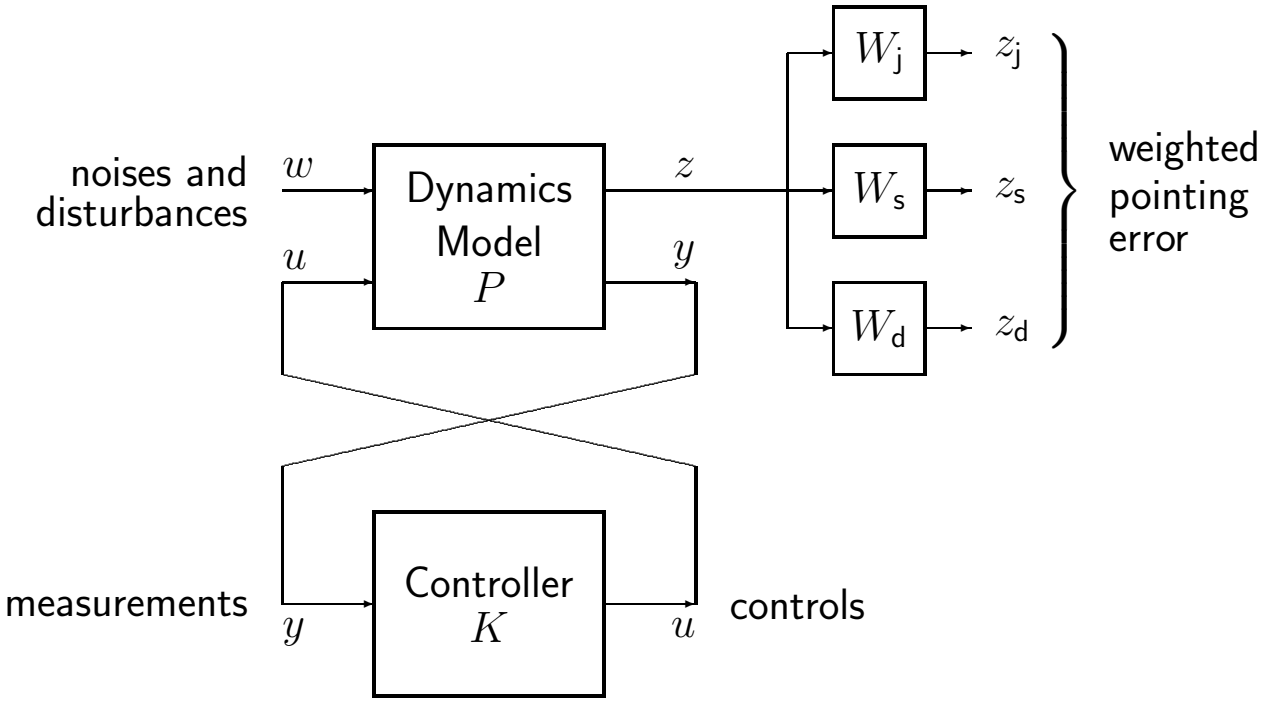

The closed-loop transfer function is computed as the Linear Fractional Transformation (LFT) $G = \mathcal{F}_\ell(P, K)$ of the plant P and controller K [36, Ch 4]

Model for Frequency Response Analysis

- Discrete-Time controller includes
  - Sample-and-hold with integrators (e.g., star tracker model, IMU filtering)
  - Attitude determination filter (suitably modeled for frequency response analysis)
  - Anti-alias filtering in the IMU (may be simplified for down-sampling)
  - Loop-shaping compensator (typically PID)
  - Structural mode filter
- Structural modes in the dynamics model should be separated into two parts, below and above approximately $10\times$ control loop bandwidth.
  - Reduces the order of the closed-loop system, facilitates analysis, improves numerical properties.
  - ▲ Closed-loop damping of structural modes in & near the control loop bandwidth can be decreased, increased, or made unstable, by feedback. Structural mode contribution to pointing motion (displacement, smear, jitter) may be diminished or amplified.

Pointing Performance Evaluation – Frequency Domain

- Feedback control design is inherently a frequency domain exercise, so frequency domain design and analysis methods are perferred.
- Linear and linearized transfer function models can be analyzed quickly and accurately, and significant system information (e.g., gain and phase margins) can be obtained.
- Interconnect continuous plant and multirate discrete-time controller with care.
- Pointing performance metrics are easy to compute from frequency domain data.
- Frequency response of a structural model is evaluated quickly and accurately.
- Low and high frequency modes can be separated to facilitate closed-loop frequency response and stability analysis. (Separate modes in and near the controller bandwidth, and modes well outside the controller bandwidth.)

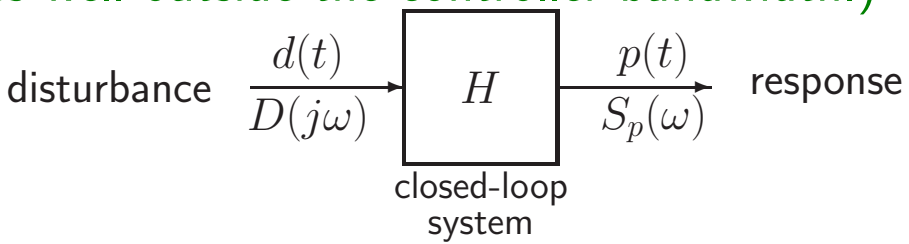

Disturbance Sources and Sensitivities

Disturbance Sources

- pointing command input (navigation error)
- sensor noise, aliasing
- RW, CMG, cryocooler, heat pump
- RCS (reaction control system thrusters)
- magnetic torque rods/coils
- antenna & solar array drives (stepper motors)
- thermal changes (solar array and boom thermal snap, thermal distortion, stick/slip)
- shutters, filter wheels
- Transient response from attitude maneuver (slosh, structural vibration)

Disturbance Sensitivities

- optical sensors
- optical communication
- star trackers
- IMU (gyros, accelerometers)
- clock chips
- microvibration transducers (analog signal conductors)
- solar array tip deflection

Know your Spectra, Watch out for Spectres

Representative mode locations are from a Nastran model.
Reaction Wheel speed range is 120 to 3000 rpm (2 Hz to 50 Hz)
Cryocooler operates at a set frequency within 51 to 63 Hz.
* Aerodynamic and gravity gradient torque

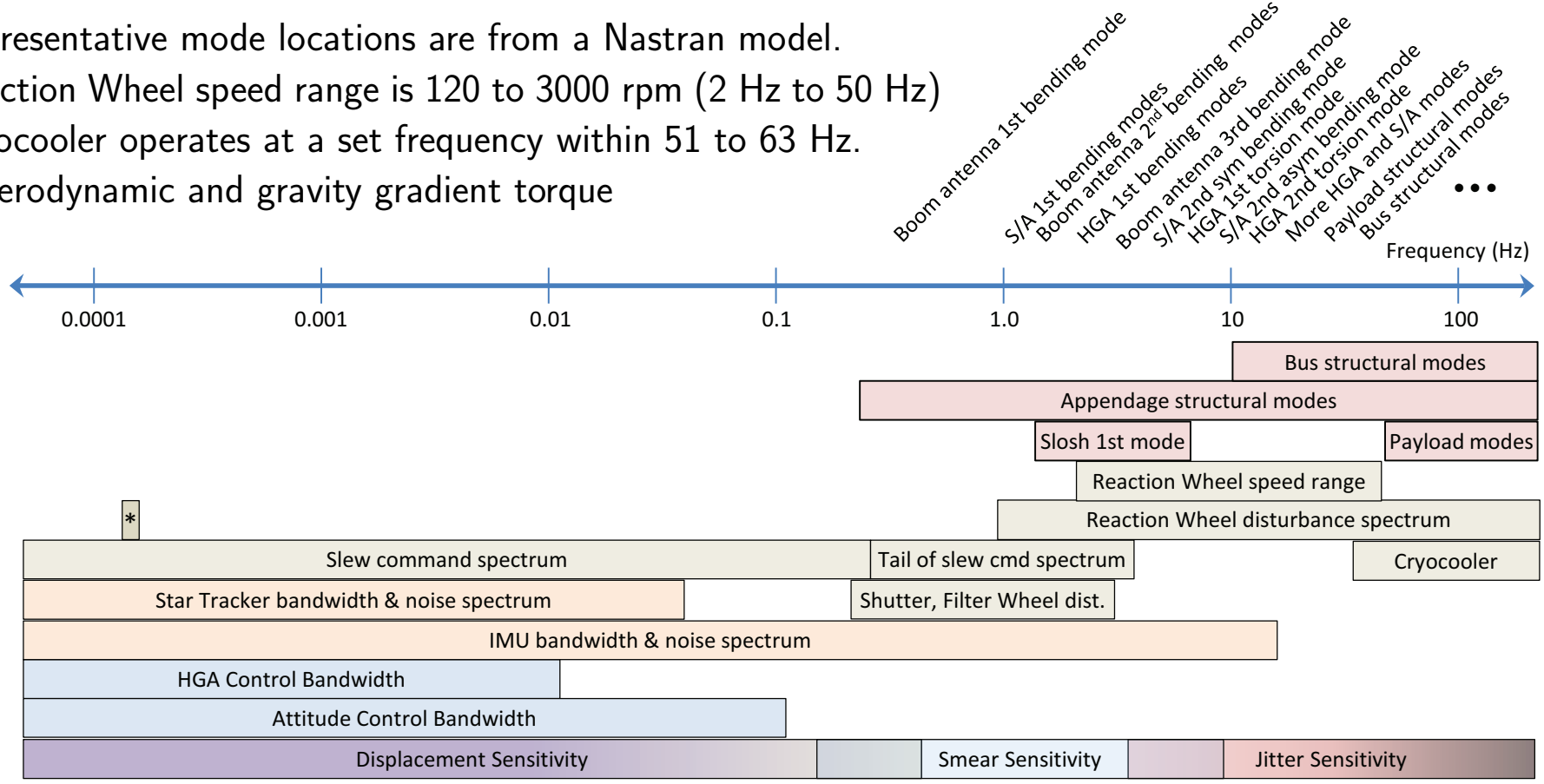

Dynamic Modeling and Analysis Flow [4]

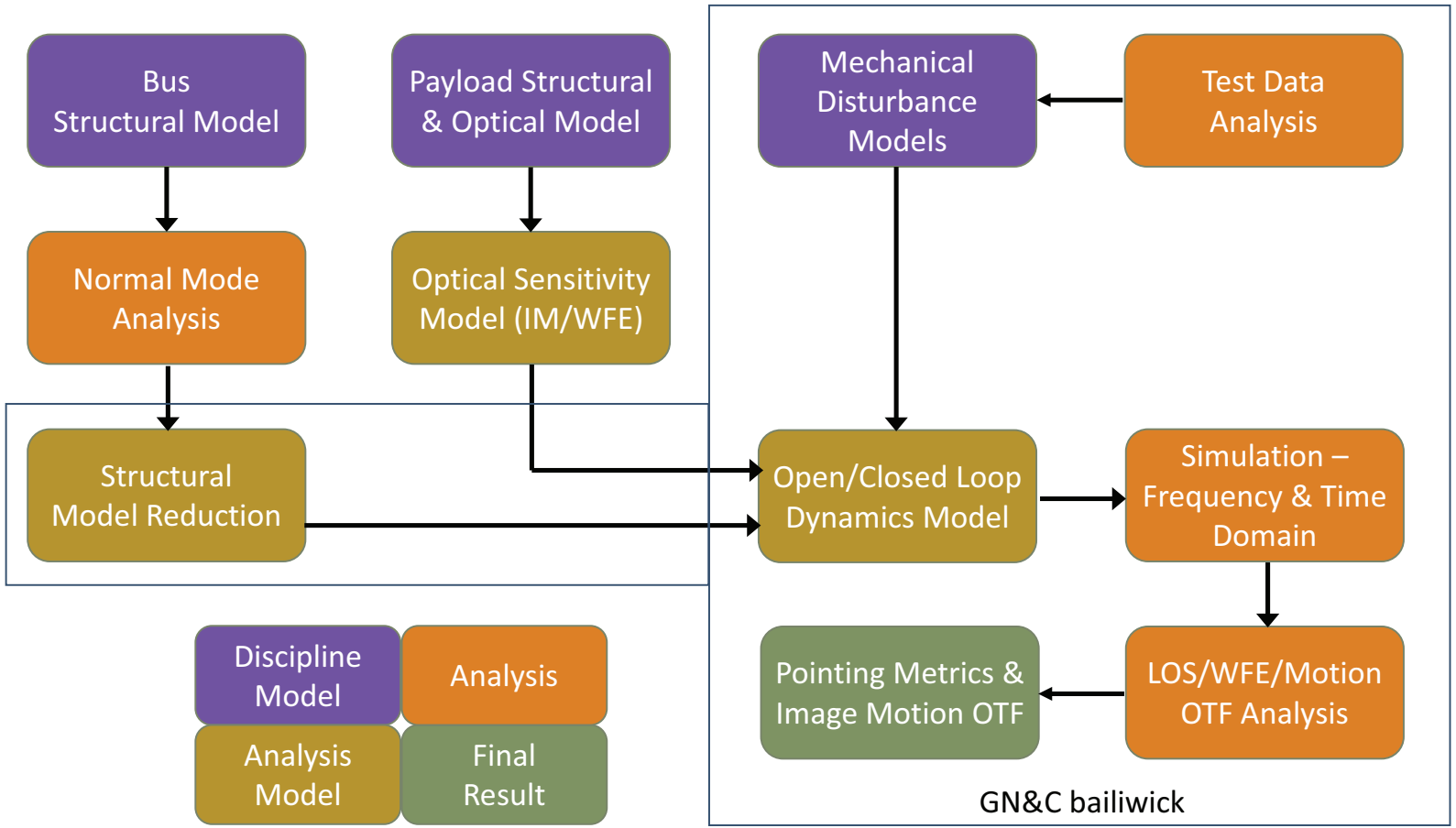

2. Pointing Performance Metrics (PPM)

- The Pointing Error Metrics are means and covariance matrices that parameterize the statistical Image Motion OTFs
  - Displacement: $\boldsymbol{\mu}$ ($\boldsymbol{\Sigma}_{\mathsf{D}}$ is not presently used)
  - Statistical Smear: $\boldsymbol{s}$, $\boldsymbol{\Sigma}_{\mathsf{S}}$
  - Jitter: $\boldsymbol{\Sigma}_{\mathsf{J}}$
- We also have (defined in the next section)
  - Accuracy metric $\boldsymbol{\Sigma}_{\mathsf{A}}$
  - Windowed Stability metric $\boldsymbol{\Sigma}_{\mathsf{WS}}$

Pointing Performance Metrics

- Pointing performance requirements should specify lower bounds on the IM OTFs, or MTFA and spatial frequency at some MTF amplitude, since the objective is image performance of the optical sensor.
- The Image Motion OTFs are parameterized by means & covariances of image motions (displacement, smear, jitter, etc.). These means & covariances are the PPMs.
  - Inverse Problem: derive the PPMs from the required $\mathrm{OTF}_{\mathsf{motion}}(\boldsymbol{\xi})$
  - Forward Problem: compute $\mathrm{OTF}_{\mathsf{motion}}(\boldsymbol{\xi})$ from the PPMs.
  - The Inverse Problem is more difficult than the Forward Problem.
- In what follows, references to pointing motion refer (primarily) to image motion (which has the unfortunate mnemonic $\boldsymbol{p}(t)$ for the 2D image motion).

Pointing Definitions Illustrated

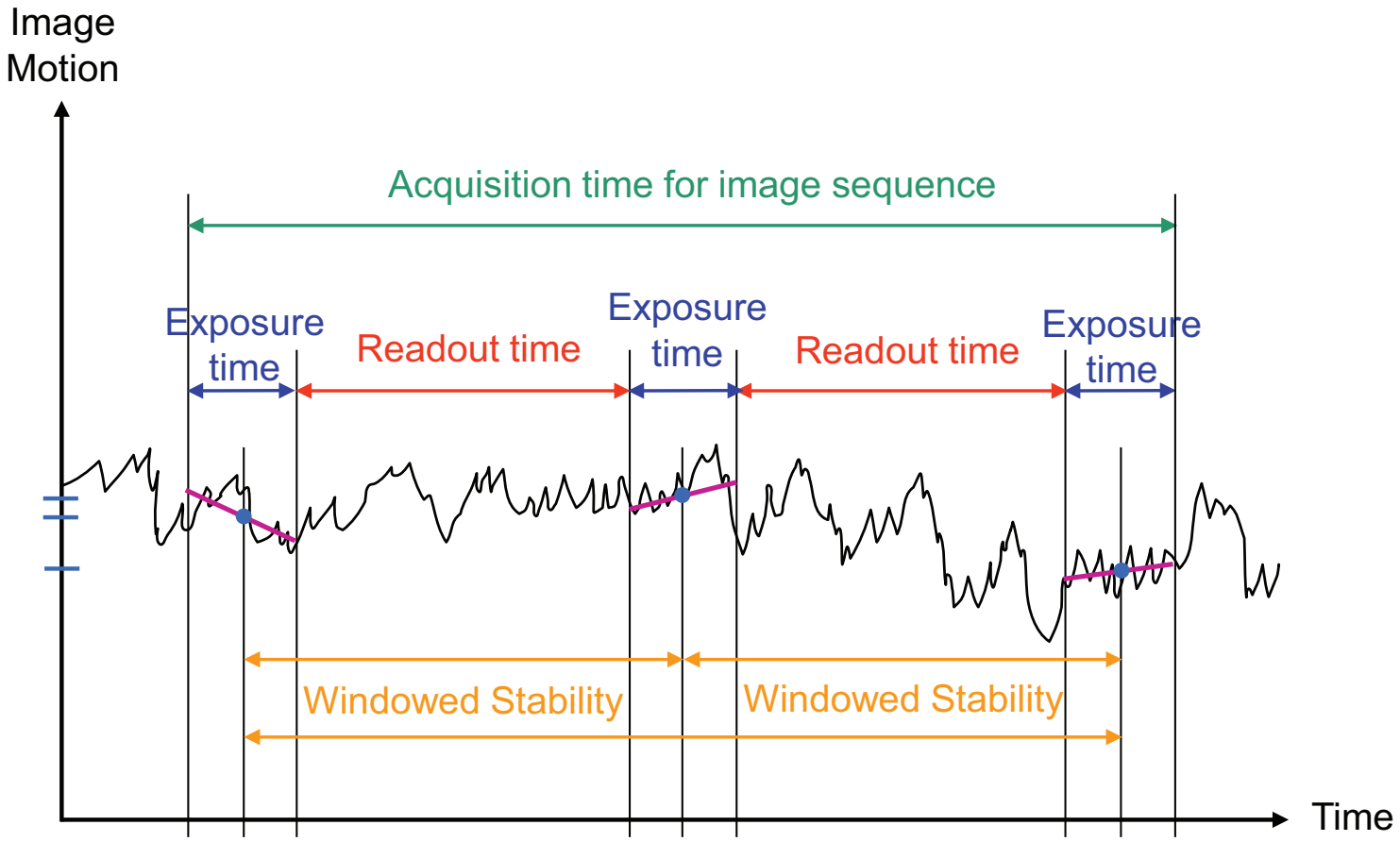

Image Motion versus LOS Pointing Motion

- We have distinguished between Image Motion and Line-Of-Sight Pointing Motion
- We are primarily concerned with the Image Motion $\boldsymbol{p}(t) = \begin{bmatrix} x(t) \\ y(t) \end{bmatrix}$.
- Line-Of-Sight (LOS) pointing motion, in general, is not equivalent to image motion.
  - "Pointing Error Metrics" is a misnomer in the context of Image Motion.
  - LOS pointing error is not well defined when the optical elements are not rigid.
  - In this work we refer to image motion. An optical sensor model is discussed later.
  - Image motion includes rotational and translational relative motion due to motion of optical elements, bus disturbances, and tracking error or pushbroom motion.
  - In this context, image motion does not include aspect changes (e.g., target rotation)
- Displacement, smear, and jitter are defined in the previous section.
- Repeatability has not been formally defined.

Revised Pointing Error [Performance] Metrics since 2003

- 2003 PEMs are the mean and covariance of displacement, jitter.
- 2015 PEMs are the mean and covariance of displacement, smear, jitter.
  - Smear and jitter affect the IM OTF differently. Smear is less detrimental to the OTF than jitter because the smear OTF decreases more slowly than the jitter OTF.
  - The jitter PM defined in 2003 ("smitter", or smear + jitter) has no direct bearing on image quality analysis and should no longer be used.
  - Displacement is unchanged.
- Other Pointing Performance Metrics not directly related to the IM OTF:
  - Windowed Stability and Point-to-Point Stability metrics are unchanged.
  - Windowed Stability is still valid and useful (e.g., for image registration).
  - Point-to-Point Stability does not seem particularly useful. Deprecate it.
- A displacement (shift) covariance can be defined. Shift is important, e.g., lock a fine error sensor on a star, keep an occulter on the Sun, or ensure a FOR is within the FOV

Estimated Image Motion Model / Relative LOS Pointing Motion

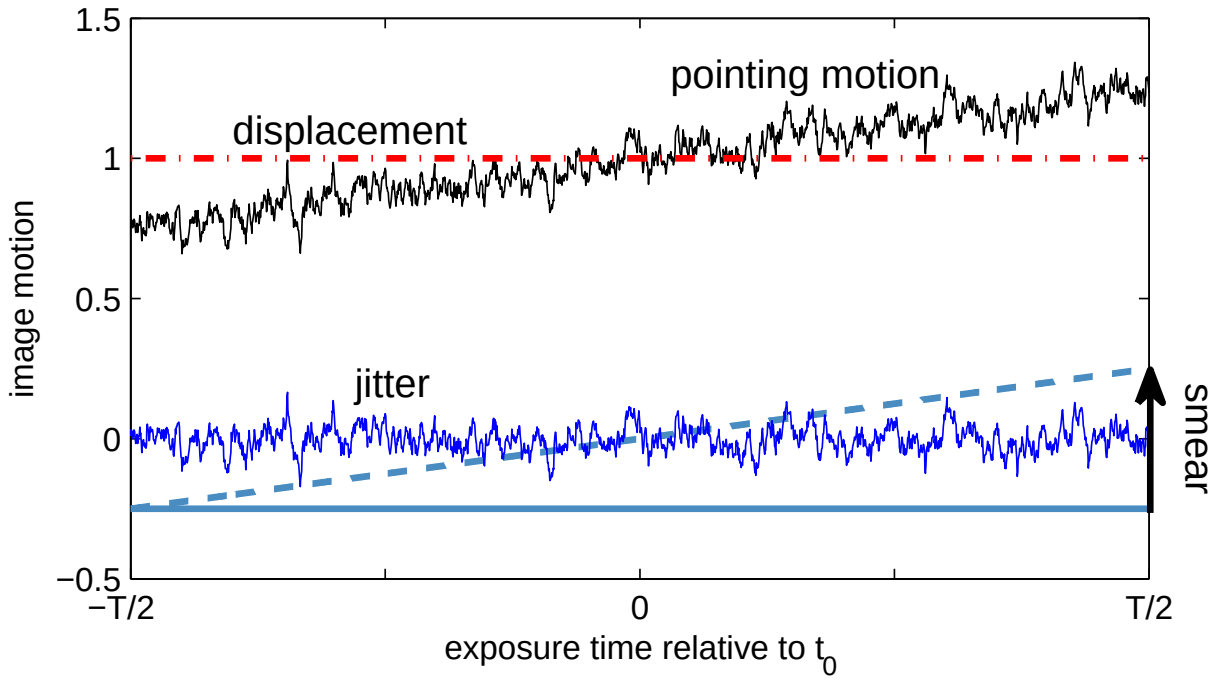

$\hat{\boldsymbol{p}}_o = \hat{\boldsymbol{p}}_o =$ est. displacement

$\hat{\boldsymbol{v}}_o = \hat{\boldsymbol{v}}_o =$ est. smear rate

$\hat{\boldsymbol{s}}_o = T\hat{\boldsymbol{v}}_o =$ estimated smear

$\hat{\boldsymbol{\psi}}(t) =$ estimated jitter

$$\boldsymbol{p}(t) = \hat{\boldsymbol{p}}_o + (t - t_0)\hat{\boldsymbol{v}}_o + \hat{\boldsymbol{\psi}}(t) \qquad t \in [t_0 - T/2,\, t_0 + T/2] \equiv \mathcal{I}(t_0)$$

$$\hat{\boldsymbol{p}}(t_0 + \alpha) = \hat{\boldsymbol{p}}_o + \alpha\hat{\boldsymbol{v}}_o + \hat{\boldsymbol{\psi}}_o(\alpha) \qquad \alpha \in [-T/2,\, T/2]\,, \quad \hat{\boldsymbol{\psi}}_o(\alpha) = \hat{\boldsymbol{\psi}}(t_o + \alpha)$$

Jitter, Displacement, Smear Rate

Jitter over $\mathcal{I}(t_0)$ is

$$\hat{\boldsymbol{\psi}}_o \equiv \hat{\boldsymbol{\psi}}(t_0+\alpha) = \boldsymbol{p}(t_0+\alpha) - \hat{\boldsymbol{p}}_o - \alpha\hat{\boldsymbol{v}}_o \qquad \alpha \in [-T/2, T/2]$$

Mean square jitter

$$\boldsymbol{J}(t_0) = \frac{1}{T}\int_{-T/2}^{T/2} \hat{\boldsymbol{\psi}}(t_0+\alpha)\hat{\boldsymbol{\psi}}^T(t_0+\alpha)\,\mathrm{d}\alpha\,, \qquad J(t_o) = \mathrm{tr}(\boldsymbol{J}(t_o))$$

Displacement: solve $\partial J/\partial \boldsymbol{p} = 0$ for $\hat{\boldsymbol{p}}$

$$\hat{\boldsymbol{p}}_o \equiv \hat{\boldsymbol{p}}(t_0) = \frac{1}{T}\int_{-T/2}^{T/2} \boldsymbol{p}(t_0+\alpha)\,\mathrm{d}\alpha$$

Smear Rate: solve $\partial J/\partial \boldsymbol{v} = 0$ for $\hat{\boldsymbol{v}}$

$$\hat{\boldsymbol{v}}_o \equiv \hat{\boldsymbol{v}}(t_0) = \frac{12}{T^3}\int_{-T/2}^{T/2} \alpha\,\boldsymbol{p}(t_0+\alpha)\,\mathrm{d}\alpha$$

Estimated Pointing Performance Metrics (PPM)

The PPMs are means and covariances that parameterize the Image Motion OTFs.

The PPMs may be **specified** in a requirements document from an IM OTF allocation or other rationale.

The PPMs must be **estimated** from data (simulated or telemetry) to verify performance.

Estimated Pointing Performance Metrics

Accuracy	$\boldsymbol{\mu} = \mathcal{E}\{\boldsymbol{p}_o\}$	$\boldsymbol{\Sigma}_\mathsf{A} = \mathrm{cov}\{\boldsymbol{p}_o\}$
Displacement	$\boldsymbol{\mu} = \mathcal{E}\{\hat{\boldsymbol{p}}_o\}$	$\boldsymbol{\Sigma}_\mathsf{D} = \mathrm{cov}\{\hat{\boldsymbol{p}}_o\}$
Smear Rate	$\boldsymbol{\rho} = \mathcal{E}\{\hat{\boldsymbol{v}}_o\}$	$\boldsymbol{\Sigma}_\mathsf{R} = \mathrm{cov}\{\hat{\boldsymbol{v}}_o\}$
Smear	$\boldsymbol{s} = T\boldsymbol{\rho}$	$\boldsymbol{\Sigma}_\mathsf{S} = T^2\boldsymbol{\Sigma}_\mathsf{R}$
Jitter	$\mathbf{0} = \mathcal{E}\{\boldsymbol{\psi}_o(\alpha)\}$	$\boldsymbol{\Sigma}_\mathsf{J} = \mathcal{E}\{\boldsymbol{J}(t_o)\}$

Covariance Matrix Computation

- The covariances Σ_X can be computed in one of three ways:
  1. Frequency response: Compute the power spectral density. This can be used for broadband and harmonic disturbance inputs, and also steps and impulses.
  2. Discrete-time or continuous-time stochastic input: Solve a Lyapunov equation.
  3. Discrete-time-domain simulation data:
     - **A.** Compute the autocovariance and PSD.
     - **B.** Direct autocorrelation.
- A combination of these methods is performed in most analyses, principally 1, or 1 and 2.
- Methods 1 and 2 are preferred whenever possible. Method 3B is not recommended.
- Covariance matrices can be computed for each disturbance & noise source, then added.
- Frequency resolution does not have to be the same for all power spectral densities.
- Sample rates do not have to be the same for all time-domain data.

Power Spectral Density (PSD)

- The Wiener-Khintchine (Khinchin) Theorem says the Power Spectral Density $\boldsymbol{S}(\omega)$ of a continuous-time signal $\boldsymbol{p}(t)$ is the Fourier Transform (FT) of the autocovariance $\boldsymbol{R}(\tau)$ of $\boldsymbol{p}(t)$, in units of power/Hz,

$$\boldsymbol{S}(\omega) = \int_{-\infty}^{\infty} \boldsymbol{R}(\tau)\, e^{-j\omega\tau}\, \mathrm{d}\tau \qquad \boldsymbol{S}(f) = \int_{-\infty}^{\infty} \boldsymbol{R}(\tau)\, e^{-j2\pi f\tau}\, \mathrm{d}\tau$$

- $\boldsymbol{S}(\omega)$ and $\boldsymbol{R}(\tau)$ are a Fourier Transform pair,

$$\boldsymbol{R}(\tau) = \frac{1}{2\pi} \int_{-\infty}^{\infty} \boldsymbol{S}(\omega)\, e^{j\omega\tau}\, \mathrm{d}\omega = \int_{-\infty}^{\infty} \boldsymbol{S}(f)\, e^{j2\pi f\tau}\, \mathrm{d}f$$

- Since $\boldsymbol{R}(0)$ is a covariance, the PPMs are computed from equations of the form

$$\boldsymbol{\Sigma}_{\mathsf{X}} = \frac{1}{2\pi} \int_{-\infty}^{\infty} \boldsymbol{S}(\omega) W_{\mathsf{X}}(\omega T)\, \mathrm{d}\omega$$

- $W_{\mathsf{X}}(\omega T)$ is a frequency-dependent weighting function corresponding to a pointing error metric (displacement, smear, jitter, etc.) It is a function of the exposure time T.

Summary of Pointing Performance Metrics (PPM)

Pointing Error	Pointing Error Metric (Covariance)	Weighting Function
Accuracy	$\boldsymbol{\Sigma}_{\mathsf{A}} = \mathrm{cov}\{\boldsymbol{p}\} = \frac{1}{2\pi}\int_{-\infty}^{\infty} \boldsymbol{S}(\omega) W_{\mathsf{A}}(\omega T)\,\mathrm{d}\omega$	$W_{\mathsf{A}}(\omega T) = 1$
Displacement	$\boldsymbol{\Sigma}_{\mathsf{D}} = \mathrm{cov}\{\bar{\boldsymbol{p}}\} = \frac{1}{2\pi}\int_{-\infty}^{\infty} \boldsymbol{S}(\omega) W_{\mathsf{D}}(\omega T)\,\mathrm{d}\omega$	$W_{\mathsf{D}}(\omega T) = \mathrm{sinc}^2(\omega T/2)$
Smear Rate	$\boldsymbol{\Sigma}_{\mathsf{R}} = \mathrm{cov}\{\bar{\boldsymbol{v}}\} = \frac{1}{2\pi}\int_{-\infty}^{\infty} \boldsymbol{S}(\omega) W_{\mathsf{R}}(\omega T)\,\mathrm{d}\omega$	$W_{\mathsf{R}}(\omega T) = \left[\frac{12}{\omega T^2}\big[\,\mathrm{sinc}(\omega T/2) - \cos(\omega T/2)\big]\right]^2$
Smear	$\boldsymbol{\Sigma}_{\mathsf{S}} = T^2 \boldsymbol{\Sigma}_{\mathsf{R}}$	$W_{\mathsf{S}}(\omega T) = T^2\, W_{\mathsf{R}}(\omega T)$
Jitter	$\boldsymbol{\Sigma}_{\mathsf{J}} = \mathcal{E}\{\boldsymbol{J}(t_0)\} = \frac{1}{2\pi}\int_{-\infty}^{\infty} \boldsymbol{S}(\omega) W_{\mathsf{J}}(\omega T)\,\mathrm{d}\omega$	$W_{\mathsf{J}}(\omega T) = 1 - W_{\mathsf{D}}(\omega T) - \frac{1}{12} W_{\mathsf{S}}(\omega T)$
Smitter	$\boldsymbol{\Sigma}_{\mathsf{SJ}} = \frac{1}{12}\boldsymbol{\Sigma}_{\mathsf{S}} + \boldsymbol{\Sigma}_{\mathsf{J}} = \frac{1}{2\pi}\int_{-\infty}^{\infty} \boldsymbol{S}(\omega) W_{\mathsf{SJ}}(\omega T)\,\mathrm{d}\omega$	$W_{\mathsf{SJ}}(\omega T) = 1 - W_{\mathsf{D}} = \frac{1}{12} W_{\mathsf{S}} + W_{\mathsf{J}}$
Point Stability	$\boldsymbol{\Sigma}_{\mathsf{PS}} = \frac{1}{2\pi}\int_{-\infty}^{\infty} \boldsymbol{S}(\omega) W_{\mathsf{PS}}(\omega T_{\mathsf{PS}})\,\mathrm{d}\omega$	$W_{\mathsf{PS}}(\omega T_{\mathsf{PS}}) = 2(1 - \cos(\omega T_{\mathsf{PS}})) = 4\sin^2(\omega T_{\mathsf{PS}}/2)$
Windowed Stability	$\boldsymbol{\Sigma}_{\mathsf{WS}} = \frac{1}{2\pi}\int_{-\infty}^{\infty} \boldsymbol{S}(\omega) W_{\mathsf{WS}}(\omega T, \omega T_{\mathsf{WS}})\,\mathrm{d}\omega$	$W_{\mathsf{WS}}(\omega T, \omega T_{\mathsf{WS}}) = W_{\mathsf{D}}(\omega T) W_{\mathsf{PS}}(\omega T_{\mathsf{WS}})$

Frequency Domain Weighting Functions $W_{\mathsf{X}}(\omega T)$

- $W_{\mathsf{X}}(\omega T) =$ weighting function,
  $\mathsf{X} =$ D, S, J. $T =$ exposure time.

$$\boldsymbol{\Sigma}_{\mathsf{X}} = \frac{1}{2\pi}\int_{-\infty}^{\infty} \boldsymbol{S}(\omega) W_{\mathsf{X}}(\omega T)\,\mathrm{d}\omega$$

- $\boldsymbol{S}(\omega)$ is the PSD computed by
  - Frequency response of image motion
  - Autocorrelation $\boldsymbol{R}(\tau)$ (BT algorithm)

$$\boldsymbol{S}(\omega) = \int_{-\infty}^{\infty} \boldsymbol{R}(\tau)\, e^{-j\omega\tau}\,\mathrm{d}\tau$$

- Could compute PMs *directly* from auto-correlation. (Discouraged)

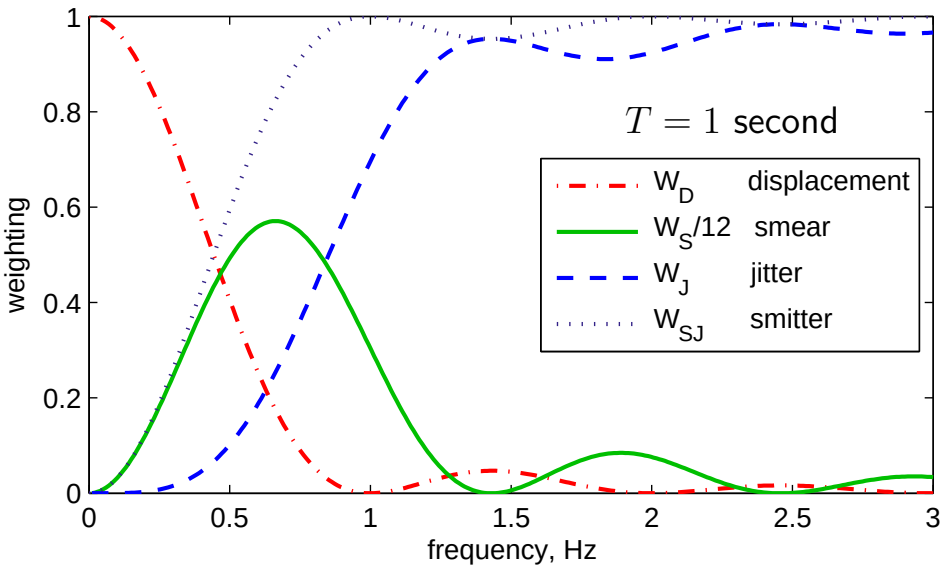

$$W_{\mathsf{A}} = W_{\mathsf{D}} + \tfrac{1}{12} W_{\mathsf{S}} + W_{\mathsf{J}} = 1$$

$$\boldsymbol{\Sigma}_{\mathsf{A}} = \boldsymbol{\Sigma}_{\mathsf{D}} + \tfrac{1}{12} \boldsymbol{\Sigma}_{\mathsf{S}} + \boldsymbol{\Sigma}_{\mathsf{J}}$$

Effect of Decreasing (or Increasing) Exposure Time T

- The weighting functions stretch out to the right as T is decreased. ($T = 1/2$ shown.)
- Equivalently, the frequency axis is scaled by $1/T$.
- Half-power point of W_J is at about $f = 1/T$, but lower frequency disturbances of high amplitude contribute to jitter.
- For smaller T, lower frequencies contribute less to jitter and more to smear and displacement.
- Ex: For $T = 20$ s, $W_J \simeq 0.95$ at the jitter corner frequency $f \simeq 0.07$ Hz. (In or near control BW.)

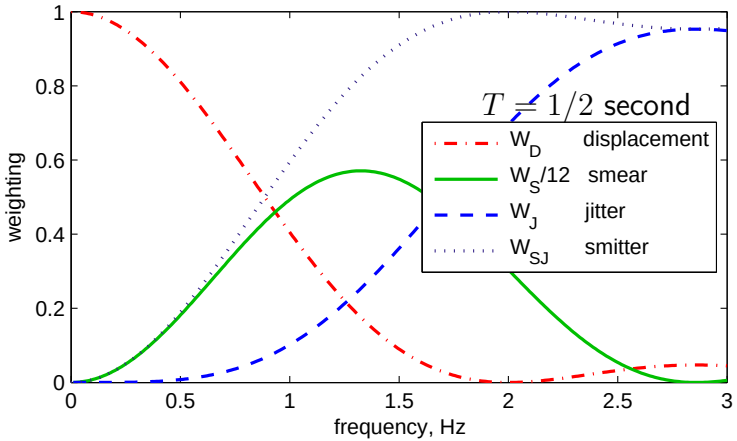

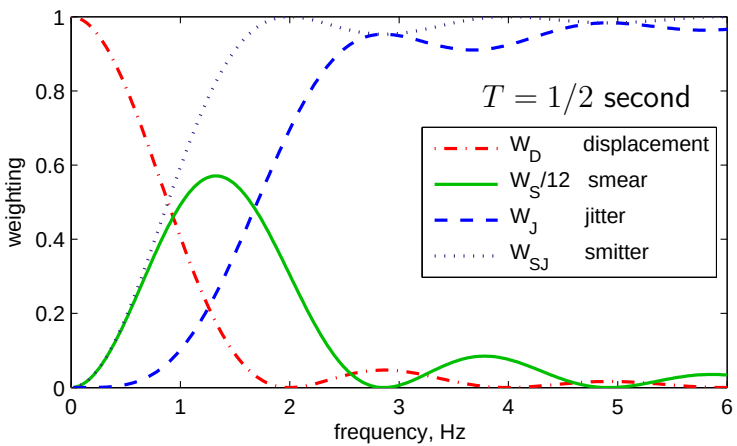

Some Useful Facts

- The weighting functions $W_{\mathsf{X}}(\omega T)$ are computed from the FT of the autocorrelations of the estimates $\hat{\boldsymbol{p}}_o$, $\hat{\boldsymbol{v}}_o$, $\hat{\boldsymbol{\psi}}_o(\alpha)$.
- Displacement, Smear, and Jitter (and the weighting functions) are not independent – they are subject to a constraint and vary together with the exposure time T.
- The jitter weighting function has a corner frequency greater than the old jitter weighting function (defined in 2003 and prior), so
  - the jitter signal will have a shorter coherence time (defined below),
  - a jitter requirement is easier to meet (but now you have a smear requirement), and
  - the old jitter weighting function should not be used, even if no smear is expected.
- The bandwidth of the attitude control loop has no bearing on what contitutes jitter.
  - Disturbance contributions to jitter depend only on the jitter weighting function.
  - Feedback affects the damping and stability of structural modes in and near the BW.

A Dirty Little Secret

- The estimated displacement, smear, jitter are correlated, even if the actual displacement, smear, and jitter are not.
  - Independence of the actual displacement, smear, and jitter was assumed in deriving the IM OTFs.
  - Analysis shows that the correlation is usually not severe. (Unpublished but circulatd among some TDT members in 2020.)
  - Optical engineers have always introduced correlation when removing smear and jitter from an image by image processing (deconvolution) techniques.

Coherence Time for the Jitter (1/2)

- The covariance of the jitter is a valid jitter metric when the coherence time τ_c of the jitter $\hat{\boldsymbol{\psi}}(t)$ is short relative to the exposure time, $\tau_c \ll T$.
- The coherence time is obtained from a second-order Taylor series approximation of the autocovariance $\boldsymbol{C}_{\hat{\boldsymbol{\psi}}}(\tau_c)$ of the jitter $\hat{\boldsymbol{\psi}}(t)$,

$$\tau_c = \left[-2\boldsymbol{C}_{\hat{\boldsymbol{\psi}}}(0)/\boldsymbol{C}''_{\hat{\boldsymbol{\psi}}}(0)\right]^{1/2}$$

  $\boldsymbol{C}''_{\hat{\boldsymbol{\psi}}}(\tau)$ is the second derivative of $\boldsymbol{C}_{\hat{\boldsymbol{\psi}}}(\tau)$ with respect to τ.
- Another definition (not used here) is

$$\tau_c = \frac{1}{\boldsymbol{C}_{\hat{\boldsymbol{\psi}}}(0)} \int_0^\infty \boldsymbol{C}_{\hat{\boldsymbol{\psi}}}(\tau)\,\mathrm{d}\tau$$

- The coherence time is computed per-channel when $\boldsymbol{C}_{\hat{\boldsymbol{\psi}}}$ is a matrix.

Ref: [27, Appendix B, Eq. (B7)]

Coherence Time for the Jitter (2/2)

- The PSD of the jitter is $\boldsymbol{S}_{\hat{\psi}}(\omega) = \boldsymbol{S}(\omega) W_{\text{J}}(\omega)$.
- Compute the autocorrelations from the inverse FT of the PSD $\boldsymbol{S}_{\hat{\psi}}(\omega)$ of $\hat{\boldsymbol{\psi}}(t)$,

$$\boldsymbol{C}_{\hat{\psi}}(\tau) = \frac{1}{2\pi} \int_{-\infty}^{\infty} \boldsymbol{S}(\omega) W_{\text{J}}(\omega)\, e^{-j\omega\tau}\, \mathrm{d}\omega$$

$$\boldsymbol{C}''_{\hat{\psi}}(\tau) = \frac{1}{2\pi} \int_{-\infty}^{\infty} -\omega^2 \boldsymbol{S}(\omega) W_{\text{J}}(\omega)\, e^{-j\omega\tau}\, \mathrm{d}\omega$$

- Evaluating $\boldsymbol{C}_{\hat{\psi}}(\tau)$ and $\boldsymbol{C}''_{\hat{\psi}}(\tau)$ at $\tau = 0$ yields

$$\boldsymbol{C}_{\hat{\psi}}(0) = \frac{1}{2\pi} \int_{-\infty}^{\infty} \boldsymbol{S}(\omega) W_{\text{J}}(\omega)\, \mathrm{d}\omega$$

$$\boldsymbol{C}''_{\hat{\psi}}(0) = \frac{1}{2\pi} \int_{-\infty}^{\infty} -\omega^2 \boldsymbol{S}(\omega) W_{\text{J}}(\omega)\, \mathrm{d}\omega$$

Variable Exposure Time

- Multiple intervals T (and T_{WS}) may be specified for an instrument with variable exposure and for various instruments on the same platform (aircraft, missile, spacecraft, etc).
  - Performance is easily evaluated for various T, such as min, median max values.
  - Performance specifications should take the range of exposure times into account.
- The displacement and jitter weighting functions move right as the interval decreases, so the jitter covariance decreases

$$\boldsymbol{\Sigma}_{\mathsf{J}}(\tau) \leq \boldsymbol{\Sigma}_{\mathsf{J}}(T) \quad \text{for all } \tau < T \qquad \left(\boldsymbol{\Sigma}_{\mathsf{J}}(\tau) \to 0 \text{ as } \tau \to 0 \right)$$

Windowed Stability Weighting Function

$$W_{\mathsf{WS}}(\omega T_{\mathsf{S}}, \omega T_{\mathsf{D}}) = W_{\mathsf{D}}(\omega T) W_{\mathsf{PS}}(\omega T_{\mathsf{WS}})$$

$T = 1, \quad T_{\mathsf{WS}} = 1$

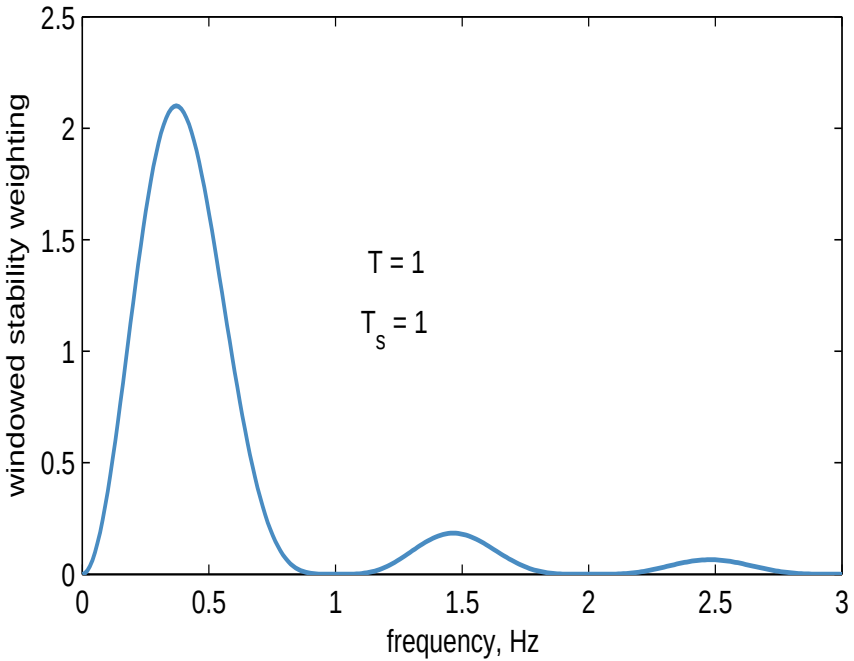

$T = 1, \quad T_{\mathsf{WS}} = 4$

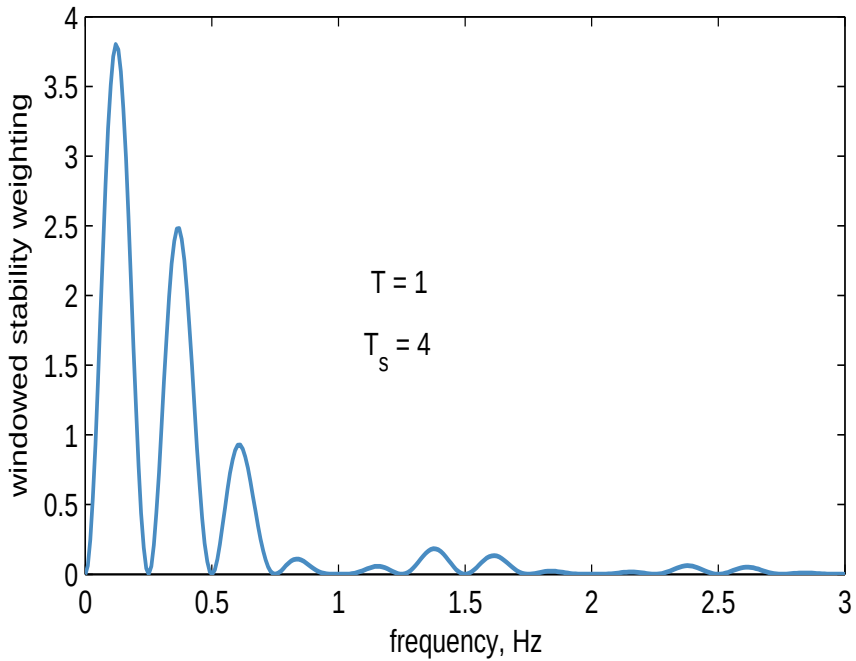

Allan Variance

- The **Allan Variance (AVAR)** was used originally to define the stability of atomic clocks, radio frequency sources, and later to measure the performance of gyros.
- In the time domain, the Allan Variance is a convergent estimate of the variance.
- In the frequency domain, the AVAR is a product of $W_{\mathsf{PS}}(\omega T)$ and $W_{\mathsf{D}}(\omega T)$, and the PSD of the data

  The Allan Variance is a consistent estimator of variance and accounts for the finite record length (window) of the data.
- $W_{\mathsf{WS}}(\omega T, \omega T)$ models the change in displacement between image centroids with no time between the imaging intervals.

$$W_{\mathsf{allan}} = W_{\mathsf{WS}}(\omega T, \omega T) = W_{\mathsf{PS}}(\omega T) W_{\mathsf{D}}(\omega T) = \frac{\sin^4(\omega T/2)}{(\omega T/2)^2}$$

3. Methods to Compute the PSD

- The methods described for evaluating the Pointing Performance Metrics (PPM) provides an effective and efficient means to evaluate pointing system performance.
  - PPMs computed from frequency-domain data (or Fourier transform of time-domain data) give insight into sensitivity to noise and disturbances at various frequencies and amplitudes.
  - PPMs can be computed individually for independent noise and disturbance sources, then combined additively.
  - PPMs can be evaluated for a variety of operating conditions for each disturbance.
- Methods to compute the PPMs (Covariance Matrices $\boldsymbol{\Sigma}_X$)
  1. Frequency response
  2. Lyapunov equation
  3. Time response (2 methods)

3.1 Power Spectral Density – Frequency Response Method (1/5)

A continuous-time linear time-invariant (LTI) state-space system (A, B, C, D) is

$$\dot{\boldsymbol{x}} = A\boldsymbol{x}(t) + B\boldsymbol{u}(t)$$
$$\boldsymbol{y} = C\boldsymbol{x}(t) + D\boldsymbol{u}(t)$$

The frequency-domain transfer function from $\boldsymbol{u}(s)$ to $\boldsymbol{y}(s)$ is

$$G(s) = D + C(sI - A)^{-1}B\,, \qquad s = j\omega$$

We assume that A is stable, $\operatorname{Re}\lambda(A) < 0$. Usually $D = \mathbf{0}$, so it is omitted henceforth.

The power spectral density of the input $\boldsymbol{u}(t)$ is $\boldsymbol{S}_u(\omega)$.

The power spectral density $\boldsymbol{S}_y(\omega)$ of the output $\boldsymbol{y}(t)$ is

$$\boldsymbol{S}_y(s) = G(s)\boldsymbol{S}_u(s)G^*(-s^*)$$

"$*$" is complex conjugate transpose or Hermetian transpose, depending on context

Power Spectral Density – Frequency Response Method (2/5)

Abuse notation, write $\boldsymbol{S}(\omega) \equiv \boldsymbol{S}(s)$, $s = j\omega$. Let's see how we might compute $\boldsymbol{S}_y(\omega)$

$$H(j\omega) = (j\omega I - A)^{-1} B$$
$$\boldsymbol{S}_x(\omega) = H(j\omega)\boldsymbol{S}_u(\omega)H^*(j\omega)$$
$$\boldsymbol{S}_y(\omega) = C\boldsymbol{S}_x(\omega)C^T$$

Some observations

- $\boldsymbol{S}_u$ may be of moderate dimension and sparse (ex: 4 RW, cryo, RCS, 2 SA, 2 ST, 1 IMU).
- $\boldsymbol{S}_x$ is typically of large dimension (ex: state vector includes 20 to 200 modes).
- $\boldsymbol{S}_y$ may be of modest dimension (ex: payload, 2 ST, IMU [gyro, accelerometer]).
- We do not need the cross-covariance between different outputs, so we do not have to compute the cross spectral density between different outputs.
- We want to compute the individual contributions of each disturbance source to the covariance at each output so that we can compute relative contributions.

Power Spectral Density – Frequency Response Method (3/5)

Partition B and $\boldsymbol{S}_u$ according to d independent disturbance sources so that we can evaluate the response to each separately.

$$B = \begin{bmatrix} B_1 & B_2 & \cdots & B_d \end{bmatrix}$$

$$\boldsymbol{S}_u = \begin{bmatrix} S_1 & \mathbf{0} & \cdots & \mathbf{0} \\ \mathbf{0} & S_2 & \ddots & \vdots \\ \mathbf{0} & \mathbf{0} & \cdots & S_d \end{bmatrix}$$

Each S_i, $i = 1, 2, \ldots, d$ is up to 6×6 in dimension, representing forces and torques in each coordinate axis.

Either B_i or S_i must incorporate coordinate transformations and unit conversions! (Model the orientations of disturbance sources mounted on the structure modeled in A.)

Important: B and $\boldsymbol{S}_u$ are partitioned this way because each disturbance input is applied at a different location on the flexible structure, hence applied to different mode shapes.

Power Spectral Density – Frequency Response Method (4/5)

The transfer function from disturbance source i to the state $\boldsymbol{x}$ is

$$H_i(j\omega) = (j\omega I - A)^{-1} B_i$$

The spectral response to disturbance source i is

$$\boldsymbol{S}_{x,i}(\omega) = H_i(j\omega) B_i S_i(\omega) B_i^T H_i^*(j\omega)$$

Factor the input spectral density matrix $\boldsymbol{S}_i(\omega) = \boldsymbol{U}_i(\omega)\, \boldsymbol{U}_i^H(\omega)$, then compute

$$\boldsymbol{X}_i(\omega) = H_i(j\omega) B_i\, \boldsymbol{U}_i(\omega)$$

The spectral density matrix of the state vector due to input i is then

$$\boldsymbol{S}_{x,i}(\omega) = \boldsymbol{X}_i(\omega)\, \boldsymbol{X}_i^*(\omega)$$

The spectral response to all disturbance sources is

$$\boldsymbol{S}_x(\omega) = \sum_{i=1}^{d} \boldsymbol{S}_{x,i}(\omega) = \sum_{i=1}^{d} \boldsymbol{X}_i(\omega)\, \boldsymbol{X}_i^*(\omega)$$

Power Spectral Density – Frequency Response Method (5/5)

Partition C according to each output of interest.

$$C = \begin{bmatrix} C_1 \\ C_2 \\ \vdots \\ C_q \end{bmatrix}$$

The C_o, $o = 1, 2, \ldots, q$, output translational or rotational displacements and rates.

The C_o must incorporate coordinate transformations and unit conversions!

Outputs of interest include motion at gyro and star tracker mounts, motion of a focal plane or optical elements in an optical payload, or motion of a boom tip.

Total State Covariance From All Disturbance Sources

The state covariance due to disturbance source i is

$$\begin{aligned}\boldsymbol{\Sigma}_{x,i} &= \frac{1}{2\pi}\int_{-\infty}^{\infty} \boldsymbol{S}_{X,i}(\omega)\, W_{\mathsf{X}}(\omega T)\,\mathrm{d}\omega \\ &= \frac{1}{2\pi}\int_{-\infty}^{\infty} \boldsymbol{X}_i(\omega)\, \boldsymbol{X}_i^*(\omega)\, W_{\mathsf{X}}(\omega T)\,\mathrm{d}\omega \\ &\simeq \frac{1}{2\pi}\sum_{k=-N}^{N} \boldsymbol{X}_i(\omega_k)\, \boldsymbol{X}_i^*(\omega_k)\, W_{\mathsf{X}}(\omega_k T)\,\Delta\omega\end{aligned}$$

$\Delta\omega = \omega_{\mathsf{max}}/N$ with ω_{max}, N suitably large so that rectangular integration error is small.

The total state covariance due to all d disturbance sources is

$$\boldsymbol{\Sigma}_x = \sum_{i=1}^{d} \boldsymbol{\Sigma}_{x,i}$$

Total Output Covariance From All Disturbance Sources

The covariance at output o due to disturbance source i is

$$\boldsymbol{\Sigma}_{y,oi} = C_o \boldsymbol{\Sigma}_{x,i} C_o^T$$

The total covariance at output o due to all d disturbance sources is

$$\boldsymbol{\Sigma}_{y,o} = C_o \boldsymbol{\Sigma}_x C_o^T = \sum_{i=1}^{d} \boldsymbol{\Sigma}_{y,oi}$$

Define $\boldsymbol{Y}_i(\omega) = C_o \boldsymbol{X}_i(\omega)$. The covariance at output o due to source i can be computed as

$$\begin{aligned}
\boldsymbol{\Sigma}_{y,i} &= \frac{1}{2\pi} \int_{-\infty}^{\infty} \boldsymbol{Y}_i(\omega)\, \boldsymbol{Y}_i^*(\omega)\, W_{\mathsf{X}}(\omega T)\, \mathrm{d}\omega \\
&\simeq \frac{1}{2\pi} \sum_{k=-N}^{N} \boldsymbol{Y}_i(\omega_k)\, \boldsymbol{Y}_i^*(\omega_k)\, W_{\mathsf{X}}(\omega_k T)\, \Delta\omega
\end{aligned}$$

Power Spectral Density – Harmonic Disturbance Sources (1/2)

Each $S_i(\omega)$ comprises p_i spectral components ω_r, $r = 1, 2, \ldots, p_i$ (harmonic, pure sine) so the disturbance spectrum is

$$S_i(\omega) = \sum_{r=1}^{p_i} S_{i,r} \pi \left[\delta(\omega + \omega_r) + \delta(\omega - \omega_r) \right]$$

The $S_{i,r}$ are, in general, constant Hermetian positive semidefinite 6×6 matrices. Example:

$$S_{i,r} = \tfrac{1}{2} \operatorname{diag}\begin{pmatrix} F_x^2 & F_y^2 & F_z^2 & T_x^2 & T_y^2 & T_z^2 \end{pmatrix}$$

where F_x, F_y, F_z are peak force disturbance amplitudes, and T_x, T_y, T_z are peak torque disturbance amplitudes, all at the harmonic frequency ω_r and in the coordinate axes of the disturbance source. The amplitudes vary with frequency, though not annotated with r. $F_x = F_y$, $T_x = T_y$. F_z and T_z are the axial force and torque.

In general the cross-spectral densities (cross-axes) may not be zero.

Covariance – Harmonic Disturbance Sources (2/2)

The state covariance due to harmonic disturbance source i is

$$\begin{aligned}
\boldsymbol{\Sigma}_{x,i} &= \frac{1}{2\pi}\int_{-\infty}^{\infty} H_i(j\omega)B_i S_i(\omega)B_i^T H_i^*(j\omega)\, W_{\mathsf{X}}(\omega T)\,\mathrm{d}\omega \\
&= \frac{1}{2\pi}\int_{-\infty}^{\infty} \sum_{r=1}^{p_i} H_i(j\omega)B_i S_{i,r}B_i^T H_i^*(j\omega)\,\pi\big[\delta(\omega+\omega_r)+\delta(\omega-\omega_r)\big]\, W_{\mathsf{X}}(\omega_r T)\,\mathrm{d}\omega \\
&= \sum_{r=1}^{p_i} \mathrm{Re}\big[H_i(j\omega_r)B_i S_{i,r}B_i^T H_i^*(j\omega_r)\big]\, W_{\mathsf{X}}(\omega_r T) \\
&= \sum_{r=1}^{p_i} \mathrm{Re}\big[\boldsymbol{X}_{i,r}\boldsymbol{X}_{i,r}^*\big]\, W_{\mathsf{X}}(\omega T)
\end{aligned}$$

where $S_{i,r} = U_{i,r}\,U_{i,r}^*$ and $\boldsymbol{X}_{i,r} = H_i(j\omega_r)B_i U_{i,r}$

Power Spectral Density – Frequency Response, Discrete System

A discrete-time linear time-invariant (LTI) state-space system (A, B, C, D), with constant sample time T, is

$$\begin{aligned} \boldsymbol{x}_{k+1} &= A\boldsymbol{x}_k + B\boldsymbol{u}_k \\ \boldsymbol{y}_k &= C\boldsymbol{x}_k + D\boldsymbol{u}_k \end{aligned}$$

The frequency-domain transfer function from $\boldsymbol{u}(s)$ to $\boldsymbol{y}(s)$ is

$$G(z) = D + C(zI - A)^{-1}B\,, \qquad z = \exp(j\omega T)$$

We assume that A is stable, $|\lambda(A)| < 1$. Usually have $D = \mathbf{0}$, so it is omitted henceforth.

The power spectral density of the input $\boldsymbol{u}_k$ is $\boldsymbol{S}_u(z)$.

The power spectral density $\boldsymbol{S}_y(z)$ of the output $\boldsymbol{y}_k$ is

$$\boldsymbol{S}_y(z) = G(z)\boldsymbol{S}_u(z)G^*(1/z^*)$$

Covariance – Frequency Response Method, Discrete System

Computations proceed as before, but with $z = \exp(j\omega T)$ and frequency range $|\omega T| < \pi$

Abuse notation again, write $\boldsymbol{S}(\omega) = \boldsymbol{S}(z)$, $\boldsymbol{X}(\omega) = \boldsymbol{X}(z)$

$$\begin{aligned}\boldsymbol{\Sigma}_{x,i} &= \frac{1}{2\pi}\int_{-\infty}^{\infty} \boldsymbol{X}_i(e^{j\omega})\,\boldsymbol{X}_i^*(e^{j\omega})\,W_{\mathsf{X}}(\omega_k T)\,\mathrm{d}\omega \\ &\simeq \frac{1}{2\pi}\sum_{k=-N}^{N} \boldsymbol{X}_i(\omega_k)\,\boldsymbol{X}_i^*(e^{j\omega})\,W_{\mathsf{X}}(\omega_k T)\,\Delta\omega\end{aligned}$$

where $\omega_{\mathsf{max}} = \pi/T$ and $\Delta\omega = \omega_{\mathsf{max}}/N = \pi/NT$, and N is suitably large so that the rectangular integration has sufficiently small error.

3.2 Pointing Performance Evaluation – Lyapunov Equation

The pointing performance metrics for a continuous-time or discrete-time system driven by zero-mean white noise can be evaluated by solving a Lyapunov equation.

- Continuous-time white noise input
  - Noise sources include RW bearing noise, torque noise
  - Integrate the weighted PSD (rectangular integration), or
  - Solve a continuous-time Lyapunov equation.
- Discrete-time white noise input
  - Noise sources include star trackers, gyros
  - Integrate the weighted PSD (rectangular integration), or
  - Solve a discrete-time Lyapunov equation, or
  - Compute the FT of the autocorrelation of simulated time-domain data.

Lyapunov Equation – Continuous System

- A Lyapunov equation can be solved for the covariance of the state and output of a continuous-time system with zero-mean white noise input.
- A continuous-time linear time-invariant (LTI) state-space system (A, B, C, D) is

$$\dot{\boldsymbol{x}}(t) = A\boldsymbol{x}(t) + B\boldsymbol{u}(t)$$
$$\boldsymbol{y}(t) = C\boldsymbol{x}(t) + D\boldsymbol{u}(t)\,, \qquad D = \mathbf{0}$$

  $\boldsymbol{u}(t)$ is a zero-mean white noise input with constant spectral density $\boldsymbol{Q}_u$
- Solve a Lyapunov equation for $\boldsymbol{P}$ and the covariance $\boldsymbol{\Sigma}_y$ of the output $\boldsymbol{y}(t)$

$$A\boldsymbol{P} + \boldsymbol{P}A^T + B\boldsymbol{Q}_u B^T = \mathbf{0}$$
$$\boldsymbol{\Sigma}_y = C\boldsymbol{P}C^T$$

  Note that $\boldsymbol{u}(t)$ does not have to be Gaussian.
- Gregory's method for structural model reduction is derived from a Lyapunov equation. It applies to open-loop continuous-time structural response to white noise input.

Lyapunov Equation – Discrete System

- A Lyapunov equation can be solved for the covariance of the state and output of a discrete-time system with zero-mean white noise input.
- A discrete-time linear time-invariant (LTI) state-space system (A, B, C, D) is

$$\boldsymbol{x}_{k+1} = A\boldsymbol{x}_k + B\boldsymbol{u}_k$$
$$\boldsymbol{y}_k = C\boldsymbol{x}_k + D\boldsymbol{u}_k$$

  $\boldsymbol{u}_k$ is a zero-mean white noise input with constant covariance $\boldsymbol{\Sigma}_u$
- Solve a Lyapunov equation for $\boldsymbol{P}$ and the covariance $\boldsymbol{\Sigma}_y$ of the output $\boldsymbol{y}_k$

$$A\boldsymbol{P}A^T + B\boldsymbol{\Sigma}_u B^T = \boldsymbol{0}$$
$$\boldsymbol{\Sigma}_y = C\boldsymbol{P}C^T + D\boldsymbol{\Sigma}_u D^T$$

  Note that $\boldsymbol{u}_k$ does not have to be Gaussian.
- The BT PSD algorithm is a time-domain alternative to the discrete-time Lyapunov equation. The BT algorithm can serve as a check.

System Modeling

- We need to have a discussion about modeling a continuous-discrete system and model conversion. This is a topic for another seminar.
  - Spacecraft structure, reaction wheels, and most disturbances are continuous-time.
  - Pointing controller and attitude sensors (e.g., star trackers, gyros) are discrete-time.
  - Does one convert continuous part to a discrete model or convert the discrete to continuous model?
  - How does one compute a valid frequency response?
- Weighting functions $\sqrt{W_{\mathsf{X}}(\omega T)}$ must be approximated by rational transfer functions, which are then augmented to the continuous-time system (A, B, C, D) for Lyapunov analysis.
  - Certain kinds of "tricks" may be used instead.

3.3 Pointing Performance Evaluation – Time Domain

- Time-domain simulation is useful where frequency response may be difficult to apply.
  - Nonlinear effects, transient events, and discrete-time events can be evaluated in the frequency domain via linearization, or in the time domain.
- Time domain simulation could be useful for verification or blunder detection.
- Pointing error evaluation is primarily a frequency domain analysis!
- Time-domain simulation and analysis can be slow, especially Monte Carlo simulation.
- A wide range of time scales can significantly slow a time-domain simulation and introduce numerical errors. This is especially true of structural modes.
- Simulation time and time step must be carefully considered. Numerical integration error may interfere with the pointing error analysis.
- Numerical integration of states driven by continuous noise must be statistically valid.
- Ensure that pointing errors are stationary, otherwise bound the statistics, etc.
- Autocorrelations require data outside of a time window, but that data may not exist.

Autocorrelation – Continuous-Time Data

Autocorrelation of $\boldsymbol{x}(t) = \begin{bmatrix} x(t) \\ y(t) \end{bmatrix}$,

$$\boldsymbol{R}(\tau) = \mathcal{E}\{\boldsymbol{x}(t+\tau)\boldsymbol{x}^H(t)\}$$
$$= \begin{bmatrix} r_{xx}(\tau) & r_{xy}(\tau) \\ r_{yx}(\tau) & r_{yy}(\tau) \end{bmatrix}$$

$$r_{xx}(\tau) = \mathcal{E}\{x(t+\tau)x^*(t)\}$$
$$r_{yy}(\tau) = \mathcal{E}\{y(t+\tau)y^*(t)\}$$
$$r_{xy}(\tau) = \mathcal{E}\{x(t+\tau)y^*(t)\}$$
$$r_{yx}(\tau) = \mathcal{E}\{y(t+\tau)x^*(t)\}$$

Autocovariance matrix

$$\boldsymbol{C}(\tau) = \boldsymbol{R}(\tau) - \boldsymbol{\mu}\boldsymbol{\mu}^T, \qquad \boldsymbol{\mu} = \mathcal{E}\{\boldsymbol{x}(t)\}$$

Autocorrelation Matrix – Properties – Continuous-Time

Properties of the multichannel autocorrelation matrix (extends to discrete-time)

$r_{xx}(\tau) = r_{xx}(-\tau)$	even function
$r_{yy}(\tau) = r_{yy}(-\tau)$	even function
$r_{xy}(\tau) = r^*_{yx}(-\tau)$	not an even function
$r_{yx}(\tau) = r^*_{xy}(-\tau)$	not an even function
$\boldsymbol{R}(\tau) \neq \boldsymbol{R}(-\tau)$	not an even function
$\boldsymbol{R}(\tau) \neq \boldsymbol{R}^H(\tau)$	not hermetian
$\boldsymbol{R}(-\tau) = \boldsymbol{R}^H(\tau)$	
$\boldsymbol{R}(0) \geq 0$	nonnegative definite (at lag 0)

Tip: Our data $\boldsymbol{x}(t)$ is real, so we can replace Hermetian (H, complex conjugate transpose) with transpose (T).

Detrending the Data

Tip: We will assume that bias and trend, or polynomial motion in general (which is nonstationary) have been removed from $\boldsymbol{x}(t)$, so the autocorrelation matrix $\boldsymbol{R}(\tau)$ is an autocovariance matrix.

The bias $\boldsymbol{\mu}$ and trend $\boldsymbol{s}$ are IM OTF parameters.

3.3A Power Spectral Density (PSD) – Continuous-Time

The Wiener-Khintchine Theorem says the Power Spectral Density $\boldsymbol{S}(\omega)$ of a continuous-time signal $\boldsymbol{x}(t)$ is the Fourier Transform (FT) of the autocovariance $\boldsymbol{R}(\tau)$ of $\boldsymbol{x}(t)$,

$$\boldsymbol{S}(\omega) = \int_{-\infty}^{\infty} \boldsymbol{R}(\tau)\, e^{-j\omega\tau}\, \mathrm{d}\tau \qquad \text{power/Hz, } \omega \text{ in rad/sec}$$

$$\boldsymbol{S}(f) = \int_{-\infty}^{\infty} \boldsymbol{R}(\tau)\, e^{-j2\pi f\tau}\, \mathrm{d}\tau \qquad \text{power/Hz, } f \text{ in Hz}$$

$\boldsymbol{S}(f) = \boldsymbol{S}^H(f)$ (Hermetian) and positive semidefinite. $\boldsymbol{S}(\omega) \leftrightarrow \boldsymbol{R}(\tau)$ (transform pair)

$$\boldsymbol{R}(\tau) = \frac{1}{2\pi}\int_{-\infty}^{\infty} \boldsymbol{S}(\omega)\, e^{j\omega\tau}\, \mathrm{d}\omega \qquad \text{units of power, } \boldsymbol{x}\boldsymbol{x}^H$$

$$= \int_{-\infty}^{\infty} \boldsymbol{S}(f)\, e^{j2\pi f\tau}\, \mathrm{d}f$$

Abuse of notation: $\boldsymbol{S}(\omega) \equiv \boldsymbol{S}(f)$ with $\omega = 2\pi f$ (meaning should be clear from context)

Covariance and Pointing Metrics – Continuous-Time Data

The PPMs can be computed from the frequency-weighted power spectral density

$$\boldsymbol{\Sigma}_{\mathsf{X}} = \boldsymbol{R}_{\mathsf{X}}(0) = \frac{1}{2\pi}\int_{-\infty}^{\infty} \boldsymbol{S}(\omega)\, W_{\mathsf{X}}(\omega T)\,\mathrm{d}\omega \qquad \text{real, symmetric}$$

$$= \int_{-\infty}^{\infty} \boldsymbol{S}(f)\, W_{\mathsf{X}}(2\pi f T)\,\mathrm{d}f$$

$W_{\mathsf{X}}(\omega T)$ is a weighting function, X is one of A, D, S, J, PS, WS – viz. PPM Summary Table

The Accuracy Metric (with $W_{\mathsf{A}}(\omega T) = 1$) is the covariance (average power)

$$\boldsymbol{\Sigma}_{\mathsf{A}} = \boldsymbol{R}_{\mathsf{A}}(0) = \frac{1}{2\pi}\int_{-\infty}^{\infty} \boldsymbol{S}(\omega)\,\mathrm{d}\omega$$

$$= \int_{-\infty}^{\infty} \boldsymbol{S}(f)\,\mathrm{d}f$$

Spectral Estimation Methods

- Non-Parametric methods
  - Periodogram
  - Blackman-Tukey Correlogram
- Parametric methods
  - Yule-Walker Autoregressive Moving Average (ARMA) algorithm

The ARMA model is general, but the model order has to be chosen. There are ways to do this automatically.

AR and MA models model only poles and zeros, respectively.

The BT spectral density estimator is statistically consistent for stochastic processes.

Other spectral estimation algorithms are not applicable here. For example, harmonic models do not allow for damping or correlated random processes.

Autocovariance – Stochastic Discrete-Time Data

The statistical autocovariance of a stochastic (random) sampled-data sequence $\boldsymbol{x}_k$ is

$$\boldsymbol{R}(k, k+\ell) = \mathcal{E}\{\boldsymbol{x}_{k+\ell}\boldsymbol{x}_k^H\}$$

If the sequence has constant mean and the autocovariance depends only on the lag ℓ (and not k) we say that $\boldsymbol{x}_k$ is second-order stationary, which implies that it is wide-sense stationary (WSS) (but not vice versa unless $\boldsymbol{x}_k$ is Gaussian, in which case it is also strict-sense stationary). We shall assume that $\boldsymbol{x}_k$ is zero mean.

The autocovariance of a WSS sequence $\boldsymbol{x}_k$ is then

$$\boldsymbol{R}(\ell) = \mathcal{E}\{\boldsymbol{x}_{k+\ell}\boldsymbol{x}_k^H\}$$

If $\boldsymbol{x}_k$ is ergodic, the statistical autocovariance is obtained equivalently as a time average

$$\boldsymbol{R}(\ell) = \mathcal{E}\{\boldsymbol{x}_{k+\ell}\boldsymbol{x}_k^H\} = \lim_{N\to\infty} \frac{1}{2N+1} \sum_{k=-N}^{N} \boldsymbol{x}_{k+\ell}\boldsymbol{x}_k^H$$

Autocorrelation – Discrete-Time Data

Autocorrelation of $\boldsymbol{x}_k = \begin{bmatrix} x_k \\ y_k \end{bmatrix}$,

$$\boldsymbol{R}(\ell) = \mathcal{E}\{\boldsymbol{x}_{k+\ell}\, \boldsymbol{x}_k^H\}$$

$$= \begin{bmatrix} r_{xx}(\ell) & r_{xy}(\ell) \\ r_{yx}(\ell) & r_{yy}(\ell) \end{bmatrix} \qquad \ell = 0,\, \pm 1,\, \pm 2,\, \ldots$$

$$r_{xx}(\ell) = \mathcal{E}\{x_{k+\ell}\, x_k^*\}$$
$$r_{yy}(\ell) = \mathcal{E}\{y_{k+\ell}\, y_k^*\}$$
$$r_{xy}(\ell) = \mathcal{E}\{x_{k+\ell}\, y_k^*\}$$
$$r_{yx}(\ell) = \mathcal{E}\{y_{k+\ell}\, x_k^*\}$$

Autocovariance matrix

$$\boldsymbol{C}(\ell) = \boldsymbol{R}(\ell) - \boldsymbol{\mu}\boldsymbol{\mu}^T\,, \qquad \boldsymbol{\mu} = \mathcal{E}\{\boldsymbol{x}_k\}$$

Autocorrelation Matrix – Properties – Discrete-Time Data

Properties of the multichannel autocorrelation matrix (similar to continuous-time)

$$\boldsymbol{R}(\ell) \neq \boldsymbol{R}(-\ell)$$ not an even function

$$\boldsymbol{R}(\ell) \neq \boldsymbol{R}^H(\ell)$$ not hermetian

$$\boldsymbol{R}(\ell) = \boldsymbol{R}^H(-\ell)$$

$$\boldsymbol{R}(-\ell) = \boldsymbol{R}^H(\ell)$$

$$\boldsymbol{R}(0) \geq 0$$ nonnegative definite (at lag 0)

Tip: Our data $\boldsymbol{x}_k$ is real, so we can replace Hermetian (H, complex conjugate transpose) with transpose (T).

Autocorrelation – More Properties – Discrete-Time Data

The matrix entries in $\boldsymbol{R}(\ell)$ have the following properties

$$
\begin{aligned}
r_{xx}(0) &> 0 & r_{yy}(0) &> 0 \\
|r_{xx}(\ell)| &\leq r_{xx}(0) & |r_{yy}(\ell)| &\leq r_{yy}(0) \\
r_{xx}(-\ell) &= r_{xx}^*(\ell) & r_{yy}(-\ell) &= r_{yy}^*(\ell) \\
r_{xy}(-\ell) &\neq r_{xy}^*(\ell) & r_{yx}(-\ell) &\neq r_{yx}^*(\ell) \\
r_{xy}(-\ell) &= r_{yx}^*(\ell) & r_{yx}(-\ell) &= r_{xy}^*(\ell)
\end{aligned}
$$

$$
|r_{xy}(\ell)|^2 \leq r_{xx}(0) r_{yy}(0)
$$

The matrix $\boldsymbol{R}(\ell)$ may, in many contexts, be replaced by a vector (since $r_{yx}(\ell)$ is redundant)

$$
\boldsymbol{r}(\ell) = \begin{bmatrix} r_{xx}(\ell) \\ r_{yy}(\ell) \\ r_{xy}(\ell) \end{bmatrix}
$$

Power Spectral Density (PSD) – Discrete-Time Data

The Wiener-Khintchine Theorem says the PSD $\boldsymbol{S}_d(\omega)$ of a discrete-time signal $\boldsymbol{x}_k$ is the Discrete-Time Fourier Transform (DTFT) of the autocovariance $\boldsymbol{R}(\ell)$ of $\boldsymbol{x}_k$,

$$\boldsymbol{S}_d(\omega) = T \sum_{\ell=-\infty}^{\infty} \boldsymbol{R}(\ell) \exp(-j\omega\ell T)$$

where T is the sample time.

We can write the PSD in terms of frequency f in Hz (with a slight abuse of notation)

$$\boldsymbol{S}_d(f) = T \sum_{\ell=-\infty}^{\infty} \boldsymbol{R}(\ell) \exp(-j2\pi f\ell T)$$

Units of $\boldsymbol{S}_d(\omega)$ and $\boldsymbol{S}_d(f)$ are power/Hz = units of $\boldsymbol{x}\boldsymbol{x}^T$ per Hz

Autocovariance – Discrete-Time Data

The autocovariance can be computed from the inverse DTFT of $\boldsymbol{S}_d(\omega)$ or $\boldsymbol{S}_d(f)$,

$$\boldsymbol{R}(\ell) = \frac{1}{2\pi}\int_{-\pi/T}^{\pi/T} \boldsymbol{S}_d(\omega)\, e^{j\omega\ell T}\,\mathrm{d}\omega$$

$$= \int_{-1/2T}^{1/2T} \boldsymbol{S}_d(f)\, e^{j2\pi f\ell T}\,\mathrm{d}f$$

The covariance of $\boldsymbol{x}_k$ is

$$\boldsymbol{\Sigma} = \boldsymbol{R}(0) = \frac{1}{2\pi}\int_{-\pi/T}^{\pi/T} \boldsymbol{S}_d(\omega)\,\mathrm{d}\omega$$

$$= \int_{-1/2T}^{1/2T} \boldsymbol{S}_d(f)\,\mathrm{d}f$$

Autocorrelation, Autocovariance Estimate – Discrete-Time Data

The autocorrelation of $\boldsymbol{x}_k$ can be expressed as a time average, provided that $\boldsymbol{x}_k$ has finite energy and is WSS (mean-ergodic and autocorrelation-ergodic). An infinite sequence $\boldsymbol{x}_k$ is not available, so we estimate the autocorrelation from N samples $\boldsymbol{x}_k$, $k = 0, 1, \ldots, N-1$,

$$\hat{\boldsymbol{R}}(\ell) = \lim_{N\to\infty} \frac{1}{N} \sum_{k=0}^{N-1-\ell} \boldsymbol{x}_{k+\ell}\, \boldsymbol{x}_k^H \qquad\qquad \ell = 0, 1, \ldots, N-1$$

$$\hat{\boldsymbol{R}}(-\ell) = \hat{\boldsymbol{R}}^H(\ell)$$

This is a biased estimator of $\boldsymbol{R}(\ell)$ because $\mathcal{E}\{\hat{\boldsymbol{R}}(\ell)\} = \dfrac{N-|\ell|}{N}\boldsymbol{R}(\ell)$.

The unbiased estimator $\check{\boldsymbol{R}}(\ell) = \dfrac{N}{N-|\ell|}\hat{\boldsymbol{R}}(\ell)$ has a large variance for large ℓ.

Tip: Remove the mean and trend, or polynomial motion, from $\boldsymbol{x}_k$. Then $\boldsymbol{R}(\tau)$ is an autocovariance matrix. The mean $\boldsymbol{\mu}$ and trend $\boldsymbol{s}$ are IM OTF parameters.

Discrete Fourier Transform (DFT)

Discrete Time Fourier Transform (DTFT) of a data sequence $\boldsymbol{x}_k$, $k = 0, 1, \ldots, N-1$

$$\boldsymbol{X}(f) = T \sum_{n=0}^{N-1} \boldsymbol{x}_n \, e^{-j2\pi f n T}$$

The Discrete Fourier Transform (DFT) is computed on a grid of frequencies $f_m = m\Delta f$, $m = -(N-1), \ldots, -1, 0, 1, \ldots, N-1$, $\Delta f = 1/NT$,

$$\boldsymbol{X}_m = \boldsymbol{X}(f_m) = T \sum_{n=0}^{N-1} \boldsymbol{x}_n \, e^{-j2\pi f_m n T}$$

$$= T \sum_{n=0}^{N-1} \boldsymbol{x}_n \, e^{-j2\pi m n / N}$$

Pad the data sequence with $(K-1)N$ zeros and compute a KN-point DFT. Equivalent to the N-point DFT on a finer grid with $\Delta f = 1/KNT$ and $\pm m = 0, 1, \ldots, KN-1$. Avoids missing a spectral line, resolves a possibly split spectral line, interpolates the DFT.

Power Spectral Density Estimation – Periodogram

For a purely deterministic signal $\boldsymbol{x}_k$, the periodogram estimate of the PSD is

$$\boldsymbol{S}_m = \frac{1}{NT} |\boldsymbol{X}_m|^2$$

The total power in the PSD is obtained by rectangular integration of the continuous PSD,

$$\boldsymbol{\Sigma} = \left[\sum_{m=-(N/2-1)}^{N/2-1} \boldsymbol{S}_m \right] \Delta f$$

The periodogram is statistically inconsistent for stochastic (random, noisy) data $\boldsymbol{x}_k$ — its variance increases with increasing N.

The periodogram can be used for deterministic data, but should be avoided for noisy data. If the data sequence is long enough, average the periodograms of segments. Welch periodogram uses overlapping segments. The resolution of the periodogram is reduced.

The Blackman-Tukey PSD estimator is statistically consistent for stochastic data.

Blackman-Tukey (BT) PSD Estimator (1/3)

Blackman-Tukey (BT) algorithm computes an estimate of the PSD from the estimated autocovariance matrix, using M lags, where $M \ll N$,

$$\hat{\boldsymbol{S}}_d(f) = T \sum_{\ell=-M/2}^{M/2} w(\ell) \hat{\boldsymbol{R}}(\ell)\, e^{-j2\pi f \ell T} \qquad \text{units: power/Hz}$$

- $w(\ell)$ is a length $2M+1$ symmetric window function such that $w(\ell) = 0$ for $|\ell| > M$.
- It is recommended that M is about $1/5$ to $1/10$ of the number of lags (N) to reduce bias and error in the estimated PSD.
- The window $w(\ell)$ effectively reduces the frequency resolution from $1/NT$ to $1/MT$.
- Averaging periodograms of segmented data is equivalent to applying the BT algorithm to the windowed autocorrelation.
- Evaluate the PSD on a fine grid $f_m = m\Delta f$, $\Delta f = 1/KMT$, $m = 0, 1, \ldots, KM-1$, $K \gg 1$ (e.g., $K \simeq 10$) [else $w(\ell)\hat{\boldsymbol{R}}(\ell)$ or $w(\ell)$ can be padded with zeros]

Blackman-Tukey (BT) PSD Estimator (2/3)

The estimated power spectral density should be positive semidefinite at each frequency. This is the case when

- The window ("lag") function $w(\ell)$ is a positive semidefinite sequence (non-negative definite). Equivalently, the FT of $w(\ell)$ is positive semidefinite.
  - Window functions that are positive semidefinite include Bartlett, Parzen, Nutall.
- The unbiased autocorrelation estimate $\hat{\boldsymbol{R}}(\ell)$ is positive semidefinite
  - The biased estimate $\check{\boldsymbol{R}}(\ell)$ can be negative definite or negative semidefinite.
- A seq. $\boldsymbol{R}(\ell)$ is positive semidefinite if the Toeplitz matrix $\mathbf{C}$ is positive semidefinite:

$$\mathbf{C} = \begin{bmatrix} \boldsymbol{R}(0) & \boldsymbol{R}(1) & \cdots & \boldsymbol{R}(M) \\ \boldsymbol{R}(-1) & \boldsymbol{R}(0) & \cdots & \boldsymbol{R}(M-1) \\ \vdots & \vdots & \ddots & \vdots \\ \boldsymbol{R}(-M) & \boldsymbol{R}(-M+1) & \cdots & \boldsymbol{R}(0) \end{bmatrix}$$

Blackman-Tukey Algorithm (3/3)

The autocovariance is the inverse Discrete-Time Fourier Transform (DTFT) of $\boldsymbol{S}_d(\omega)$,

$$\hat{\boldsymbol{R}}(\ell) = \sum_{m=-M/2}^{M/2} \hat{\boldsymbol{S}}_d(f_m)\, e^{j2\pi f_m \ell T}\, \Delta f$$

where $\Delta f = 1/MT$. The covariance matrix is obtained at lag $\ell = 0$,

$$\boldsymbol{\Sigma} = \hat{\boldsymbol{R}}(0) = \sum_{m=-M/2}^{M/2} \hat{\boldsymbol{S}}_d(f_m)\, \Delta f$$

The frequency-domain weighting functions for a pointing error metric is included to get

$$\boldsymbol{\Sigma}_{\mathsf{X}} = \sum_{m=-M/2}^{M/2} \hat{\boldsymbol{S}}_d(f_m) W_{\mathsf{X}}(f_m T)\, \Delta f$$

Check the Total Power in the Power Spectral Density

Be sure to correctly scale the DFT to a power spectrum! (Software packages may not.)

From Parseval's Energy Theorem, the total power in the power spectral density must equal the power in the time-domain signal

$$\boldsymbol{\Sigma} = \left[\sum_{m=-M/2}^{M/2} \hat{\boldsymbol{S}}_d(f_m) \right] \Delta f = \frac{1}{NT} \left[\sum_{n=0}^{N-1} \boldsymbol{x}_n \boldsymbol{x}_n^H \right] T$$

These may differ slightly due to truncation and windowing of the autocovariance $\hat{\boldsymbol{R}}(\ell)$, and the coarseness of the frequency grid.

For a white noise process $\boldsymbol{x}_k$ with covariance $\boldsymbol{\Sigma}_x$, the mean "noise floor" of the diagonal terms in the PSD, when plotted per axis, should be $\boldsymbol{\Sigma}_x/M$. (A statistical statement is omitted.)

Results are not be valid if these simple checks are not passed.

Coherence Function

The coherence function between signals $\boldsymbol{x}_k$ and $\boldsymbol{u}_k$ is

$$\gamma(f) = \frac{|S_{xu}(f)|}{\sqrt{S_{xx}(f)}\sqrt{S_{uu}(f)}}$$

The Magnitude Square Coherence between signals $\boldsymbol{x}_k$ and $\boldsymbol{u}_k$ is

$$\mathsf{MSC}(f) = |\gamma(f)|^2 = \frac{|S_{xu}(f)|^2}{S_{xx}(f)S_{uu}(f)}$$

$$0 \leq |\gamma(f)| \leq 1$$

The Phase Coherence Function is

$$\Phi(f) = \arctan\Big(\mathsf{Im}(\gamma(f)), \mathrm{Re}(\gamma(f))\Big)$$

When x or u is a vector, the coherence functions are computed component-wise.

Example - PSD of a Sinusoid from Autocorrelation (1/2)

A deterministic sinusoidal sequence x_n is not WSS: Its mean is not constant and its autocorrelation depends on n.

A random sinusoidal process is WSS:

$$x_n = A\sin(2\pi f n T + \theta)$$

where A is a fixed amplitude and θ is a random phase uniformly distributed on $[0,\, 2\pi)$.

Its mean is constant: $$\mathcal{E}\{x_n\} = \int_0^{2\pi} A\sin(2\pi f n T + \theta)\,\frac{1}{2\pi}\,\mathrm{d}\theta = 0$$

Its autocorrelation depends only on m, not on n,

$$r_{xx}(m) = \mathcal{E}\{x_{n+m}x_n\} = \int_0^{2\pi} A\sin(2\pi f(n+m)T + \theta)\,A\sin(2\pi f n T + \theta)\,\frac{1}{2\pi}\,\mathrm{d}\theta$$

$$= \frac{A^2}{2}\cos(2\pi f m T)$$

Example - PSD of a Sinusoid from Autocorrelation (2/2)

For a sum of L independent sinusoids with amplitudes A_i, frequencies f_i, and phases θ_i,

$$r_{xx}(m) = \sum_{i=1}^{L} \frac{A_i^2}{2} \cos(2\pi f_i m T)$$

The PSD is

$$S_{xx}(f) = \sum_{i=1}^{L} \frac{A_i^2}{4} \left[\delta(f + f_i) + \delta(f - f_i)\right]$$

Integrate over frequency to get

$$\sigma_{xx}^2 = \sum_{i=1}^{L} \frac{A_i^2}{2}$$

Similar results are obtained for random A_i with $\mathcal{E}\{A_i^2\} = \sigma_i^2$ and $\mathcal{E}\{A_i A_j\} = 0$, $i \neq j$.

Tip: A pure tone is deterministic, but an exposure may begin at a random phase.

3.3B Time-Domain Definitions for Pointing Metrics (summary)

Metric	Time Domain
Accuracy	$\boldsymbol{\Sigma}_{\mathsf{A}} = \mathrm{cov}(\boldsymbol{p}) = \mathcal{E}\{\left[\boldsymbol{p}(t) - \mathcal{E}\{\boldsymbol{p}(t)\}\right]\left[\boldsymbol{p}(t) - \mathcal{E}\{\boldsymbol{p}(t)\}\right]^T\}$
Displacement	$\boldsymbol{\Sigma}_{\mathsf{D}} = \mathrm{cov}(\bar{\boldsymbol{p}}) = \mathcal{E}\{[\langle \boldsymbol{p}(t)\rangle_T][\langle \boldsymbol{p}(t)\rangle_T]^T\}$
Smear Rate	$\boldsymbol{\Sigma}_{\mathsf{R}} = \mathrm{cov}(\bar{\boldsymbol{v}}) = \mathcal{E}\{[\frac{12}{T^2}\langle t\boldsymbol{p}(t)\rangle_T][\frac{12}{T^2}\langle t\boldsymbol{p}(t)\rangle_T]^T\}$
Smear	$\boldsymbol{\Sigma}_{\mathsf{S}} = T^2\boldsymbol{\Sigma}_{\mathsf{R}}$
Jitter	$\boldsymbol{\Sigma}_{\mathsf{J}} = \mathcal{E}\{\langle \left[\boldsymbol{p}(t) - \langle \boldsymbol{p}(t)\rangle_T\right]\left[\boldsymbol{p}(t) - \langle \boldsymbol{p}(t)\rangle_T\right]^T\rangle_T\}$
P-P Stability	$\boldsymbol{\Sigma}_{\mathsf{PS}} = \mathcal{E}\{\left[\boldsymbol{p}(t) - \boldsymbol{p}(t - T_{\mathsf{PS}})\right]\left[\boldsymbol{p}(t) - \boldsymbol{p}(t - T_{\mathsf{PS}})\right]^T\}$ (Deprecated)
W-Stability	$\boldsymbol{\Sigma}_{\mathsf{WS}} = \mathcal{E}\{\left[\langle \boldsymbol{p}(t)\rangle_T - \langle \boldsymbol{p}(t - T_{\mathsf{WS}})\rangle_T\right]\left[\langle \boldsymbol{p}(t)\rangle_T - \langle \boldsymbol{p}(t - T_{\mathsf{WS}})\rangle_T\right]^T\}$

Average over the exposure interval of T seconds: $\langle \boldsymbol{x}(t)\rangle_T = \dfrac{1}{T}\displaystyle\int_{-T/2}^{T/2} \boldsymbol{x}(t_o + t)\,\mathrm{d}t$

T_{WS} is the time between image centroids

Direct Time-Domain vs Frequency Domain Pointing Metrics

- The time-domain and frequency domain definitions of the Pointing Performance Metrics are mathematically equivalent. See the appendices in [35].
- The time-domain calculation of the PPMs is less informative: Cumulative power vs. frequency and power in a frequency interval can be computed only by frequency domain analysis.
- Control system design for linear and linearized dynamics is inherently a frequency-domain exercise (except in trajectory optimization).
  - Frequency-domain analysis is preferred for pointing performance.
  - Time-domain analysis is useful for verification. Nonlinear or transient effects may be evaluated (assuming stationarity).

Difficulties in using Direct Time-Domain Pointing Metrics

- Although the pointing metrics are defined in continuous-time, they are evaluated from simulated discrete-time data. The integrals become sums.
- Difficulties include
  - There may not be enough samples in the exposure window.
  - Autocorrelations require data outside the window; the data may not be stationary.
  - Monte Carlo simulation is required to compute means, autocorrelations, and covariances (time consuming). $\Rightarrow$ Could compute the IM PSF and IM OTF directly.
    - Imaging intervals in a single run could be used, but the pointing motion (image motion) must be uncorrelated.
  - Computing relative contributions of disturbance and noise sources requires simulation runs for each source (with other sources off).
  - Sensitivity analysis is time consuming, requiring additional simulation.

4. Linearized Optical Model

An $k \times 1$ vector of translational and rotational displacements $\boldsymbol{d}$ of optical elements interior to the optical system, including the focal plane, (or at the mounting for a pinhole camera model) in terms of the mode shapes and slopes $\boldsymbol{\Phi_d}$ and modal displacements $\boldsymbol{q}$, is

$$\boldsymbol{d} = \boldsymbol{\Phi_d}\,\boldsymbol{q}$$

The image motion (or LOS motion) are computed from a geometric optical model

$$\boldsymbol{p} = \boldsymbol{c}(\boldsymbol{d})$$

Since $\boldsymbol{d}$ is small, and if $\boldsymbol{c}(\boldsymbol{0}) = \boldsymbol{0}$, the image motion is

$$\boldsymbol{p} = C_{\boldsymbol{d}}\,\boldsymbol{d} = C_{\boldsymbol{d}}\,\boldsymbol{\Phi_d}\,\boldsymbol{q}$$

where $C_{\boldsymbol{d}}$ is a $2 \times n$ sensitivity matrix,

$$C_{\boldsymbol{d}} = \left.\frac{\partial \boldsymbol{c}}{\partial \boldsymbol{d}^T}\right|_{\boldsymbol{d}\,=\,\boldsymbol{d}_0}$$

$\boldsymbol{d}_0$ is a nominal displacement (e.g., misalignment, displacement after gravity off-loading)

Time-Domain Evaluation of Image Motion

The modal displacement vector $\boldsymbol{q}(t)$ is the solution to

$$\ddot{\boldsymbol{q}} + D\dot{\boldsymbol{q}} + \Lambda \boldsymbol{q} = \boldsymbol{\Phi}_{\boldsymbol{\tau}} \boldsymbol{\tau}(\boldsymbol{q}, t) + \boldsymbol{\Phi}_{\boldsymbol{f}} \boldsymbol{f}(t)$$

$\boldsymbol{\tau}$ is a vector of feedback control forces/torques, $\boldsymbol{f}$ is a vector of disturbance forces/torques.
The image motion (LOS pointing) is

$$\begin{aligned} \boldsymbol{p}(t) &= C_{\boldsymbol{d}}\, \boldsymbol{d}(t) \\ &= C_{\boldsymbol{d}}\, \boldsymbol{\Phi}_{\boldsymbol{d}}\, \boldsymbol{q}(t) \end{aligned}$$

The equations are linear, so we can sum individual contributions due to the $\boldsymbol{f}^{(i)}(t)$

$$\begin{aligned} \boldsymbol{p}^{(i)}(t) &= C_{\boldsymbol{d}}\, \boldsymbol{d}^{(i)}(t) \\ &= C_{\boldsymbol{d}}\, \boldsymbol{\Phi}_{\boldsymbol{d}}^{(i)}\, \boldsymbol{q}^{(i)}(t) \end{aligned} \qquad \Longrightarrow \quad \boldsymbol{p}(t) = \sum_i \boldsymbol{p}^{(i)}(t)$$

Disturbances are deterministic or stochastic/statistically independent (a mild assumption)

$$\boldsymbol{P}_{\boldsymbol{p}}(\omega) = \sum_i \boldsymbol{P}_{\boldsymbol{p}}^{(i)}(\omega) \quad \Longrightarrow \quad \boldsymbol{\Sigma}_{\mathsf{X}} = \sum_i \boldsymbol{\Sigma}_{\mathsf{X}}^{(i)}$$

Frequency Domain Evaluation of Image Motion

Obtain the closed-loop transfer function $G(j\omega)$ for the structural modes.

The frequency response of the displacements is

$$\boldsymbol{d}(\omega) = \boldsymbol{\Phi_d}\, G(j\omega)\, \boldsymbol{\Phi_f} \boldsymbol{f}(\omega)$$

The frequency response at the LOS (or focal plane) is

$$\begin{aligned} \boldsymbol{p}(\omega) &= C_{\boldsymbol{d}}\, \boldsymbol{d}(\omega) \\ &= C_{\boldsymbol{d}}\, \boldsymbol{\Phi_d}\, G(j\omega)\, \boldsymbol{\Phi_f} \boldsymbol{f}(\omega) \end{aligned}$$

The equations are linear, so we can sum individual contributions due to the $\boldsymbol{f}^{(i)}(\omega)$

$$\boldsymbol{p}^{(i)}(\omega) = C_{\boldsymbol{d}}\, \boldsymbol{\Phi_d}\, G(j\omega)\, \boldsymbol{\Phi}_{\boldsymbol{f}}^{(i)} \boldsymbol{f}^{(i)}(\omega) \quad \Longrightarrow \quad \boldsymbol{p}(\omega) = \sum_i \boldsymbol{p}^{(i)}(\omega)$$

Disturbances are deterministic or stochastic/statistically independent (a mild assumption)

$$\boldsymbol{P}_{\boldsymbol{p}}(\omega) = \sum_i \boldsymbol{P}_{\boldsymbol{p}}^{(i)}(\omega) \quad \Longrightarrow \quad \boldsymbol{\Sigma}_{\mathsf{X}} = \sum_i \boldsymbol{\Sigma}_{\mathsf{X}}^{(i)}$$

No Optical Model Available

- There is usually an initial baseline or reference design for a camera, updated periodically
  - Rarely is there no information about an optical payload.
- In some situations an optical model is not available or can't be used because either
  - The optical system has not yet been designed, behind schedule, not released, or
  - The pointing requirements are at the optical payload-bus mounting interface,
  - Contractual or proprietary reasons, or programmatic or institutional reasons.
  - The instrument designer can't give it to the control system designer for security reasons (if the optical system and its pointing performance are SCI).
- In any of those situations, there are ways to proceed
  - Evaluate the pointing motion at the mounting interface, or
  - Use a pinhole camera model and motion at the boresight or mounting interface, or
  - Evaluate the displacements $\boldsymbol{d}(t)$ or $\boldsymbol{d}(\omega)$ and compute the power spectrum $\boldsymbol{P}_{\boldsymbol{d}}(\omega)$.

Structural Model but No Geometric Optical Model $C_{\boldsymbol{d}}$

$\boldsymbol{d}$ is of dimension $n > 2$ (usually $n \gg 2$), so we prefer to compute the power spectrum of $\boldsymbol{p}$.

In the absence of an optical model, compute $\boldsymbol{d}$,

$$\boldsymbol{d}^{(i)}(t) = \boldsymbol{\Phi}_{\boldsymbol{d}}\, \boldsymbol{q}^{(i)}(t) \quad \Longrightarrow \quad \boldsymbol{d}(t) = \sum_i \boldsymbol{d}^{(i)}(t)$$

$$\boldsymbol{d}^{(i)}(\omega) = \boldsymbol{\Phi}_{\boldsymbol{d}}\, G(j\omega)\, \boldsymbol{\Phi}_{\boldsymbol{f}}^{(i)}\, \boldsymbol{f}^{(i)}(\omega) \quad \Longrightarrow \quad \boldsymbol{d}(\omega) = \sum_i \boldsymbol{d}^{(i)}(\omega)$$

Compute the power spectrum of $\boldsymbol{d}$, and if you know the exposure time T, compute $\boldsymbol{\Sigma}_{\boldsymbol{d},\mathsf{X}}$

$$\boldsymbol{P}_{\boldsymbol{d}}(\omega) = \sum_i \boldsymbol{P}_{\boldsymbol{d}}^{(i)}(\omega) \quad \Longrightarrow \quad \boldsymbol{\Sigma}_{\boldsymbol{d},\mathsf{X}} = \sum_i \boldsymbol{\Sigma}_{\boldsymbol{d},\mathsf{X}}^{(i)}$$

If you have a pinhole camera model, $\boldsymbol{d} = \boldsymbol{\theta}$, compute $\boldsymbol{P}_{\boldsymbol{\theta}}(\omega)$ and $\boldsymbol{\Sigma}_{\boldsymbol{\theta},\mathsf{X}}$

Structural Model but No Geometric Optical Model $C_{\boldsymbol{d}}$ (cont'd)

- If the optical system is SCI, you won't know the exposure time(s) or the time between exposures, so you can't compute $\boldsymbol{\Sigma}_{\boldsymbol{d},\mathsf{X}}$.
  - $\boldsymbol{\Sigma}_{\boldsymbol{d},\mathsf{X}}$ cannot be evaluated when the exposure time is not known.
  - You can either compute $\boldsymbol{\Sigma}_{\boldsymbol{d},\mathsf{X}}$ parametrically over a range of exposure times, or
  - Throw $\boldsymbol{P}_{\boldsymbol{d}}(\omega)$ over the transom for the instrument designer to compute $\boldsymbol{\Sigma}_{\boldsymbol{p},\mathsf{X}}$

$$\boldsymbol{P}_{\boldsymbol{p}}(\omega) = C_{\boldsymbol{d}}\, \boldsymbol{P}_{\boldsymbol{d}}(\omega)\, C_{\boldsymbol{d}}^{T}$$

$$\boldsymbol{\Sigma}_{\boldsymbol{p},\mathsf{X}} = C_{\boldsymbol{d}}\, \boldsymbol{\Sigma}_{\boldsymbol{d},\mathsf{X}}\, C_{\boldsymbol{d}}^{T}$$

  - Evaluate relative contributions of each disturbance source parametrically over a range of exposure times.

6. Relative Contribution Analysis

- Provides an effective and efficient means to evaluate pointing system performance.
- Provides a means to allocate/reallocate a component-level error budget.
- Covariances are additive for *statistically independent* disturbance (vector) inputs.
- PPMs can be computed for each individual noise and disturbance source, then added.
  - Allows for changes in sensor and actuator models without recomputing everything.
  - Allows for changes in operating conditions & parameters, e.g., RW speeds, damping.
  - Gives insight into sensitivity to disturbances at various frequencies & amplitudes.
- Relative contributions to the PMs $\boldsymbol{\mu}$, $\boldsymbol{\rho}$ or $\boldsymbol{s}$, $\boldsymbol{\Sigma}_{\mathrm{X}}$ from each source are easily evaluated for various operating conditions and exposure times.
  - worst offenders
  - sensitive frequency intervals
  - worst-case sensitivities
  - cumulative power over frequency
  - power in a frequency interval
  - relative power in a frequency interval
- Weighting functions W_{X} change with exposure time, hence the $\boldsymbol{\Sigma}_{\mathrm{X}}^{(i)}$, *but not the* $\boldsymbol{S}(\omega)$.

Relative Contribution

- In general, a combination of pointing covariances from time-domain, frequency domain, and stochastic disturbance sources will be computed and added.
- The relative contribution of each disturbance source (i) can be evaluated and ranked

$$r^i_{\mathsf{X}} = \frac{\bar{\sigma}(\boldsymbol{\Sigma}^{(i)}_{\mathsf{X}})}{\bar{\sigma}(\boldsymbol{\Sigma}_{\mathsf{X}})} \times 100\% \qquad \text{or} \qquad r^i_{\mathsf{X}} = \frac{\mathrm{tr}(\boldsymbol{\Sigma}^{(i)}_{\mathsf{X}})}{\mathrm{tr}(\boldsymbol{\Sigma}_{\mathsf{X}})} \times 100\%$$

  Smear $(\boldsymbol{s})$ and displacement $(\boldsymbol{\mu})$ can be treated similarly.
- Attention can be given to the major contributors.
  - $\boldsymbol{\Sigma}_{\mathsf{X}}$ *must include all sources* for the ratio to make sense!
  - Use estimates or allocations as proxies for the non-evaluated $\boldsymbol{\Sigma}^{(i)}_{\mathsf{X}}$.
  - Or use an allocation (plus margin) for $\boldsymbol{\Sigma}_{\mathsf{X}}$ or the missing $\boldsymbol{\Sigma}^{(i)}_{\mathsf{X}}$.
- Optical systems typically operate over a range of exposure times, so multiple $\boldsymbol{\Sigma}^{(i)}_{\mathsf{X}}$, $\boldsymbol{\Sigma}_{\mathsf{X}}$, and r^i_{X} have to be computed. Consider how results change with $W_{\mathsf{X}}(\omega T)$ and T.
- The r^i_{X} are not square root of the ratios because OTFs are functions of the covariance.

Cumulative Power

- Cumulative Weighted Power ($M+1$ frequency components in the discrete PSD)

$$\boldsymbol{P}_{\mathsf{X}}(m) = \sum_{i=-m}^{m} \boldsymbol{S}(\omega_i) W_{\mathsf{X}}(\omega_i T) \,, \qquad 0 \le m \le M$$

  (Expressed as an integral for a continuous power spectral density.)

  Plot $\bar{\sigma}(\boldsymbol{P}_{\mathsf{X}}(m))$ or $\mathrm{tr}(\boldsymbol{P}_{\mathsf{X}}(m))$ versus m.

- Relative Cumulative Weighted Power

$$q_{\mathsf{X}}(m) = \frac{\bar{\sigma}(\boldsymbol{P}_{\mathsf{X}}(m)}{\bar{\sigma}(\boldsymbol{P}_{\mathsf{X}}(M))} \qquad \text{or} \qquad q_{\mathsf{X}}(m) = \frac{\mathrm{tr}(\boldsymbol{P}_{\mathsf{X}}(m)}{\mathrm{tr}(\boldsymbol{P}_{\mathsf{X}}(M))}$$

  Note: $\boldsymbol{P}_{\mathsf{X}}(M) \equiv \boldsymbol{\Sigma}_{\mathsf{X}}$ is the total cumulative power.

Power in a Frequency Interval

- The power in a frequency interval $[\omega_m, \omega_n]$ is

$$\boldsymbol{P}_{\mathsf{X}}(m,n) = \sum_{i=-n}^{-m} \boldsymbol{S}(\omega_i) W_{\mathsf{X}}(\omega_i T) + \sum_{i=m}^{n} \boldsymbol{S}(\omega_i) W_{\mathsf{X}}(\omega_i T)\,, \qquad 0 \le m \le M$$

- The Relative Weighted Power in a frequency interval is computed by the same formula as the Relative Cumulative Weighted Power

What to do If Pointing Requirements are not Met

- If the IM OTF requirements are met, it may be less important that a Pointing Petric exceeds its requirement.
- Determine which IM OTF exceeds its requirements (displacement, smear, jitter), then focus on the corresponding Pointing Metric.
  - Focus on the most offending responses to each disturbance, based on the relative contribution analysis.
  - Locate the frequency range where the weighting function is large.
  - Consider operational changes to mitigate the disturbance in the sensitive frequency range (e.g., avoid imaging during thermal transient on S/A, change exposure time).
  - Consider hardware modifications to reduce the disturbance amplitude or shift its frequency to a less sensitive range (e.g., improved RW balancing, change structural modes).
  - Consider design changes (e.g., change structural modes, higher speed RW).

Part 5: Reaction Wheel Disturbance Model

6 DOF Reaction Wheel Dynamics Model [39, 40]

Dynamics model exhibits 3 vibration modes axial translation, radial translation, radial rocking (negative whirl and positive whirl modes)

Natural frequencies of the vibrational modes depend on the wheel speed

Torque noise includes bearing noise, motor ripple, many other effects.

The model is semi-analytical: Its parameters are determined from design data, specifications, and test data.

The model permits simulation and analysis of pointing motion over a range of wheel speeds.

Figure is from Fig. 4-5 in [39]

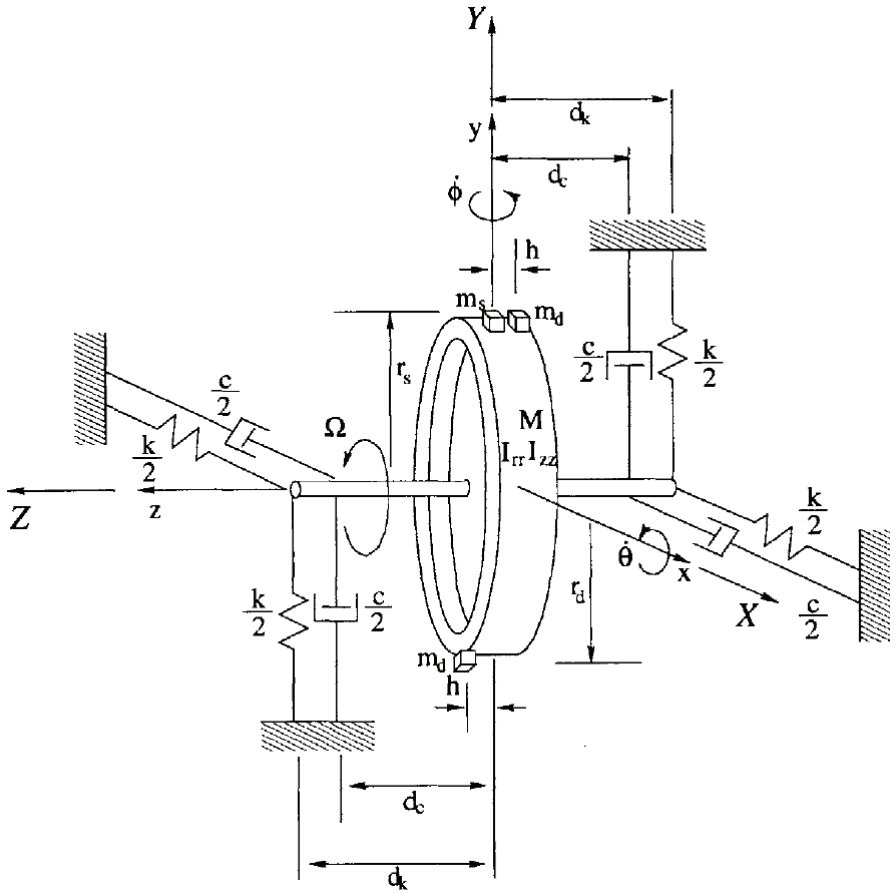

Semi-Analytical Reaction Wheel Model

Semi-Analytical model, aka "empirical", "hybrid", or "extended" model: Additional harmonics and sub-harmonics g_i, h_j and amplitudes B_i, C_j $(i \neq i^* \;\; j \neq j^*)$ and noise parameters are identified from test data.

Static and Dynamic imbalance coefficients ($i*$, $j*$ index the fundamental harmonics)

$B_{i^*} = U_s$	$g_{i^*} = 1$	$U_s = m_s r_s$	static imbalance
$C_{j^*} = U_d$	$h_{j^*} = 1$	$U_d = 2 m_d r_d h$	dynamic imbalance

and in addition

D_{ℓ^*}	$\gamma_{\ell^*} = 1$	axial force coefficient

Certain harmonics can be associated with bearing and race geometry.
The axial force is (assumed to be) driven by imbalances.

Reaction Wheel Radial Translation Motion $x(t)$, $y(t)$

$$\begin{bmatrix} M & 0 \\ 0 & M \end{bmatrix} \begin{bmatrix} \ddot{x} \\ \ddot{y} \end{bmatrix} + \begin{bmatrix} b & 0 \\ 0 & b \end{bmatrix} \begin{bmatrix} \dot{x} \\ \dot{y} \end{bmatrix} + \begin{bmatrix} k & 0 \\ 0 & k \end{bmatrix} \begin{bmatrix} x \\ y \end{bmatrix} = \sum_{i=1}^{m} B_i \Omega^2 \begin{bmatrix} -\sin(g_i \Omega t) \\ \cos(g_i \Omega t) \end{bmatrix} + \begin{bmatrix} w_x(t) \\ w_y(t) \end{bmatrix}$$

which can be written as two equations with a 90° phase relationship.

The radial translation mode, damping ratio, and poles are

$$\omega_T = \sqrt{k/M} \qquad \text{modal frequency, radial translation}$$

$$\zeta_T = b_z / 2\omega_T M \qquad \text{damping ratio}$$

$$\omega_{1,2} = -\zeta_T \omega_T \pm j\omega_T \sqrt{1 - \zeta_T^2} \qquad \text{pole frequencies}$$

total mass $M = M_o + m_s + 2m_d$, wideband noise $w_x(t)$, $w_y(t)$

Reaction Wheel Cross-Axial Rotation Motion $\theta(t)$, $\phi(t)$

$$\begin{bmatrix} I_\theta & \frac{1}{2}\tilde{I}\sin(2\Omega t) \\ \frac{1}{2}\tilde{I}\sin(2\Omega t) & I_\phi \end{bmatrix} \begin{bmatrix} \ddot{\theta} \\ \ddot{\phi} \end{bmatrix} + \begin{bmatrix} c - \Omega\tilde{I}\sin(2\Omega t) & \Omega\big(I_{zz} + 2\tilde{I}\cos^2(\Omega t)\big) \\ -\Omega\big(I_{zz} + 2\tilde{I}\sin^2(\Omega t)\big) & c + \Omega\tilde{I}\sin(2\Omega t) \end{bmatrix} \begin{bmatrix} \dot{\theta} \\ \dot{\phi} \end{bmatrix}$$

$$+ \begin{bmatrix} \kappa & 0 \\ 0 & \kappa \end{bmatrix} \begin{bmatrix} \theta \\ \phi \end{bmatrix} = \sum_{j=1}^{n} C_j \Omega^2 \begin{bmatrix} \cos(h_j \Omega t) \\ \sin(h_j \Omega t) \end{bmatrix} + \begin{bmatrix} w_\theta(t) \\ w_\phi(t) \end{bmatrix}$$

$$\begin{aligned} I_\theta &= I_{rr} + 2m_d h^2 + \tilde{I}\cos^2(2\Omega t) \\ I_\phi &= I_{rr} + 2m_d h^2 + \tilde{I}\sin^2(2\Omega t) \\ I_{zz} &= I_{zz} + 2\tilde{I}\cos^2(\Omega t) \\ \tilde{I} &= 2m_d r_d^2 + m_s r_s^2 \end{aligned}$$

rotational damping $c = bd_k^2$, stiffness $\kappa = kd_c^2$, wideband noise $w_\theta(t)$, $w_\phi(t)$

Reaction Wheel Cross-Axial Rotation Motion – LTI Model

$$\cos^2(2\Omega t) = \tfrac{1}{2} + \tfrac{1}{2}\cos(2\Omega t) \simeq \tfrac{1}{2}$$
$$\sin^2(2\Omega t) = \tfrac{1}{2} - \tfrac{1}{2}\cos(2\Omega t) \simeq \tfrac{1}{2}$$

Linear time-invariant (LTI) approximation

$$\begin{aligned} I_\theta &\simeq I_{rr} + 2m_d h^2 + \tfrac{1}{2}\tilde{I} \\ I_\phi &\simeq I_{rr} + 2m_d h^2 + \tfrac{1}{2}\tilde{I} \\ I_z &\simeq I_{zz} + \tilde{I} \end{aligned} \qquad \text{or} \qquad \begin{aligned} I_\theta &\simeq I_{rr} \\ I_\phi &\simeq I_{rr} \\ I_z &\simeq I_{zz} \end{aligned}$$

$$\begin{bmatrix} I_\theta & \frac{1}{4}\tilde{I} \\ \frac{1}{4}\tilde{I} & I_\phi \end{bmatrix} \begin{bmatrix} \ddot{\theta} \\ \ddot{\phi} \end{bmatrix} + \begin{bmatrix} c - \frac{1}{2}\Omega\tilde{I} & \Omega I_z \\ -\Omega I_z & c + \frac{1}{2}\Omega\tilde{I} \end{bmatrix} \begin{bmatrix} \dot{\theta} \\ \dot{\phi} \end{bmatrix} + \begin{bmatrix} \kappa & 0 \\ 0 & \kappa \end{bmatrix} \begin{bmatrix} \theta \\ \phi \end{bmatrix} = \sum_{j=1}^{n} C_j \Omega^2 \begin{bmatrix} \cos(h_j \Omega t) \\ \sin(h_j \Omega t) \end{bmatrix} + \begin{bmatrix} w_\theta(t) \\ w_\phi(t) \end{bmatrix}$$

positive, negative whirl modes (rocking modes) $\omega_r^{\pm} = \pm \dfrac{\Omega I_{zz}}{2I_{rr}} + \sqrt{\left(\dfrac{\Omega I_{zz}}{2I_{rr}}\right)^2 + \dfrac{\kappa}{I_{rr}}}$

Rotational Particular Solutions, Rocking Mode Resonance

The frequencies and damping ratios where the harmonic frequencies are equal to the rocking modes are obtained by setting $\omega_{r_j}^{\pm} = \omega_j = h_j\Omega$ and solving for $\omega_{r_j}^{\pm}$,

$$(\omega_{r_j}^{\pm})^2 = \frac{h_j\kappa}{h_j I_{rr} \mp I_{zz}}$$

$$\zeta_{r_j}^{\pm} = \frac{h_j c}{2\omega_{r_j}^{\pm}(h_j I_{rr} + I_{zz})}$$

The particular solutions to the rotational EOM at the harmonic frequency $\omega_{r_j} = h_j\Omega$ are

$$\theta_{p_j}(t) = \frac{h_j B_j \Omega^2/(h_j I_{rr} - I_{zz})}{\left(2\omega_i\zeta_{r_j}^{+}\omega_{r_j}^{+}\right)^2 + \left(\omega_j^2 - (\omega_{r_j}^{+})^2\right)^2}\left[2\omega_j\zeta_{r_j}^{+}\omega_{r_j}^{+}\sin\omega_j t - \left(\omega_j^2 - (\omega_{r_j}^{+})^2\right)\cos\omega_j t\right]$$

$$\phi_{p_j}(t) = \frac{-h_j B_j \Omega^2/(h_j I_{rr} - I_{zz})}{\left(2\omega_i\zeta_{r_j}^{+}\omega_{r_j}^{+}\right)^2 - \left(\omega_j^2 - (\omega_{r_j}^{+})^2\right)^2}\left[2\omega_j\zeta_{r_j}^{+}\omega_{r_j}^{+}\cos\omega_j t + \left(\omega_j^2 - (\omega_{r_j}^{+})^2\right)\sin\omega_j t\right]$$

Radial Translation Particular Solutions, Resonant Frequencies

The particular solutions to the translational EOM at the harmonic frequency $\omega_i = g_i\Omega$ are

$$x_{p_i}(t) = \frac{C_i\Omega/M}{\left(2\omega_i\zeta_T\omega_T\right)^2 + \left(\omega_i^2 - \omega_T^2\right)^2}\left[2\omega_i\zeta_T\omega_T\cos\omega_i t + \left(\omega_i^2 - \omega_T^2\right)\sin\omega_i t\right]$$

$$y_{p_i}(t) = \frac{C_i\Omega/M}{\left(2\omega_i\zeta_T\omega_T\right)^2 + \left(\omega_i^2 - \omega_T^2\right)^2}\left[2\omega_i\zeta_T\omega_T\sin\omega_i t - \left(\omega_i^2 - \omega_T^2\right)\cos\omega_i t\right]$$

The denominator has two roots where resonance occurs,

$$(\omega_i^{\pm})^2 = \omega_T^2\left(1 - 2\zeta_T^2\right) \pm 2\zeta_T\omega_T^2\sqrt{\zeta_T^2 - 1}$$

The wheel speeds at resonance are $\Omega^{\pm} = \omega_i^{\pm}/g_i$. When $\zeta_T \ll 1$ we have $\omega_i \simeq \omega_T$.
The total response, excluding the homogeneous solution, is

$$x(t) = \sum_{i=1}^{m} x_{p_i}(t) \qquad y(t) = \sum_{i=1}^{m} y_{p_i}(t)$$

PSD of Reaction Wheel Disturbances

The contour plot shows the PSD in $(\text{N-m})^2/\text{s}$ and frequency in Hz of several harmonic radial torque disturbances as a function of wheel speed in revolutions per second (RPS, Hz).

The nearly vertical lines that begin at 60 RPS are the negative and positive whirl (rocking) modes. A strong resonance occurs at wheel speeds where the rocking modes cross a harmonic frequency, that is, where the harmonic frequency equals a rocking mode frequency.

Torque noise is also seen in the contour plot.

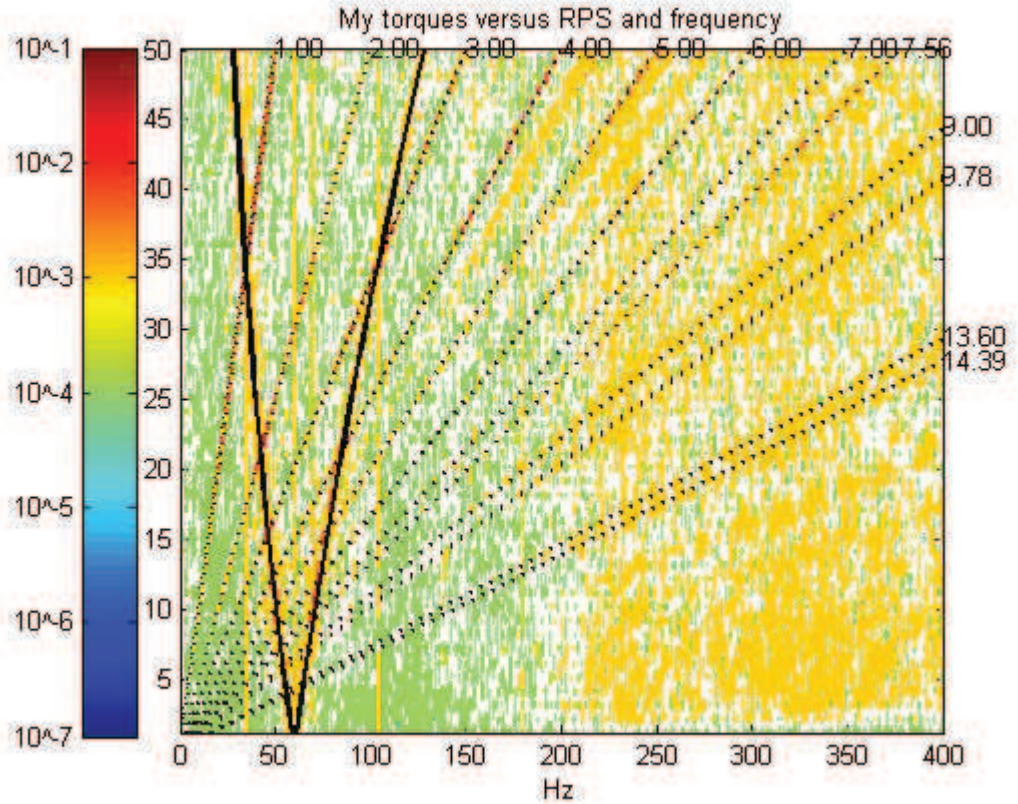

Figure 13 in Liu, et al., 2007 [41]

Reaction Wheel Axial Translation Motion $z(t)$

The axial disturbance force is modeled as

$$F_z(t) = \sum_{\ell=1}^{p} F_{z_\ell} = \sum_{\ell=1}^{p} D_\ell \cos(\gamma_\ell \Omega\, t + \varphi_\ell) + w_z(t)$$

where D_ℓ is the axial force coefficient, γ_ℓ is the ℓth harmonic, and φ_ℓ is the phase angle w.r.t. the radial and rotational disturbance forces, and $w_z(t)$ is wideband noise.
Second-order spring-mass model assumed for axial translation

$$M\ddot{z} + b_z\dot{z} + k_z z = F_z(t)$$

$$\omega_z = \sqrt{k_z/M} \qquad \text{modal frequency, radial translation}$$

$$\zeta_z = b/2\omega_z M \qquad \text{damping ratio}$$

$$\omega_{1,2} = -\zeta_z\omega_z \pm j\omega_z\sqrt{1-\zeta_z^2} \qquad \text{pole frequencies}$$

Reaction Wheel Output Force and Torque Disturbances

$$F_x(t) = kx(t) \qquad T_x(t) = \kappa\theta(t)$$
$$F_y(t) = ky(t) \qquad T_y(t) = \kappa\phi(t)$$
$$F_z(t) = k_z z(t) \qquad T_z(t) = 0$$

The axial torque disturbance T_z due to imbalance is negligible [39].

Motor torque noise is added to T_z.

Wideband noise includes bearing noise. Bearing noise is due to bearing imperfections and lubricant dynamics.

Angular rate vector $\boldsymbol{\omega} = \begin{bmatrix} \dot{\theta} \\ \dot{\phi} \\ \Omega \end{bmatrix}$

PSD of Reaction Wheel Force and Torque

The PSD of the output disturbances is obtained directly from the analytical solutions from the translational and rotational disturbance responses.

$$\boldsymbol{u}_i(t) = \begin{bmatrix} \boldsymbol{F}_i(t) \\ \boldsymbol{T}_i(t) \end{bmatrix} \qquad \boldsymbol{u}(t) = \begin{bmatrix} \boldsymbol{F}(t) \\ \boldsymbol{T}(t) \end{bmatrix} = \sum_{i=0}^{q} \boldsymbol{u}_i(t)$$

$$\boldsymbol{S}_{u,i}(\omega) = \begin{bmatrix} \boldsymbol{S}_{FF,i}(\omega) & \boldsymbol{S}_{FT,i}(\omega) \\ \boldsymbol{S}_{TF,i}(\omega) & \boldsymbol{S}_{TT,i}(\omega) \end{bmatrix} \qquad \boldsymbol{S}_{u}(\omega) = \begin{bmatrix} \boldsymbol{S}_{FF}(\omega) & \boldsymbol{S}_{FT}(\omega) \\ \boldsymbol{S}_{TF}(\omega) & \boldsymbol{S}_{TT}(\omega) \end{bmatrix} = \sum_{i=0}^{q} \boldsymbol{S}_{u,i}(\omega)$$

$$\boldsymbol{S}_{u,i}(\omega) = \mathsf{FT}\{\boldsymbol{u}_i(t)\boldsymbol{u}_i^T(t)\}$$

Time Domain Fcn	**Fourier Transform**	
$\cos \omega t$	$\pi[\delta(\omega + \omega_o) + \delta(\omega - \omega_o)]$	$\delta(\omega) =$ Dirac delta function
$\sin \omega t$	$j\pi[\delta(\omega + \omega_o) - \delta(\omega - \omega_o)]$	$\int_{-\infty}^{\infty} \delta(\omega)\, \mathrm{d}\omega = 1$

Example 1 – Back of the Envelope Calculation

Structural dynamics model, rigid body

$$H(s) = \frac{1}{Js^2}$$

Sinusoidal disturbance from reaction wheel imbalance, n wheels at different speeds ω_k

$$d(t) = \sum_{k=1}^{n} A_k \sin \omega_k t \qquad A_k = (U_d + rU_s)\omega_k^2$$

$U_d =$ dynamic imbalance, $U_s =$ static imbalance, $r =$ moment arm length

Power Spectral Density (PSD) of the disturbance

$$|D(\omega)|^2 = \sum_{k=1}^{n} \frac{A_k^2}{2} \pi \left[\delta(\omega + \omega_k) + \delta(\omega - \omega_k)\right]$$

$\delta(\omega) =$ Dirac delta function, $\int_{-\infty}^{\infty} \delta(\omega)\, \mathrm{d}\omega = 1$

Example 1 (cont'd)

Jitter Variance

$$\sigma_{\text{J}}^2 = \frac{1}{2\pi}\int_{-\infty}^{\infty} \left|H(j\omega)\right|^2 \left|D(\omega)\right|^2 W_{\text{J}}(\omega T)\,\mathrm{d}\omega$$

$$= \sum_{k=1}^{n} \left|H(j\omega_k)\right|^2 \frac{A_k^2}{2} W_{\text{J}}(\omega_k T)$$

$$= 2\sum_{k=1}^{n} \left|\frac{1}{-J\omega_k^2}\right|^2 \frac{1}{2}\left((U_d + rU_s)\omega_k^2\right)^2 W_{\text{J}}(\omega_k T)$$

$$= \left(\frac{U_d + rU_s}{J}\right)^2 \sum_{k=1}^{n} W_{\text{J}}(\omega_k T)$$

Example 2 – Back of the Envelope Calculation

Structural dynamics model, rigid body + flexible body mode

$$H(s) = \frac{1}{Js^2} + \frac{\phi_o \phi_i}{s^2 + 2\zeta\omega_k^2 s + \omega_k^2}$$

Sinusoidal disturbance due to reaction wheel imbalance, wheel k at speed ω_k

$$d(t) = A_k \sin \omega_k t \qquad A_k = (U_d + rU_s)\omega_k^2$$

$U_d =$ dynamic imblance, $U_s =$ static imbalance, $r =$ moment arm length

Power Spectral Density (PSD) of the disturbance

$$|D(\omega)|^2 = \sum_{k=1}^{n} \frac{A_k^2}{2} \pi \left[\delta(\omega + \omega_k) + \delta(\omega - \omega_k)\right]$$

$\delta =$ Dirac delta function, $\int_{-\infty}^{\infty} \delta(\omega)\, \mathrm{d}\omega = 1$

Example 2 (cont'd)

Jitter Variance

$$\sigma_{\text{J}}^2 = \frac{1}{2\pi}\int_{-\infty}^{\infty} \left|H(j\omega)\right|^2 |D(\omega)|^2 W_{\text{J}}(\omega T)\,\mathrm{d}\omega$$

$$= \sum_{k=1}^{n} \left|H(j\omega_k)\right|^2 \frac{A_k^2}{2} W_{\text{J}}(\omega_k T)$$

$$= 2\left|\frac{1}{-J\omega_k^2} + \frac{\phi_o\phi_i}{j2\zeta\omega_k^2}\right|^2 \frac{1}{2}\left((U_d + rU_s)\omega_k^2\right)^2 W_{\text{J}}(\omega_k T)$$

$$= (U_d + RU_s)^2 \left[\left(\frac{1}{J}\right)^2 + \left(\frac{\phi_o\phi_i}{2\zeta}\right)^2\right] W_{\text{J}}(\omega_k T)$$

In a preliminary analysis, flexible-body modes can be treated by assuming some modal gain and damping so that $20\log(\phi_o\phi_i/2\zeta)$ is, for example, 30 or 40 dB

Part 6: Summary & Recommendations

Summary of Pointing Performance Analysis Methodology

1. The statistical Image Motion OTF describes the average OTF due to image motion. IM OTF requirements translate (in a nonlinear way) into requirements on shift, smear, and jitter covariance. A lower bound on the IM OTF, or a minimum image resolution and minimum MTF area, should be specified with a confidence level. It's likely that margin is already built into an IM OTF requirement.
2. The IM OTFs augment traditional deterministic and Monte Carlo methods of optical payload performance analysis.
3. Identify and model all disturbance sources, steady-state and transient. Make a chart of disturbance frequency bands. Classify steady-state disturbances as tonal fixed (tunable, non-tunable, variable) including harmonics, wide band/broadband/stochastic (stationary). Specify sweep rate of tonal variable.
4. Develop time domain and frequency domain models of disturbance sources, discrete or continuous.
5. Develop a continuous-time, discrete-time, or continuous-discrete model of the system. (Controller is discrete, plant is continuous.) Be careful with model conversions when stochastic inputs are involved.
6. Vary wheel speeds to find the average, median, worst-case responses. Use knowledge of damped natural frequencies and modal gain of the structure to hit peak resonances. Note: Transient response is smaller, e.g., frequency sweep through a mode.

Pointing Performance Analysis Summary (cont'd)

7. Evaluate the power spectral density of the disturbance response. Then weight and sum to get covariance matrices (the PPMs).
8. The covariance response to continuous or discrete sensor noise (white noise) input can be evaluated as the solution to a Lyapunov equation. Frequency weighting functions can be included, but must be approximated by rational transfer functions. (However, see [30].)
9. Determine the sensitivity of outputs to parameters such as modal frequency, modal damping, coupled damping, modal gain, and disturbance amplitude and frequency. Sensitivity may have to be evaluated at various nominal parameters. Sensitivity analysis is essential to performance analysis.
10. Evaluate the closed-loop response from each disturbance input to each output at critical locations such as star trackers, gyros, accelerometers, and payload focal plane (or LOS if no payload model is available).
11. Evaluate the relative contribution of each disturbance source to the overall performance.
12. Evaluate performance under various operating conditions (e.g., wheel speeds, control modes, BOL, EOL) and various geometrical configurations (e.g., SA rotation angle).

⚠ Cautions – Avoiding Problems

- Control system design is inherently a frequency-domain exercise. PPMs are most efficiently and accurately evaluated by using frequency response analysis.
- Frequency-domain and time-domain formulas apply to deterministic and stochastic signals.
- The weighting functions $W_{\mathsf{X}}(\omega)$ weight the power spectrum $\boldsymbol{S}(\omega)$, not an amplitude spectrum
  For example, the jitter weighting function $W_{\mathsf{J}}(\omega)$ does not apply to the structural response $\boldsymbol{q}$.
- The weighting functions are H_2 weightings, not H_∞ weightings.
- Frequency-domain and time-domain formulas for the PPMs are (theoretically) equivalent.
  Frequency domain methods are preferred for most pointing error analyses.
- Time-domain analysis can be slow and inaccurate due to time scales. Ensemble data (Monte Carlo or segmented data) may be required. Time-domain analysis can be used for specific cases and as a check on frequency-domain and Lyapunov analyses.
- Frequency-domain and time-domain resolution do not have to be uniform when using superposition of statistically independent disturbance responses. They have to be small enough to faithfully simulate essential features of pointing motion and image motion. Frequency resolution results from the finite length of a sampled-data record.

⚠ Cautions (cont'd)

- The error weighting functions have to be approximated by rational transfer functions (Laplace transforms) to use linear control system analysis methods such as state-space models and rational transfer functions. Be cognizant of approximation errors affecting results of analyses.
- Don't confuse the power spectrum and power spectral density. Software packages may not provide the proper scaling.
- When computing the power spectrum from time-domain data, use the biased autocovariance of the data, use 1/4 to 1/10 of the available lags, and window the autocovariance data using a positive-definite weighting function.
- Ensure that the total power in the frequency domain equals the total power in the time domain when computing the power spectral density from time-domain data.
- Pure sinusoidal motion may manifest as split spectral lines (leakage) in the power spectrum, due to the finite record length. Split spectral lines can be distinguished by evaluating the PSD over a fine grid of frequencies, or by zero padding the data. These do not improve the resolution of the BT periodogram.
- Be careful of aliasing. It may exist in an actual system and affect performance. It can also be created in a model of the system.

▲ Cautions (cont'd)

- Zero-order holds provide additional filtering – don't leave them out of the model where they are required.
- Traditionally the cutoff frequency for jitter motion is $1/T$ Hz, but motion at frequencies below $1/T$ Hz also contributes to jitter and displacement, smear. The half-power frequency is about $0.85/T$ Hz. If one has to define a cutoff frequency, specify the frequency at 10% gain at about $0.5/T$ Hz.

⚠ Cautions (cont'd)

- Apply model uncertainty factors (MUFs) with care. Identify and mitigate hidden margin and margin-on-margin.
- Modal damping within and near the controller bandwidth will increase or decrease with changes in modal frequency, modal gain, controller parameters, sensor and actuator performance, and latency.
- The closed-loop response of structural modes at or near the control loop bandwidth should not be evaluated open-loop.
  - Gain-stabilized modes are not controlled, but feedback can increase or decrease modal damping.
  - Phase-stabilized modes are controlled; greater loop gain yields greater damping.
- The RMS of Gaussian random amplitudes of sinusoidal motion is the factor that determines the IM OTF.
  - Random phase does not matter to average performance. Coherent, deterministic, or specific phases do matter.
  - The IM OTF in the presence of a dominant tonal disturbance is a zero-order Bessel function J_0.
  - Smear, statistical smear, and jitter OTFs cannot, in general, be separated into x and y-axis OTFs.

Are we there yet? What more is there to do?

- Get feedback from GN&C and optical engineers regarding application and effectiveness of IM OTF and PPMs in design and operation (reports, presentations, publications).
- Develop guidelines to allocate an OTF requirement to IM OTF, to allocate an IM OTF requirement to $\mathrm{OTF}_{\mathsf{D}}$, $\mathrm{OTF}_{\mathsf{S}}$, $\mathrm{OTF}_{\mathsf{J}}$; to state requirements, and to verify IM OTF and pointing requirements.
- Develop guidelines to define PPM requirements for ρ, $\boldsymbol{\Sigma}_{\mathsf{S}}$ from an $\mathrm{OTF}_{\mathsf{S}}$ requirement.
- Analyze and document the Harmonic OTF further and describe its average properties and behavior with multiple sinusoids over various distributions
- Investigate and 2D Harmonic OTF with vibration in two axes, including circular and ellipsoidal (relative phase) vibration.
- Develop a statistical Wave Front OTF (WF OTF).
- Develop statistical Image Motion OTFs for other types of optical detectors such as a time-delay-integration (TDI) line scan (pushbroom) and shutter (APS detector).

Nomenclature & Definitions

$$\boldsymbol{\xi} = \text{2D spatial frequency}$$

$$\operatorname{sinc}(x) = \frac{\sin x}{x} = \text{sinc function}$$

$$\boldsymbol{S}(\omega) = \text{power spectral density}$$

$$\boldsymbol{R}(\ell) = \text{correlation matrix}$$

$$\mathcal{E}\{\cdot\} = \text{statistical expectation}$$

$$\langle\cdot\rangle_T = \text{time average over a time window of width } T$$

Acronyms & Abbreviations (1/2)

FWHM	full-width half-maximum
PSF	point spread function
LSF	line spread function
OTF	optical transfer function
IM OTF	image motion optical transfer function
PTF	phase transfer function
MTF	modulation transfer function
MTFA	area under the modulation transfer function, above the NEM
NEM	noise equivalent modulation
CTF	contrast transfer function
WFE	wavefront error
PM	pointing metrics
PPM	pointing performance metrics
PEM	pointing error metrics

Acronyms & Abbreviations (2/2)

PSD	power spectral density
BT	Blackman-Tukey
RCS	reaction control system (thrusters)
SA	solar array
cryo	cryo cooler (cryo pump)
HGA	high gain antenna
RW	reaction wheel
ST	star tracker
IMU	inertial measurement unit (gyros)
LOS	line of sight
EOL	end of life
BOL	beginning of life
MUF	model uncertainty factor

References

[1] M. Hagopian, "Predicting, managing, controlling, and testing spacecraft jitter", NASA Engineering and Safety Center (NESC) GN&C Technical Discipline Team (TDT), LOS Jitter Workshop, October 2019, Columbia, MD.

[2] G. J. Henderson, "Managing Observatory Line-of-Sight Jitter", NASA Engineering and Safety Center (NESC) GN&C Technical Discipline Team (TDT), LOS Jitter Workshop, October 2019, Columbia, MD.

[3] M. Pittelkau, "2D Image Motion Optical Transfer Functions and Pointing Error Metrics: Displacement, Smear, Jitter", NASA Engineering and Safety Center (NESC) GN&C Technical Discipline Team (TDT), LOS Jitter Workshop, October 2019, Columbia, MD.

[4] K.-C. Liu, C. Blaurock, "Integrated Modeling Pre-PDR Engineering Peer Review – WFIRST Overview", NASA/GSFC, 23 October 2019.

[5] C. Blaurock, "Jitter Experience and EllipTool", NASA Engineering and Safety Center (NESC) GN&C Technical Discipline Team (TDT), LOS Jitter Workshop, October 2019, Columbia, MD.

[6] N. Dennehy, O. S. Alvarez-Salazar, "A Survey of the Spacecraft Line-of-Sight Jitter Problem", AAS 19-131, 2nd Annual AAS Guidance & Control Conference, 31 January – 6 February 2019.

References

[7] J. Sudey, M. Hagopian, N. Dennehy, "GOES I-M – A Retrospective Look at Image Navigation and Registration (INR), Jitter and Lessons Learned", AAS 19-132, 2nd Annual AAS Guidance & Control Conference, 31 January – 6 February 2019.

[8] Sudey, Dellinger, Hagopian (1996) On-orbit jitter performance of the Proceedings of the GOES spacecraft and instruments", SPIE 1996 International Symposium on Optical Science, Engineering, and Instrumentation, Denver, CO, Vol. 2812, *GOES-8 and Beyond*, 1996.

[9] M. Pittelkau, "Pointing Performance Validation and Verification", ESA-CNES-DLR-NASA VV Workshop, 20 April 2021.

[10] K.-C. Liu, G. Mosier, "Integrated Modeling: Past, Present, and Future", seminar, 28 April 2021.

[11] *NASA Systems Engineering Handbook*, NASA SP-2016-6105 Rev 2.

[12] T. Carter, "Recommendations for the SECCHI Pointing Stability Requirements Based on the Presence of the EUVI Image Stabilization System (ISS)", Technical Memo, Space Department, JHU Applied Physics Laboratory, 21 Nov 2000.

[13] T. Carter, "Proposed Changes to the Pointing Accuracy, Pointing Stability, and Pointing Knowledge Requirements in the STEREO Mission Requirements Document", Technical Memo, Space Department, JHU Applied Physics Laboratory, 14 May 2001.

[14] B. Southard, "STEREO Spacecraft Preliminary High Frequency Jitter Analysis", HYTEC, Inc., HTN-114190-0010, 2001-09-11.

References

[15] B. Appleby, "EOS-PM GIRD Analysis Continuation Task Results", Draper Laboratory, EOS-92-001, 23 November 1993.

[16] L. Draper, "Performing Analysis of NOAA-KLM Spacecraft Displacement Using the New AMSU-A1, A2, and B Torque-Time Profiles", GE Astro Space, 27 January 1994.

[17] P. Maghami, et al., *PLATSIM: A Simulation and Analysis Package for Large-Order Flexible Systems (Version 2.0)*, NASA Technical Memorandum 4790, NASA Langley Research Center, Dec 1997. http://www.sti.nasa.gov/

[18] U.S. Patent 6988051, "Window Average Statistics Model for Pointing Stability Jitter Analysis", Filed 14 Nov 2003, Awarded 17 Jan 2006, Assignee: The Boeing Company.

[19] G. D. Boreman, *Modulation Transfer Function in Optical and Electro-Optical Systems*, Tutorial Texts in Optical Engineering, Volume TT52, SPIE Press, Bellingham, Washington, USA, 2001, available at http://ebooks.spiedigitallibrary.org/

[20] M. Born and E. Wolf, Principles of Optics: Electromagnetic Theory of Propagation, Interference and Diffraction of Light, Pergamon Press, Oxford, 7th Edition, 1999.

[21] A. Nusbaum, R. A. Phillips, *Contemporary Optics for Scientists and Engineers*, Prentice-Hall, Englewood Cliffs, NJ, 1976.

[22] G. C. Holst, "Imaging System Fundamentals", Optical Engineering 50(5), Vol. 50, No. 5, May 2011, 11 pp.

References

[23] T. Trott, "The effects of motion on resolution", *Photogrammetric Engineering*, Journal of the American Society of Photogrammetry, Vol. 26, Dec 1960, pp. 819–827.

[24] R. M. Scott, "Contrast Rendition As a Design Tool", Photographic Science and Engineering, Vol. 3, Issue 5, 1959, pp. 201–209.

[25] Shack, R. V., "The Influence of Image Motion and Shutter Operation on the Photographic Transfer Function", *Applied Optics*, Vol. 3, No. 10, October 1964, pp. 1171–1181.

[26] Sirlin, S. W.; San Martin, A. M.; "A New Definition of Pointing Stability", Jet Propulsion Laboratory, Pasadena, California, JPL Engineering Memorandum EM 343-1189, 6 Mar 1990.

[27] Lucke, R. L.; Sirlin, S. W.; San Martin, A. M.; "New Definitions of Pointing Stability: AC and DC Effects", *AAS Journal of the Astronautical Sciences*, Vol. 40, No. 4, Oct–Dec 1992, pp. 557–576.

[28] Baiocco, P., Sevaston, G., "On the Attitude Control of a High-Precision Space Interferometer", Space Guidance, Control, and Tracking, SPIE Vol. 1949, 1993, pp. 92–107.

[29] Bayard, D. S., *A Simple Analytic Method of Computing Instrument Pointing Jitter*, JPL New Technology Report NPO-30525, NASA Tech Brief Vol. 27, No. 1. (JPL Internal Document JPL D-19967, 22 November 2000)

[30] Bayard, D. S., "State-Space Approach to Computing Spacecraft Pointing Jitter", *Journal of Guidance, Control, Dynamics*, Vol. 27, No. 3, May–June 2004, pp. 426–433.

References

[31] M. Santina et al., "Line-of-sight pointing and control of electro-optical space systems – an overview", in *Advances in the Astronautical Sciences, Guidance and Control 2011*, AAS Guidance and Control Conference, 4–9 February 2011, Breckenridge, CO, Vol. 141, pp. 213–235, Paper No. AAS-11-041.

[32] Pittelkau, M. E., "Definitions, Metrics, and Algorithms for Displacement, Jitter, and Stability", Paper No. AAS 03-559, *AAS/AIAA Astrodynamics Specialist Conference*, Big Sky, MT, 3–7 Aug 2003. In *Advances in the Astronautical Sciences*, Vol. 116, Part II, 2003, pp. 901–920.

[33] Pittelkau, M. E., "Definitions, Metrics, and Algorithms for Displacement, Jitter, and Stability", *Flight Mechanics Symposium*, NASA Goddard Space Flight Center, NASA/CP-2003-212246, 28–30 October 2003.

[34] Pittelkau, M. E.; McKinley, W. G.; "Pointing Error Metrics: Displacement, Smear, Jitter, and Smitter with Application to Image Motion MTF", Paper No. AIAA-2012-4869, AIAA Guidance, Navigation, and Control Conference, 13–16 Aug 2012, Minneapolis, MN, 19 pp.

[35] Pittelkau, M. E.; McKinley, W. G.; "Optical transfer functions, weighting functions, and metrics for images with two-dimensional line-of-sight motion", SPIE, Optical Engineering, Vol. 55, Issue 6, 17 June 2016, 17 pp. *Open Access*, DOI: 10.1117/1.OE.55.6.063108, https://doi.org/10.1117/1.OE.55.6.063108

[36] M. Green, D.J.N Limebeer, *Linear Robust Control*, Prentice Hall, HJ, 1995.

References

[37] C. Blaurock, K.-C. Liu, L. Dewell, J. Alexander, "Pointing Control System Design and Jitter Analysis of the Terrestrial Planet Finder Coronagraph", FMET, 2005.

[38] K.-C. Liu, P. Maghami, C. Blaurock, "Reaction Wheel Disturbance Modeling, Jitter Analysis, and Validation Tests for Solar Dynamics Observatory", AIAA GNC Conference, Honolulu, HI, 18 August 2008.

References

[39] R. A. Masterson, *Development and Validation of Empirical and Analytical Reaction Wheel Disturbance Models*, M.S. Thesis, Department of Mechanical Engineering, MIT, June 1999.

[40] N. J. Dennehy, "A Survey of Reaction Wheel Disturbance Modeling Approaches for Spacecraft Line-of-Sight Jitter Performance Analysis", Proc. 18th European Space Mechanisms and Tribology Symposium 2019, Munich, Germany, 18–20 September 2019.

[41] K.-C. Liu, T. Kenney, P. Maghami, P. Mule, C. Blaurock, W. B Haile, "Jitter Test Program and On-Orbit Mitigation Strategies for Solar Dynamic Observatory", Proceedings of the 20th International Symposium on Space Flight Dynamics, 24 September 2007.

[42] B. Bialke, "Microvibration disturbance sources in reaction wheels and momentum wheels", Spacecraft Structures, Materials & Mechanical Testing, Technische Informationsbibliothek (TIB), pp. 765–770, 1996.

[43] B. Bialke, "A compilation of reaction wheel induced spacecraft disturbances", 20th Annual American Aeronautical Society Guidance and Control Conference, San Diego, USA, AAS Publication, 1997.

[44] A. Bronowicki, "Forensic Investigation of Reaction Wheel Nutation on Isolator", 49th AIAA/ASME/ASCE/AHS/ASC Structures, Structural Dynamics, and Materials Conference, 7–10 April 2008.

[45] F. C. Lee, M. Werner, "Reaction Wheel Jitter Analysis Including Rocking Dynamics & Bearing Harmonic Disturbances", AAS 07-006, Proceedings of the 30th Annual AAS Rocky Mountain Guidance and Control Conference, Breckenridge, CO, USA, February 3–7, 2007, *Advances in the Astronautical Sciences Volume 128*.

References

[46] PEET Standard
url: http://peet.estec.esa.int/standard/

[47] PEET Handbook, ESSB-HB-E-003, Issue 1, Rev 0, 19 July 2011.
url: http://peet.estec.esa.int/files/ESSB-HB-E-003-Issue1(19July2011).pdf
url: http://peet.estec.esa.int/handbook/

[48] PEET Tool
url: http://peet.estec.esa.int/downloads/

[49] ESA Pointing Error Handbook, 19 February 1993, ESA-NRC-502.

[50] D. G. Dungate, "Statistical Spacecraft Pointing Performance Calculation: The ESA Pointing Error Handbook and the APP Software Package", (AAS 98-013), Volume 98, Advances in the Astronautical Sciences, Guidance and Control 1998.

[51] M. Casasco, S. Salehi, S. Weikert, J. Eggert, M. Hirth, H. Su, T. Ott, "Pointing Error Engineering Framework for High Pointing Accuracy Missions", 24th International Symposium on Space Flight DynamicsAt: Laurel, MD, May 2014.

[52] M. Hirth, H. Su, T. Ott, M. Casasco, G. Ortega, "PEET V1.0: The State-of-the-Art Pointing and Performance Error Engineering Tool for Space Missions", ESA GNC 2017: 10th International ESA Conference on Guidance, Navigation, & Control Systems, Salzburg, Austria, 29 May – 2 June 2017.